Investigation of the Determinants of Reaction Specificity in the Pyridoxal 5'-Phosphate Dependent Enzymes Cystathionine β-Lyase and Cystathionine γ-Lyase

By

Ali Farsi, B. Sc.

A thesis submitted to

the Faculty of Graduate Studies and Research

in partial fulfillment of

the requirements for the degree of

Masters of Science

Biology Department

Ottawa-Carleton Institute of Biology

Carleton University

Ottawa, Ontario

May 2007

Your file Votre référence
ISBN: 978-0-494-27018-9
Our file Notre référence
ISBN: 978-0-494-27018-9

ABSTRACT

Amino acids play an important role in the production of flavor compounds in fermented foods. Cysteine and methionine, the two sulfur-containing amino acids, are the precursors of aroma-active volatile sulfur compounds, as well as an array of important cellular metabolites. Cystathionine β-Lyase (CBL) and cystathionine γ-Lyase (CGL) are pyridoxal-5'-phosphate (PLP) dependant enzymes involved in the inter-conversion of cysteine and methionine. These two enzymes bind the same pseudo-symmetric substrate, cystathionine, but in opposite orientations. Therefore, they provide a good model system to investigate the mechanism whereby PLP-dependent enzymes regulate the chemistry of this versatile cofactor. The active-sites of CBL and CGL are very similar, with a conspicuous difference being the aromatic residues Phe55 and Tyr338 in *E. coli* CBL (eCBL), which correspond to the acidic residues Glu48 and Glu333 in *S. cerevisiae* CGL (yCGL). A series of site-directed mutants of these residues were constructed to probe their role in substrate binding, catalysis and as determinants of reaction specificity. The ability of these mutants to complement methionine auxotrophy in *E. coli* strains lacking the enzymes of the transsulfuration pathway was observed to be no greater than the corresponding wild-type enzymes. The k_{cat}/K_m of the CBL Phe55Asp and Tyr338Glu mutants is reduced by two and three orders of magnitude, respectively, and a similar, although less pronounced, trend was observed for mutants of the corresponding residues in yCGL. The results provide insight into the mechanisms of eCBL and yCGL and suggest that the two residues investigated (Phe55 and Try338 of eCBL and Glu48 and Glu333 of yCGL) are not prime determinants of reaction specificity, thereby demonstrating the importance of context in protein structure-function relationships.

2. ACKNOWLEDGEMENTS

I am extremely grateful to have such a dedicated and attentive supervisor as Dr. Susan Aitken. I am forever in her debt for her valuable time and ever-available advice, which made this thesis possible. Dr. Aitken's individual guidance has provided me with a great deal of knowledge and experience. It has been an honour to learn from someone like Sue who is so dedicated to education and the field of science. Sue's expertise and willingness to listen made my time at Carleton University worth a great deal more than simply a degree.

I would also like to extend my sincere appreciation to my committee members, Dr. William Willmore and Dr. Katie Gilmour. Special thanks to my colleagues and friends for their support and advice, in particular Pratik Lodha, who enriched my experience with his companionship and assistance both inside and outside the lab.

Above all I would like to thank my mom and dad for supporting me through all these years of education, helping me make the right decisions, showing the way when I got discouraged and being the best parents ever. I also want to thank my beautiful sister for being my best friend and for bringing the most beautiful and precious baby angel to our family. Finally, I thank my extended family, especially my uncle Hossein, who have been unending in their support. Now it is my turn to come home and show my appreciation to you all.

3. DEDICATION

As a small sign of gratitude,

I would like to dedicate this work to my parents,

and to the memory of my grandmother

3. TABLE OF CONTENTS

4. LIST OF TABLES

5. LIST OF FIGURES

6. LIST OF ABBREVIATIONS

aadA	Aminoglycoside adenyltransferase
Amp	Ampicillin
AVG	Aminoethoxyvinylglycine
BSA	Bovine serum albumin
Cat	Chloramphenicol acetyltransferase
CBL	Cystathionine β-lyase
CGL	Cystathionine γ -lyase
CGS	Cystathionine γ-synthase
Chlor	Chloramphenicol
L-Cth	L-Cystathionine
Cys3	Saccharomyces cerevisiae gene encoding cystathionine γ-lyase
L-Cys	L-Cysteine
DEAE	Diethylaminoethyl cellulose
DNA	Deoxyribonucleic acid
DTNB	5,5'-Dithiobis-(2-nitrobenzoic acid)
E. coli	*Escherichia coli*
EDTA	Ethylenediamine tetraacetic acid
HCL	Hydrochloric acid
HIC	Hydrophobic interaction chromatography
L-Hcys	L-Homocysteine
IPTG	Isopropyl-β-*D*-thiogalactopyranoside
Kan	Kanamycin

LAB	Lactic acid bacteria
LB	Luria broth
L-Met	L-Methionine
metB	*Escherichia coli* gene encoding cystathionine γ-lyase
metC	*Escherichia coli* gene encoding cystathionine β-lyase
MSG	Monosodium glutamate
Ni-NTA	Ni-nitrilo triacetic acid
PAGE	Polyacrylamide gel electrophoresis
PCR	Polymerase chain reaction
PLP	Pyridoxal 5'-phosphate
RepA	Replication initiation gene
SacB	Gene encoding levansucrase from *Bacillus subtilis*
SAM	*S*-adenosylmethionine
SDS	Sodium Dodecyl Sulfate
L-Ser	L-Serine
Spec	Spectinomycin
TLC	Thin layer chromatography
trc	Hybrid *trp-lac* promoter
Tris	Tris-[hydroxymethyl]aminomethane
tsp	Periplasmic protease
UV	Ultraviolet
VSC	Volatile sulfur compounds

8. INTRODUCTION:

8.1. Amino Acids

Any organic compound that comprises both amino and carboxyl moieties may be referred to as an amino acid. However, in the field of biochemistry the term amino acid is generally applied to the α-amino acids, in which the amino and carboxyl groups are attached to the same carbon atom, and in particular to the 20 proteinogenic α-amino acids, which have the formula $NH_2CHRCOOH$ and are encoded by deoxyribonucleic acid (DNA). Ten of the 20 amino acids found in proteins are essential in humans because they are not synthesized *de novo* and therefore must be obtained from the diet (Shike, 2006). Methionine and lysine are of particular importance because they are limiting nutrients, meaning that they are present in the lowest concentration compared to other essential amino acids, in pulses, such as chickpea and lentil, and in grains, including wheat and maize, respectively (Galili and Hofgen, 2002). The amino acid cysteine is derived from methionine, *via* the transsulfuration pathway, and is therefore considered a semi-essential amino acid. Methionine and cysteine, which are the only proteinogenic amino acids that contain the element sulfur, are the precursors of an array of important cellular metabolites, including *S*-adenosylmethionine (SAM) and glutathione (Voet *et al.*, 2002).

8.1.1. Applications of amino acid metabolism

The annual industrial production of amino acids is in excess of two million tons and is dominated by glutamate, used as a food additive in the monosodium glutamate (MSG) form, and by lysine, methionine and threonine, which are largely used as livestock feed supplements (Hermann, 2003; Leuchtenberger *et al.*, 2005). Synthetic applications of amino acids in the chemical and pharmaceutical industries are also developing rapidly and, given the current 7% annual rate of increase, are expected to comprise a one-billion-dollar market by 2009 (Leuchtenberger *et al.*, 2005). Biotechnological processes, involving microorganisms, now dominate amino acid production as a result of health and environmental concerns (Wada and Takagi, 2006).

The microbial catabolism of amino acids also plays an important role in the production of flavor compounds in a variety of fermented foods, including cheese and wine. For example, compounds derived from branch-chain, aromatic and sulfur-containing amino acids produce malty and fruity, floral, and meaty and garlic flavors, respectively (Ardö, 2006). Compounds derived from the sulfur-containing amino acids cysteine and methionine in fermentation by lactic acid bacteria (LAB) contribute to flavor development in cheese during ripening (Cutin and McSweeney, 2004). For example, methionine is the precursor of aroma-active volatile sulfur compounds (VSCs), including methanethiol, which is an indicator compound for quality in aged cheddar cheese (Dias and Weimer, 1998; Weimer *et al.*, 1999). Sulfur compounds also play an important role in wine fermentation and quality. Several VSCs are produced by *Saccharomyces cerevisiae* during the fermentation process. These include hydrogen sulfide,

methanethiol, dimethylsulfide and methylthioesters, which give aromas of rotten egg, cabbage, garlic, chive and cheese, as well as the fruity volatile thiols that are potent and valued aroma components of wines and impart aromas of box tree (4-mercapto-4-methyl-pentan-2-one) and of passion fruit, grapefruit, gooseberry and guava (3-mercaptohexan-1-ol and 3-mercaptohexyl acetate) (Swiegers and Pretorius 2007; Sarrazin *et al.*, 2007; Tominaga *et al.*, 1995, Tominaga *et al.*, 1998a; Tominaga *et al.*, 1998b; Dubourdieu *et al.*, 2006) (Figure 1). The volatile thiols involved in wine aroma are present as cysteine-conjugates in grapes, necessitating cleavage by yeast carbon-sulfur lyases to release the volatile thiols. For example, yeast carbon-sulfur lyases with β-elimination activity are involved in the release of 4MMP and 3MH from Cys-4MMP and Cys-3MH, respectively (Figure 1). As a result, the fermentation conditions as well as the identity of the yeast strain employed can alter the relative and absolute amounts of these compounds, thereby affecting the character of the wine. Therefore, the process of yeast fermentation in wine production is very important for flavor development (Tominaga *et al.*, 2000; Howell *et al.*, 2004). The range of amino acid products employed in industrial applications and their resulting economic impact demonstrate that the development of a thorough understanding of amino acid biochemistry, including their biosynthesis and catabolism, is essential for the efficient microbial production of amino acids and their catabolic products.

Figure 1. Example of thiol compounds that contribute to aroma of wine. During fermentation, *S. cerevisiae* mediates the cleavage of non-volatile cysteine conjugates, such as S-4-(4-methylpentan-2-one)-L-cysteine (Cys-4MMP) and 4-mercapto-4-methylpentan-2-one (Cys-3MH), present in grape juice, in order to release the volatile thiols (Swiegers and Pretorious, 2007).

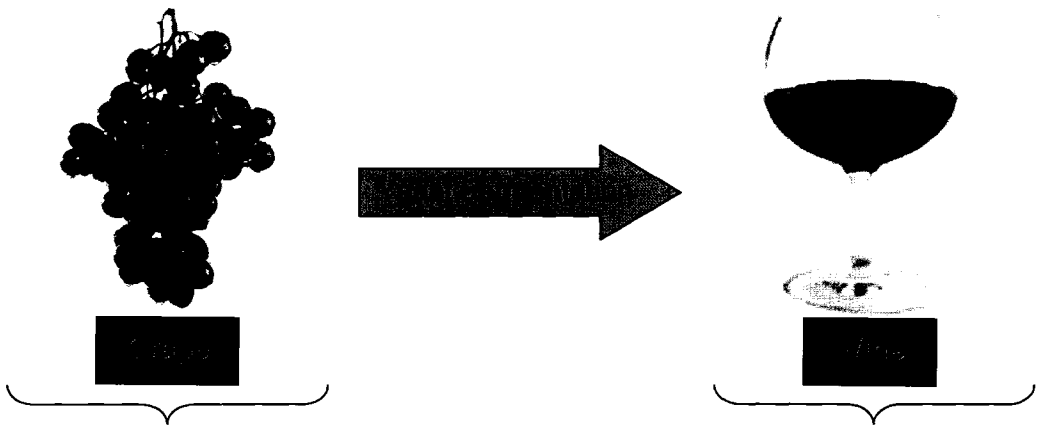

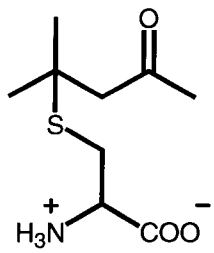

Cys-4MPP:
S-4-(4-methylpentan-2-one)-L-cysteine

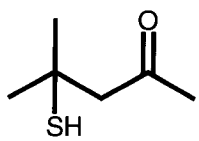

4MMP:
4-mercapto-4-methylpentan-2-one

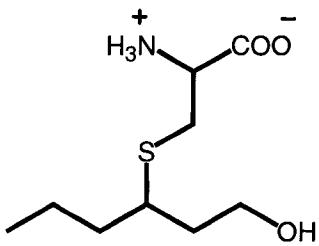

Cys-3MH:
S-3-(hexan-1-ol)-L-cysteine

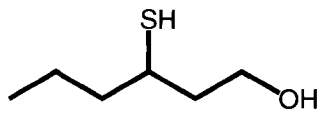

3MH:
3-mercaptohexan-1-ol

8.2. Enzymes

Most chemical reactions occur too slowly to support life. Enzymes are the biological catalysts which enable the chemical processes of living cells and organisms. Enzymes function by lowering the activation energy of a reaction, thereby increasing its rate, without affecting the position of equilibrium (Voet *et al.,* 2002). The vast majority of enzymes are proteins, although some are RNA molecules, referred to as ribozymes. The specificity and catalytic power of enzymes is central to cellular metabolism, as demonstrated by the over 4000 biochemical reactions catalyzed by enzymes (Bairoch, 2000). Their importance is further illustrated by the large number of metabolic diseases caused by the malfunction of individual enzymes (Voet *et al*, 2002). Examples of such diseases include homocystinuria and phenylketonuria, which are both hereditary diseases of amino acid metabolism and are linked to mutations in the genes encoding cystathionine β-synthase and phenylalanine hydroxylase, respectively (Mudd *et al.*, 1989; Centerwall and Centerwall, 2000).

8.2.1. Applications and engineering of enzymes

Enzymes have the capacity to accelerate reactions by many orders of magnitude, while concomitantly enabling catalysis under the mild conditions commonly found inside the cell (Voet *et al.*, 2002). This is in marked contrast to the conditions required in synthetic organic chemistry reactions, including elevated temperature and extremes of pH. Enzymes also generally demonstrate exquisite selectivity in substrate and reaction

specificity and enantioselectivity, thereby allowing yields to be increased, as compared to corresponding synthetic organic methods. Another advantage of the use of enzymes in industrial processes is their reduced environmental impact, in comparison with traditional chemical methods.

Enzymes are employed in a wide range of industrial applications, such as the use of amylase and xylanase in the production of refined flour and baking, phospholipase in the refining of edible oils, proteases and lipases in laundry detergent, xylanase in the paper industry and an array of enzymes used in the production of specialty chemicals and polymers (Ahuja *et al.*, 2004). Limitations of the use of enzymes for industrial applications are that an enzyme with a suitable substrate specificity or activity may not exist in nature and that the conditions (*i.e.* pH, temperature, presence of organic solvents) under which the enzyme is required to function may be sub-optimal for its efficient catalysis (Kuchner and Arnold, 1997). The many advantages of biological catalysts have spurred interest in the design of enzymes with novel activities or properties, as tailor-made bio-catalysts for industrial applications, to overcome these limitations (Hult and Berglund, 2003). Recent advances in protein engineering, including the techniques of rational and semi-rational design and directed evolution, now enable the modification and/or enhancement of enzyme properties. Although directed evolution is a powerful tool for engineering of proteins, it is a challenging technique, due in part to the inherent difficulty of the vastness of sequence space, and therefore, the large size of mutant libraries. Rational and semi-rational methods can provide assistance by limiting the focus of the investigation to a restricted subset of all accessible mutants (Chica *et al.*, 2005). Therefore, the ability to engineer enzymes for industrial applications is dependent on the

development of an in-depth understanding of the relationship between macromolecular structure and function.

8.3. Cofactors

Although the 20 amino acids found in proteins provide an array of chemical tools for catalysis, enzymes frequently require additional assistance from small molecules, referred to as cofactors. Cofactors bind at the active site of an enzyme and participate in catalysis, but are not considered substrates of the reaction (Kyte, 1995) and are returned to their original state when the catalytic cycle is complete. The enzyme-cofactor complex is termed the holoenzyme, while the protein component of the enzyme is the apoenzyme. Cofactors may be metal ions or organic molecules, such as pyridoxal 5'-phosphate (PLP), flavin and heme (Voet *et al.*, 2002).

8.3.1. Pyridoxal phosphate enzymes

PLP is derived from pyridoxine, also known as vitamin B6, which is a water-soluble vitamin discovered in 1938 by Paul György (György, 1971). Pyridoxine is oxidized and phosphorylated *in vivo* to the form PLP (Figure 2A) (Christen and Mehta, 2001). In PLP-dependent enzymes the cofactor is bound covalently to an active-site lysine residue *via* an aldimine linkage, referred to as the internal aldimine (Figure 2A) (Eliot and Kirsch, 2004). The α-amino group of amino acid substrate replaces the ε-

amino group of the active-site lysine residue, *via* a transaldimination reaction, to form an aldimine intermediate referred to as the external aldimine (Figure 2B). Electron withdrawal by the pyridinium nitrogen has the effect of weakening the substrate sigma bond that is orthogonal to the plane of the PLP ring (Figure 2C), thereby facilitating the cleavage of this bond and resulting in a resonance-stabilized carbanion intermediate (Figure 2B) (Eliot and Kirsch, 2004; Kyte, 1995; Dunathan, 1966).

PLP-dependent enzymes are divided into four families, fold types I through IV, based on structure and sequence similarity (Percudani and Peracchi, 2003; Jansonius, 1998). The majority of PLP-dependent enzymes are members of fold-type I, also known as the α-family, which is represented by the model enzyme aspartate aminotransferase. These enzymes function as homodimers, or homotetramers, in which active sites are typically comprised of residues from more than one monomer. Each monomer has a large and a small domain which undergo a conformational change, upon association with substrate, to create a closed conformation of the active site (Eliot and Kirsch, 2004). Tryptophan synthase is typical of the fold-type II enzymes, also referred to as the β-family. In contrast with fold-type I, fold-type II enzymes often possess a regulatory domain, as exemplified by the mammalian form of cystathionine β-synthase, and an active site that is comprised of residues from a single monomer (Hyde *et al.*, 1988). Alanine racemase and a subset of amino-acid decarboxylases comprise fold-type III and fold-type IV enzymes comprise the D-amino acid aminotransferase (Sugio *et al.*, 1995).

The PLP cofactor has the capacity to catalyze a wide variety of reactions (Figure 2B), as demonstrated by the large number of different PLP-dependent enzymes

(Percudani and Peracchi, 2003; Jansonius, 1998). The catalytic versatility of the PLP cofactor is such that PLP-dependent enzymes are found in five of the six enzyme classes (EC 2 – transferases, EC 3 – hydrolases, EC 4 – lyases, EC 5 – isomerases and EC 6 – ligases) defined by the Enzyme Nomenclature Committee of the International Union of Biochemistry and Molecular Biology (Christen and Mehta, 2001; Eliot and Kirsch, 2004). The diversity of the PLP cofactor is further demonstrated by the fact that more than 100 distinct EC numbers have been assigned to PLP-dependent enzymes (Christen and Mehta, 2001; Eliot and Kirsch, 2003). Therefore, it is the protein component of the enzyme that determines specificity by restricting the reactivity of the cofactor as well as limiting the range of potential substrates to which the cofactor has access (Eliot and Kirsch, 2004). The catalytic promiscuity of the PLP cofactor presents a challenge for the assignment of function to novel gene products. For example, a homologue of the plant enzyme 1-aminocyclopropane-1-carboxylate synthase was identified in humans, but its activity remains undetermined (Koch *et al.*, 2001). As a result, approximately one third of characterized PLP-dependent activities have yet to be associated with a particular coding sequence (Christen and Mehta, 2001). The versatility of the PLP cofactor also presents a unique opportunity, as PLP-dependent enzymes provide an ideal model system for the investigation of the mechanisms whereby enzymes control substrate and reaction specificity.

Figure 2. Structure and mechanism of PLP. (**A**) Structure (**1**) pyridoxine, (**2**) PLP and (**3**) the internal aldimine of PLP, as bound to the active-site lysine residue of an enzyme. (**B**) The PLP cofactor can catalyze a range of transformations of amino acids via resonance stabilization of the carbanion formed upon cleavage of the bond to the carbon-α moiety that is perpendicular to the plane of the pyridinium ring system, which is facilitated by (**C**) the electron withdrawing effect of the pyridinium nitrogen.

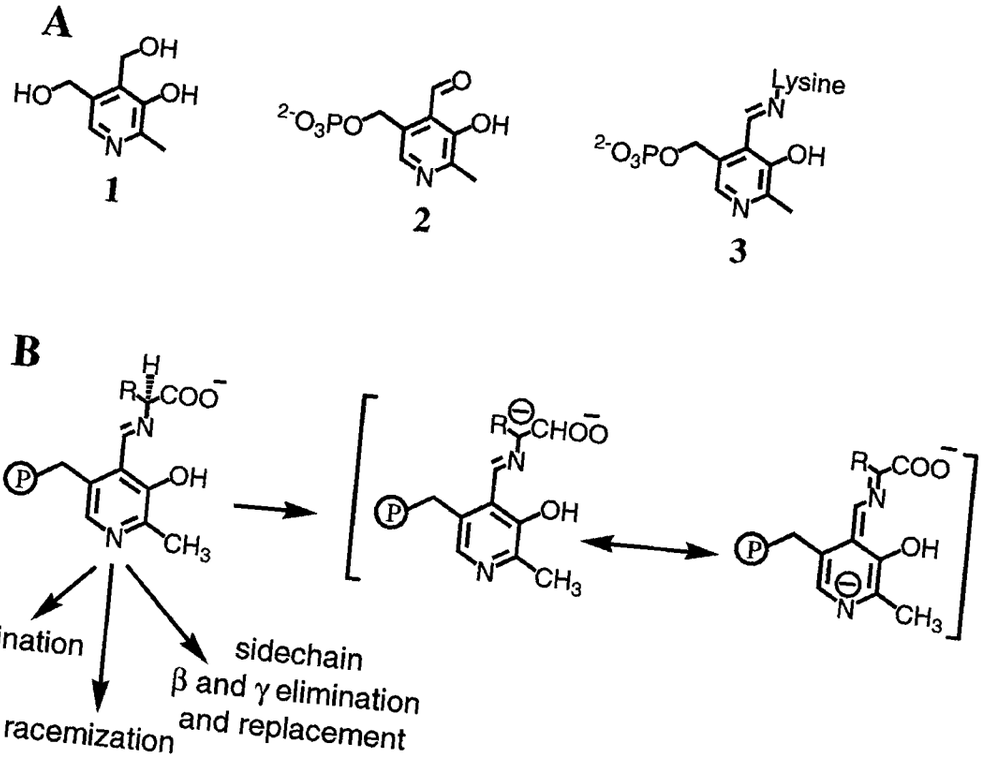

8.4. Enzymes of the transsulfuration and reverse transsulfuration pathways

In bacteria and plants, cystathionine γ-synthase (CGS) and cystathionine β-lyase (CBL), the two enzymes that comprise transsulfuration pathway, convert L-cysteine (L - Cys) to L-homocysteine (L-Hcys) (Figure 3), which is subsequently methylated by methionine synthase to form L-methionine (L-Met). In contrast, the reverse transsulfuration pathway (Figure 3), comprised of cystathionine β-synthase (CBS) and cystathionine γ-lyase (CGL), converts L-homocysteine to L-cysteine in mammals (Steegborn *et al.*, 1999).

CGS, CBL and CGL are members of the γ-subfamily of fold-type I of PLP enzymes, while CBS is a fold-type II enzyme (Percudani and Peracchi, 2003). In *E. coli* CGS and CBL are encoded by the *metB* and *metC* genes, respectively. The crystal structures of *E. coli* CGS (eCGS), *E. coli* CBL (eCBL) and *S. cerevisiae* (yeast) CGL (yCGL) have been solved at 1.5 Å, 1.83 Å and 2.6 Å, respectively (Figure 4) (Clausen *et al.*, 1998; Clausen *et al.*, 1996; Messerschmidt *et al.*, 2003). These enzymes share 30-38% sequence identity and are so similar in structure that they can be superimposed with a r.m.s. deviation of only 1.5 Å for C_α atoms of the backbone (Aitken and Kirsch, 2005; Messerschmidt *et al.*, 2003). CGS, the first enzyme of the transsulfuration pathway, catalyzes the condensation of L-Cys and *O*-activated L-homoserine to produce L-Cth *via* a γ-replacement reaction that is unique among PLP enzymes (Aitken *et al.*, 2003). CBL and CGL catalyze the second step in the transsulfuration and reverse transsulfuration pathways, in which cystathionine, is cleaved to produce homocysteine and cysteine, respectively. Therefore, these enzymes provide an ideal system to probe the mechanism(s) whereby PLP-dependent enzymes regulate cofactor chemistry.

Figure 3. The transsulfuration and reverse transsulfuration metabolic pathways of bacteria and plants and of mammals, respectively (adapted from Steegborn *et al.*, 1999).

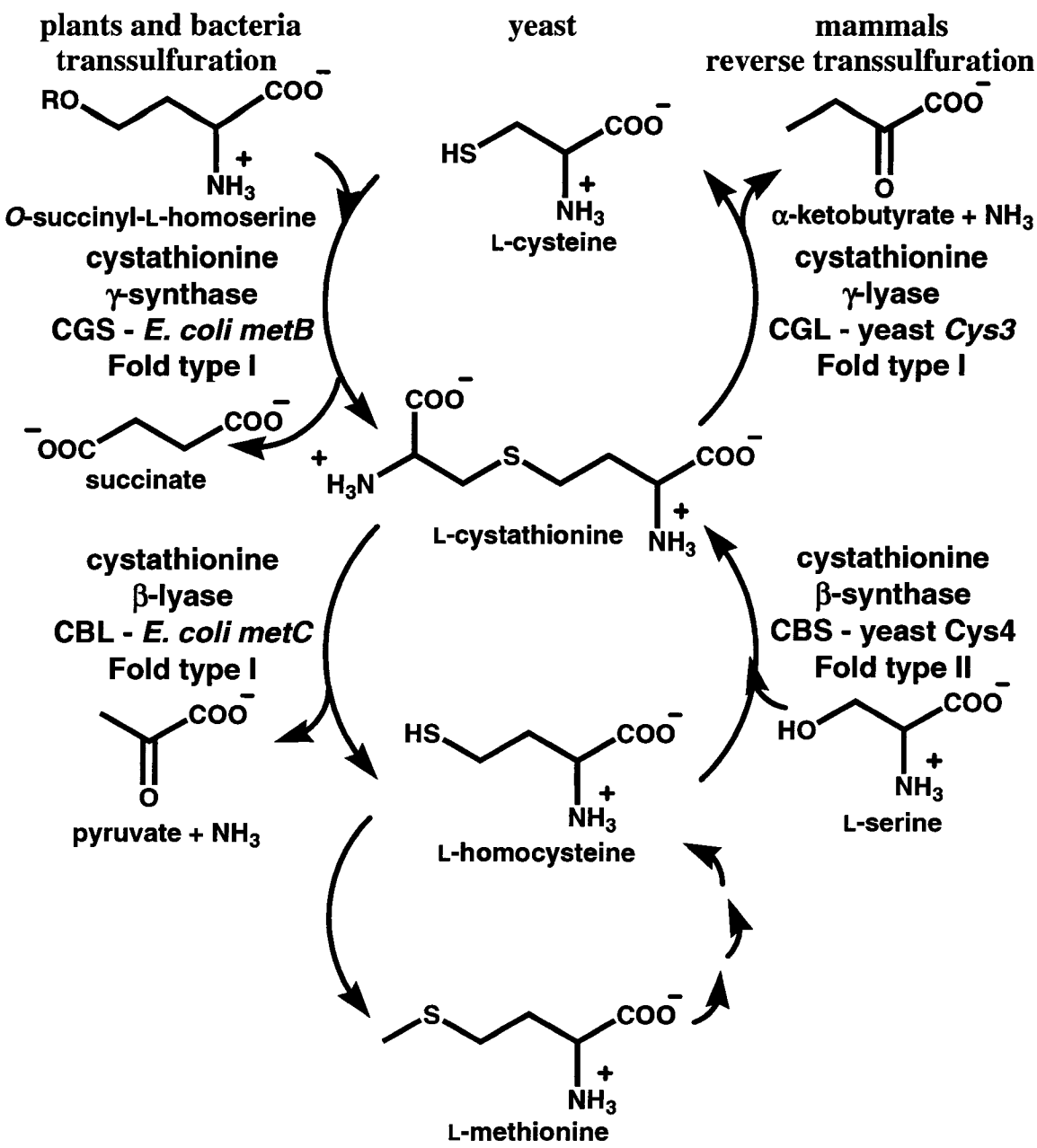

Figure 4. Similarity in the structures of eCGS, eCBL and yCGL. Structure of the (**A**) eCBL monomer, (**B**) semi-transparent surface view of the eCBL tetramer and cartoon views of the homotetrameric structures of (**C**) eCBL, (**D**) yCGL and (**E**) eCGS. The internal aldimine of PLP with the active-site lysine residue is shown in red and each subunit is given a distinct colour (Clausen *et al.*, 1996; Clausen *et al.*, 1998; Messerschmidt *et al.*, 2003; DeLano, 2002).

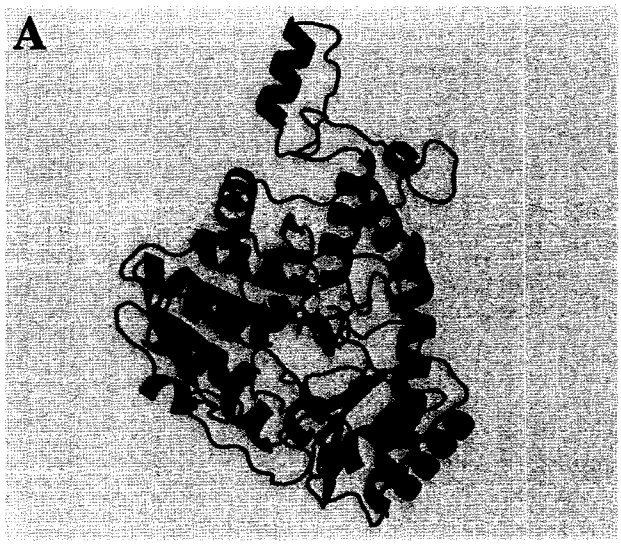

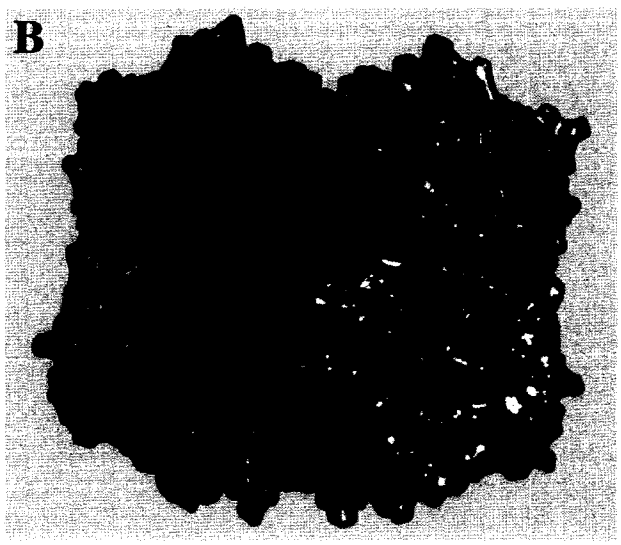

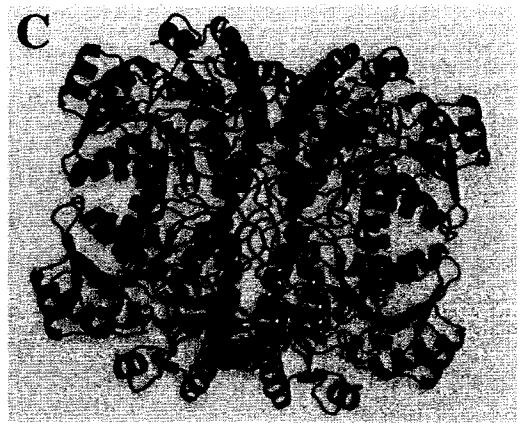

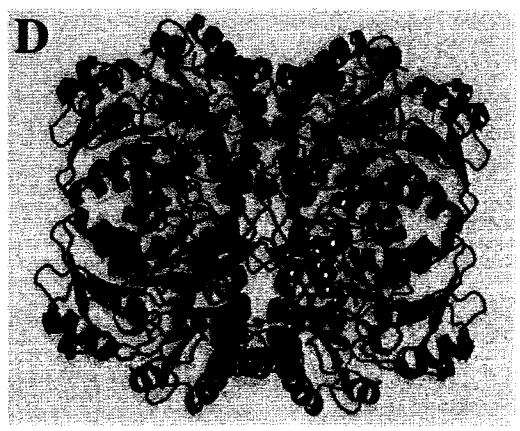

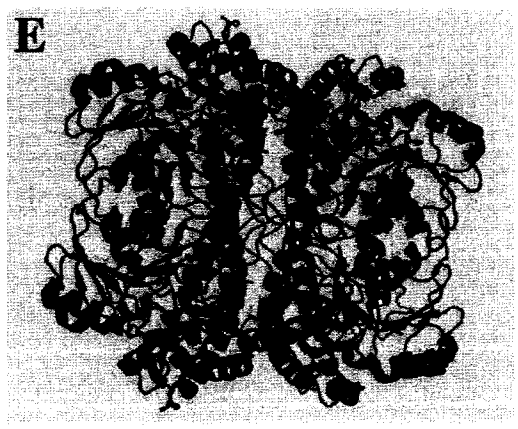

8.4.1. Cystathionine β-lyase

Cystathionine β-lyase (CBL), like CGS, is found in bacteria and plants (Figure 3). The *E. coli* CBL enzyme is encoded by the *metC* gene and was first cloned and sequenced by Belfaiza and colleagues in 1986 (Belfaiza *et al.*, 1986). Carbon-sulfur lyases, including CBL have applications in the food industry, such as the formation of flavor compounds in cheese and wine production. For example, CBL is involved in the production of VSCs, including methanethiol, from methionine and cystathionine during the cheese ripening process. The overexpression of CBL has been shown to produce higher quantities of VSCs, compared to a *Lactobacillus* wild-type strain, suggesting that the increased expression of this gene may be an effective method for intensifying cheese flavor during ripening (Lee *et al.*, 2007; Fernandez *et al.*, 2000; Alting *et al.*, 1995). As the role of CBL in the generation of VSCs has not been well characterized, a greater understanding of the substrate and reaction specificity of this enzyme is required as a precursor to its use and/or engineering for the development of flavor compounds and other industrial applications.

8.4.1.1. Mechanism

E. coli CBL catalyses the hydrolysis of L-Cth to L-Hcys, pyruvate and ammonia in the second reaction of the transsulfuration pathway (Figure 3). The first step in the mechanism of this reaction is transaldimination, in which the α-amino group of the L-Cth substrate replaces the ε-amino group of Lys210 in aldimine linkage with the cofactor, to

form the external aldimine of L-Cth (intermediate **2** of Figure 5). This is followed by abstraction of the α-proton to yield a quinonoid intermediate (intermediate **3** of Figure 5), from which L-Hcys is eliminated to form the external aldimine of aminoacrylate (intermediate **4** of Figure 5). The final step in the mechanism is a second transaldimination reaction, in which the internal aldimine form of the enzyme (intermediate **1** of Figure 5) is regenerated and aminoacrylate is released. Aminoacrylate is hydrolyzed to ammonia and pyruvate in aqueous solution (Figure 5) (Clausen *et al.*, 1997a).

8.4.1.2. Structure

Each monomer of the homotetrameric eCBL enzyme contains one PLP molecule, which is covalently bound, *via* an aldimine linkage, to the ε-amino group of an active-site lysine residue, Lys210 (Figures 4A and C) (Clausen *et al.*, 1996). The structure of eCBL, solved by X-ray crystallography in 1996, was the first of the enzymes of the transsulfuration and reverse transsulfuration pathways to be determined (Clausen *et al.*, 1996). Each eCBL subunit is divided into two domains: (i) the PLP-binding domain (residues 1 to 256) and (ii) the C-terminal domain (residues 257 to 395). Typical of fold-type I PLP enzymes, each active site of eCBL is situated at a subunit interface and comprises residues from two subunits (Figure 4C).

Figure 5. Proposed reaction mechanism of cystathionine β-lyase (Clausen *et al.*, 1997a).

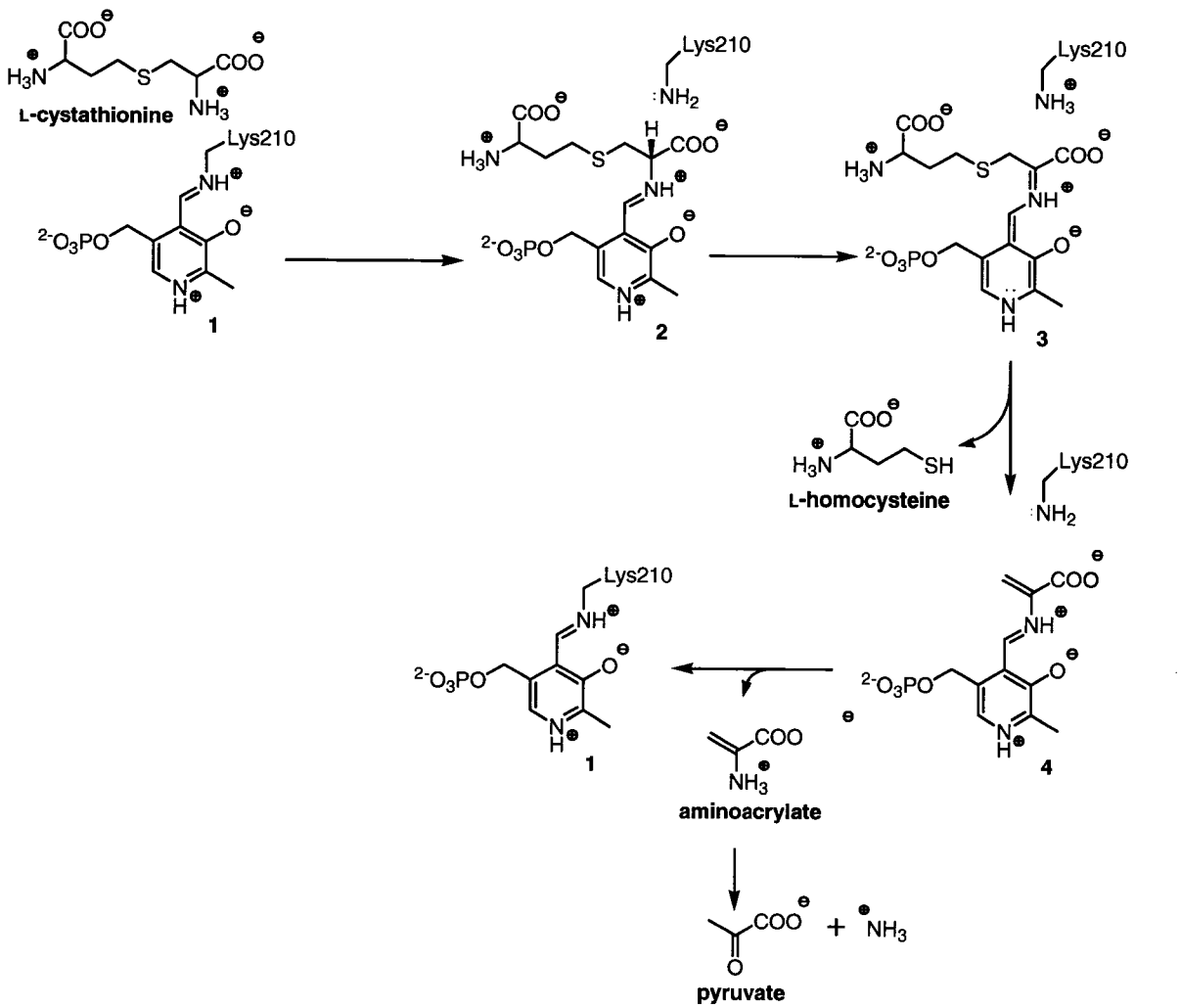

8.4.2. Cystathionine γ-lyase

CGL is found in mammals and fungi (Figure 3) and deficiency of this enzyme is associated with the hereditary metabolic disorders of cystathioninuria (Wang and Hegele, 2003) and homocystinurea (Uren *et al.,* 1978) in humans. Despite the essential metabolic role of CGL and its disease association, a detailed mechanistic understanding of this enzyme is lacking. CGL has been purified from several species, including *Neurospora crassa* (Flavin and Segal, 1964), *Streptomyces phaeochromogenes* (Nagasawa *et al.,* 1984), and rat (Uren *et al.*, 1978) and the genes encoding yeast and human CGL have been cloned, enabling their preliminary kinetic characterization (Yamagata *et al.,* 1993; Steegborn *et al.,* 1999).

8.4.2.1. Mechanism

Yeast CGL catalyses a γ-elimination reaction, in which L-Cth is hydrolyzed to produce L-Cys, α-ketobutyrate and ammonia, in the second reaction of the reverse transsulfuration pathway (Figure 3). The first step in the CGL mechanism is a transaldimination reaction in which the α-amino group of the L-Cth substrate replaces the ε-amino moiety of the active-site lysine (Lys203), to form the external aldimine of L-Cth (intermediate **2** of Figure 6). The α-proton is subsequently abstracted, forming a quinonoid intermediate (intermediate **3** of Figure 6), which is protonated at the C4' position to produce a ketimine intermediate (intermediate **4** of Figure 6). Abstraction of the Cβ proton, with subsequent release of L-Cys product, and removal of the C4' proton, produces a quinonoid intermediate (intermediate **6** of Figure 6) which undergoes electron rearrangement and protonation at the Cγ position to produce the internal aldimine of

aminocrotonate (intermediate **7** of Figure 6). The last step in the mechanism is a transaldimination reaction which regenerates the internal aldimine form of the enzyme (intermediate **7** of Figure 6) and releases aminocrotonate, which is hydrolyzed to produce α-ketobutyrate and ammonia in aqueous solution (Figure 6) (Steegborn *et al.*, 1999).

A distinguishing factor of CGL is its low catalytic efficiency. The k_{cat}/K_m of eCBL and eCGS are two-to-three orders of magnitude higher than that of yCGL (Aitken and Kirsch, 2003; Aitken *et al.*, 2003). Interestingly, the catalytic efficiency yCGL (2700 $M^{-1}s^{-1}$; S. Aitken, unpublished results) is comparable to that of the γ-elimination side reaction catalyzed by eCGS (1350 $M^{-1}s^{-1}$; Aitken *et al.*, 2003). Another characteristic of yCGL is its low reaction specificity, as this enzyme has been reported to have a ratio γ-elimination to β-elimination activity of only 2:1 with L-Cth as a substrate (Yamagata *et al.,* 1993). The γ-elimination *versus* γ-replacement reaction specificity of yCGL, and eCGS, was also proposed to be low and determined by substrate availability rather than the protein component of the enzyme (Ono *et al.,* 1999). However, preliminary steady state kinetic measurements (S. Aitken, unpublished results), suggest that the reaction specificity of yCGL and eCGS is, at least in part, determined by the enzyme.

8.4.2.2. Structure

yCGL is a homotetrameric enzyme comprising four active sites located at the subunit interfaces (Figure 4D) (Yamagata *et al.,* 1993; Messerschmidt *et al.*, 2003). Similar to eCBL, each monomer of yCGL is divided into a PLP-binding, catalytic domain, comprised of residues 1-252, and a C-terminal domain, comprised of residues 252-393 (Messerschmidt *et al.*, 2003).

Figure 6. Proposed reaction mechanism of cystathionine γ-lyase (Steegborn *et al.*, 1999).

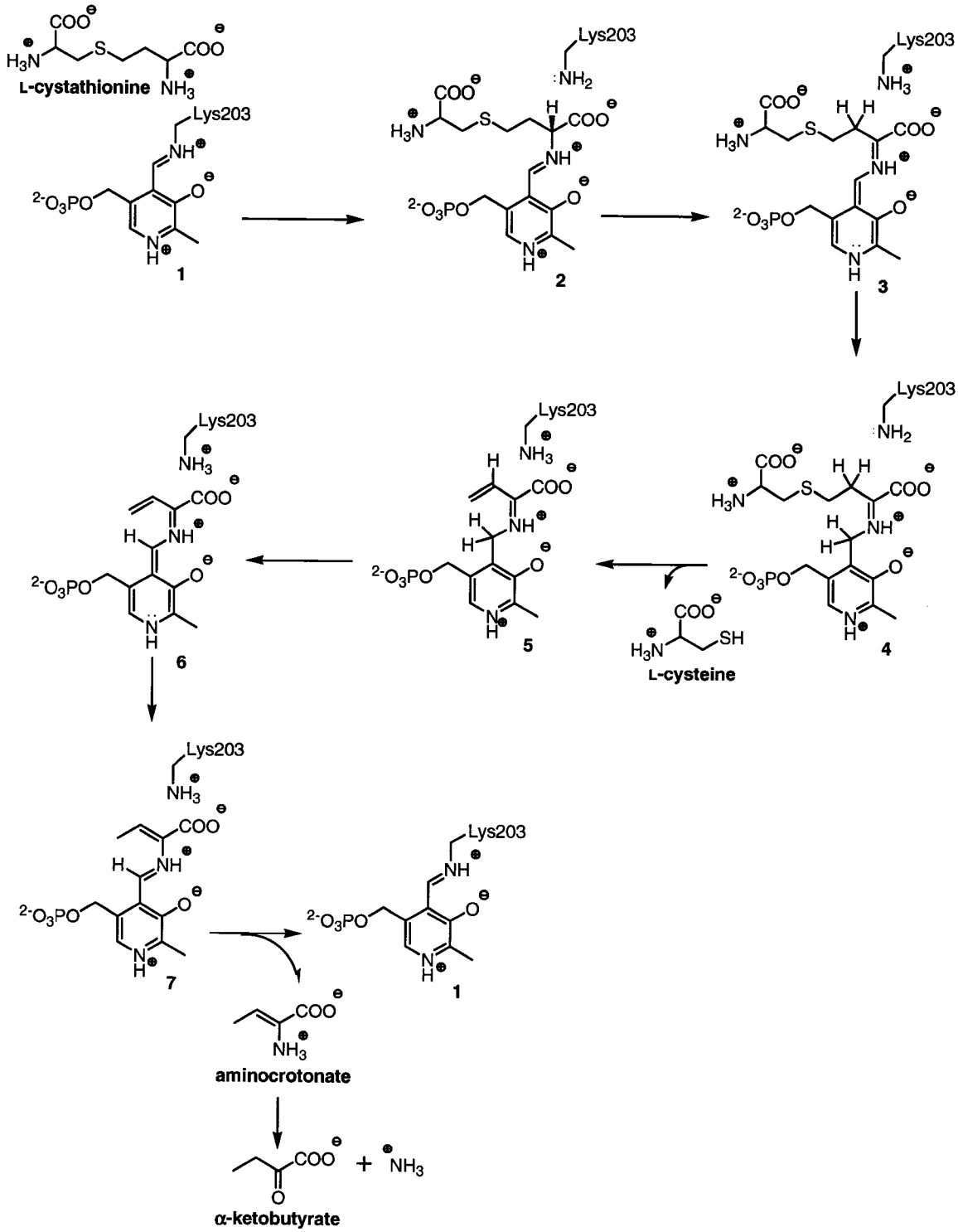

8.5. eCBL and yCGL: similarities and differences

Although eCBL and yCGL are very similar in both overall structure (Figure 4) and active-site architecture, their mechanisms are distinct (Figures 5 and 6). The pseudo-symmetric L-Cth substrate must bind with the sulfur atom in the δ-position or γ-position, with respect to the PLP cofactor, in CGL and CBL, respectively (Messerschmidt *et al.*, 2003). Examination of the active sites of eCBL and yCGL highlights five distinct active-site residues, which have been proposed to interact with the L-Cth substrate in at least one of the two enzymes, and which may act as determinants of the reaction specificity of these enzymes (Clausen *et al.*, 1996; Clausen *et al.*, 1997b; Messerschmidt *et al.*, 2003). These residues are Phe55, Arg59, Asp116, Tyr238 and Tyr338 of eCBL, which correspond to Glu48, Ser52, Arg108, Asn232 and Glu333 of yCGL (Table 1, Figures 7 and 8). Residues Phe55 and Tyr338 of eCBL, which correspond to Glu48 and Glu333 of yCGL are particularly interesting as the side chains of tyrosine and phenylalanine are nonpolar, bulky aromatic groups, whereas those of glutamate and aspartate are charged and acidic. Therefore, these residues may be expected to participate in very distinct interactions with the L-Cth substrate in eCBL and yCGL. The structure of eCBL has also been solved with the inhibitor aminoethoxyvinylglycine (AVG) bound at the active site (Clausen *et al.*, 1997b). The structure of the eCBL active site in the absence and presence of AVG are presented in Figure 9. Although AVG lacks the distal carboxylate of L-Cth and is the equivalent of one methylene carbon shorter, it provides a good model for the orientation of L-Cth within the eCBL active site, suggesting that Phe55 and Tyr338 do likely interact directly with the substrate. Interestingly, the corresponding residues in

eCGS, Asp45 and Glu325, are proposed to H-bond to the amino group of cysteine, the second substrate of the CGS reaction (Clausen *et al.*, 1998). Although no role has been proposed for Glu48 of yCGL, Glu333 is predicted to bind to the distal amino group of the L-Cth substrate. This residue is also proposed to play an important role in regulating the orientation of substrate binding in yCGL *via* electrostatic repulsion with the sulfur atom of L-Cth when the mode of substrate binding is such that the sulfur is in the γ-position, the orientation required for β-elimination, rather than the δ-position, as required for the γ-elimination reaction to proceed (Messerschmidt *et al.*, 2003). A corresponding role for Tyr338 in favoring the L-Cth binding mode required for the β-elimination reaction, with the sulfur atom in the γ-position, has not been suggested seems unlikely to be a major determinant of reaction specificity.

Table 1. Proposed functions of selected active-site amino acids of eCBL and the corresponding residues of yCGL.

eCBL active site		**yCGL active site**	
[a]**Residue**	[b]**Proposed role**	[a]**Residue**	[b]**Proposed role**
Phe55 (70%)	- Hydrophobic interaction with cystathionine	**Glu48** (70%)	- No proposed role
Tyr56 (100%)	- H-bond with phosphate of PLP	Tyr49 (100%)	- H-bond with phosphate of PLP
Arg58 (90%)	- Salt bridge with phosphate of PLP - H-bond to Tyr111	Arg51 (90%)	- Salt bridge with phosphate of PLP - H-bond with distal carboxylate of cystathionine
Arg59 (80%)	- Salt bridge with distal carboxylate of cystathionine	Ser52 (90%)	- No proposed role
Tyr111 (100%)	- π-stacking with PLP ring - H-bond with distal amino of cystathionine - H-bond with Arg58 - catalytic base	Tyr103 (100%)	- π-stacking with PLP ring - H-bond with Arg51 - catalytic base
Asp116 (nc)	- H-bond with distal amino of cystathionine	Arg108 (100%)	- Salt bridge with distal of carboxylate of cystathionine
Tyr238 (80%)	- Water-mediated H-bond to distal amino of cystathionine	Asn232 (90%)	- No proposed role
Tyr338 (70%)	- Hydrophobic interaction with cystathionine	**Glu333** (100%)	-H-bond with distal amino of cystathionine
Ser339 (100%)	- H-bond with sulfur atom of cystathionine - H-bond with ε-amino of Lys210	Ser334 (100%)	- H-bond with ε-amino of Lys203
Arg372 (100%)	- Salt bridge with α-carboxylate of cystathionine	Arg369 (100%)	- Salt bridge with α-carboxylate of cystathionine

[a]Values in parentheses are degree of conservation among proteobacterial CBL or fungal and mammalian CGL protein sequences (nc = nonconserved).

[b]Interactions involved in substrate binding and catalysis, predicted on the basis of crystal structures of yCGL, eCBL and the eCBL-AVG complex (Clausen *et al.*, 1996; Clausen *et al.*, 1997b; Messerschmidt *et al.*, 2003).

Figure 7. Predicted binding mode of L-Cth in the active site of eCBL (Clausen *et al.*, 1996). The key active site residues proposed to be involved in substrate binding and catalysis are shown in the (**A**) schematic, (**B**) stick and cartoon and (**C**) surface views. Residues are colored for ease of visualization (**B** and **C**): basic (blue), acidic (magenta), polar (pink), aldimine of PLP cofactor with Lys210 (yellow), aromatic (green) and Phe55 (cyan) and Tyr338 (cyan). Dashed lines represent proposed H-bonding and salt bridge interactions (Clausen *et al.*, 1996; Clausen *et al.*, 1997b).

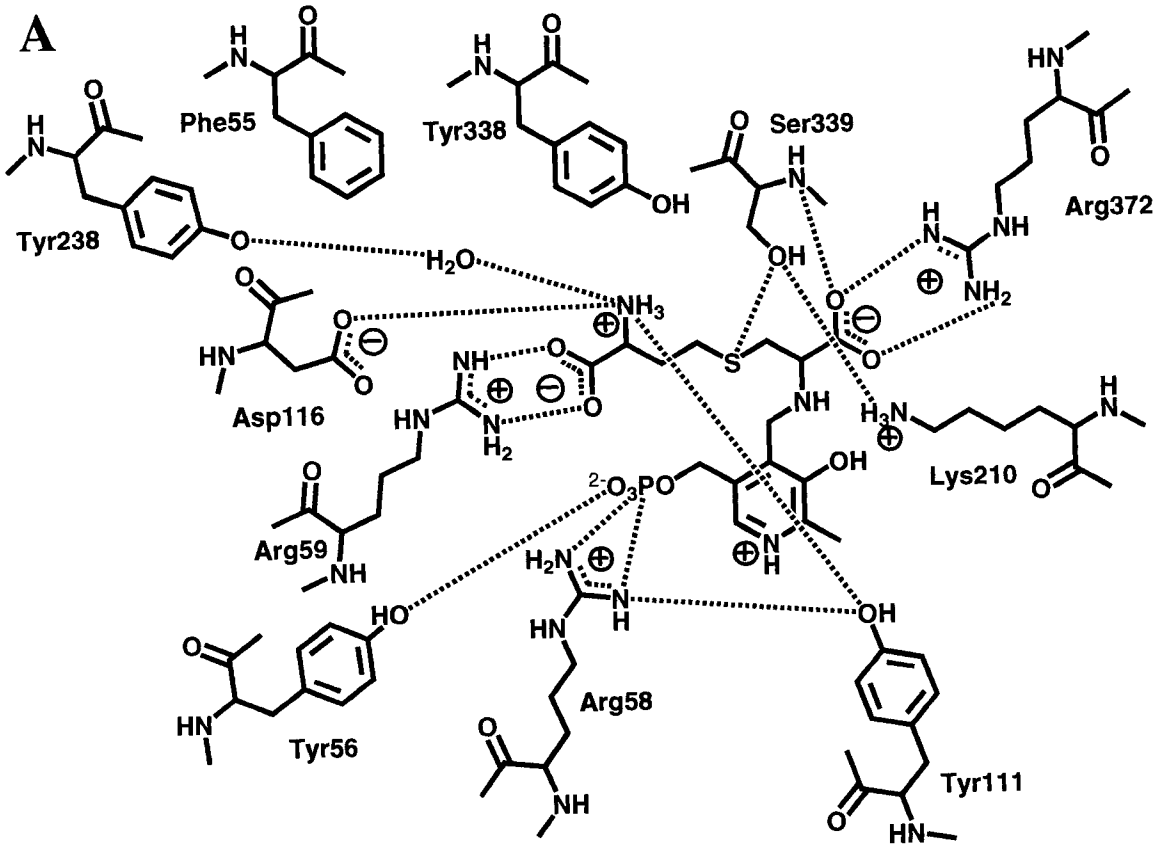

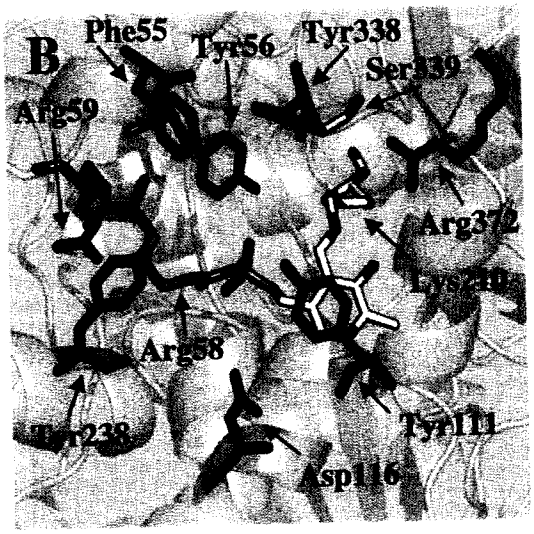

Figure 8. Predicted binding mode of L-Cth in the active site of yCGL (Messerschmidt *et al.*, 2003). The key active site residues proposed to be involved in substrate binding and catalysis are shown in the (**A**) schematic, (**B**) stick and cartoon and (**C**) surface views. Residues are colored for ease of visualization (**B** and **C**): basic (blue), acidic (magenta), polar (pink), aldimine of PLP cofactor with Lys203 (yellow), aromatic (green) and Glu48 (cyan) and Glu333 (cyan). Dashed lines represent proposed H-bonding and salt bridge interactions (Messerschmidt *et al.*, 2003).

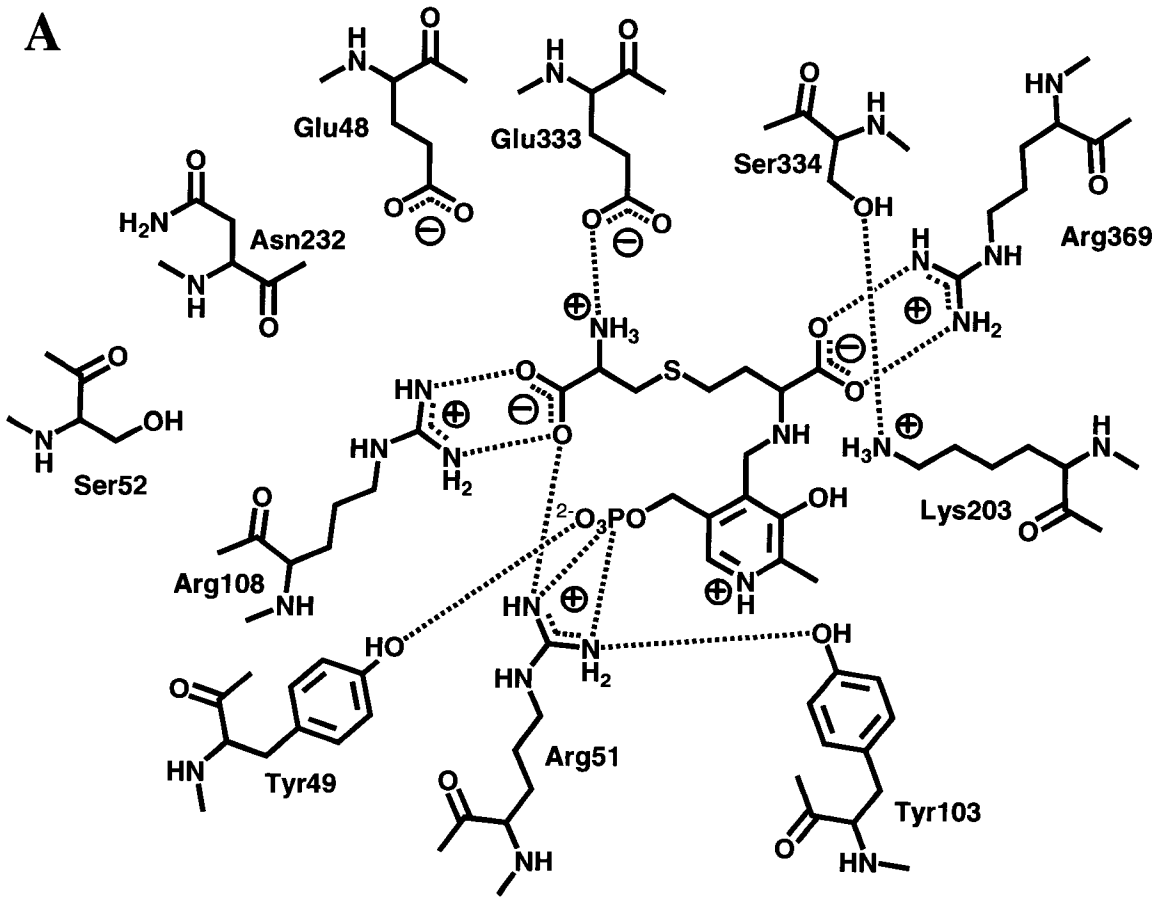

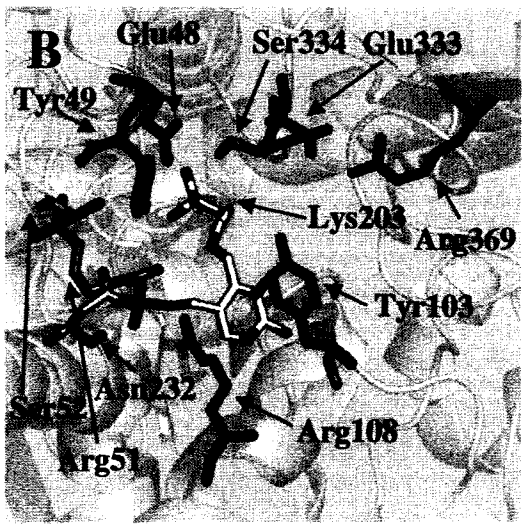

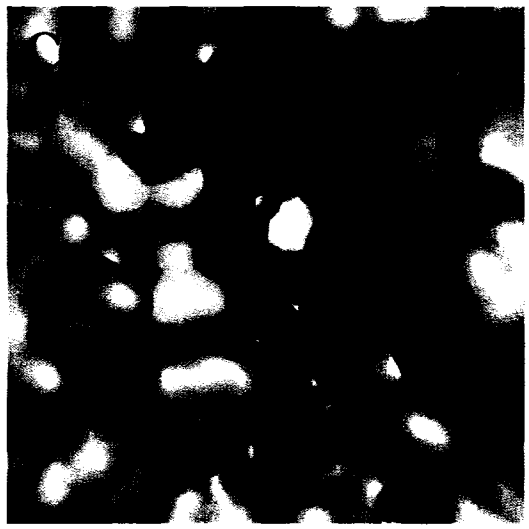

Figure 9. The active site of eCBL in the (**A**) absence and (**B**) presence of the inhibitor L-aminoethoxyvinylglycine (Clausen *et al.*, 1996; Clausen *et al.*, 1997b). In the (**A**) unliganded form of the enzyme, the PLP (yellow) is bound to Lys210 (orange) while in the (**B**) inhibitor complex, the PLP cofactor (yellow) is connected *via* an aldimine linkage to AVG (yellow) and Lys210 is shown in orange.

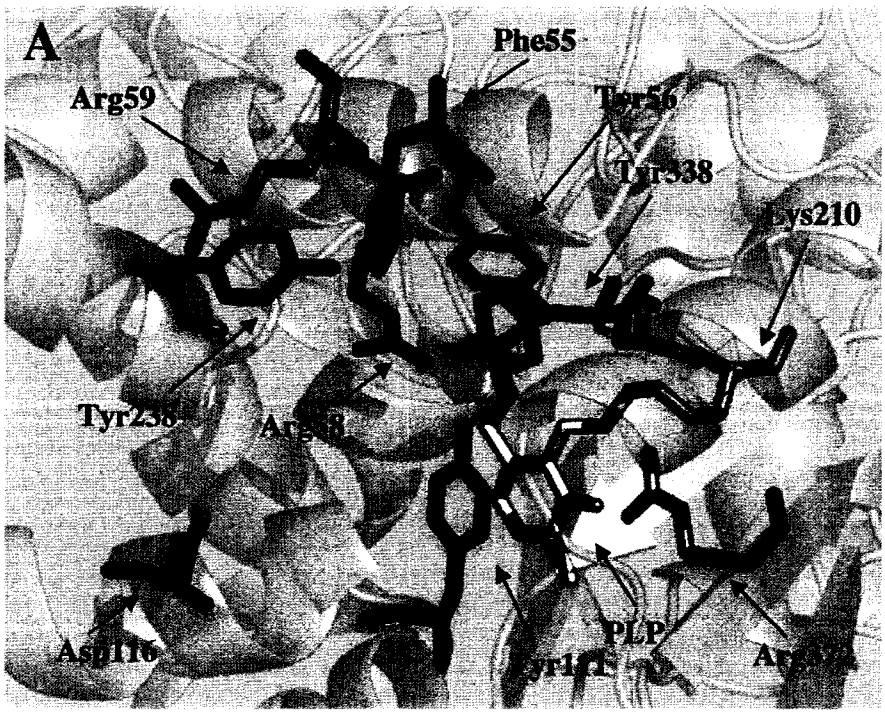

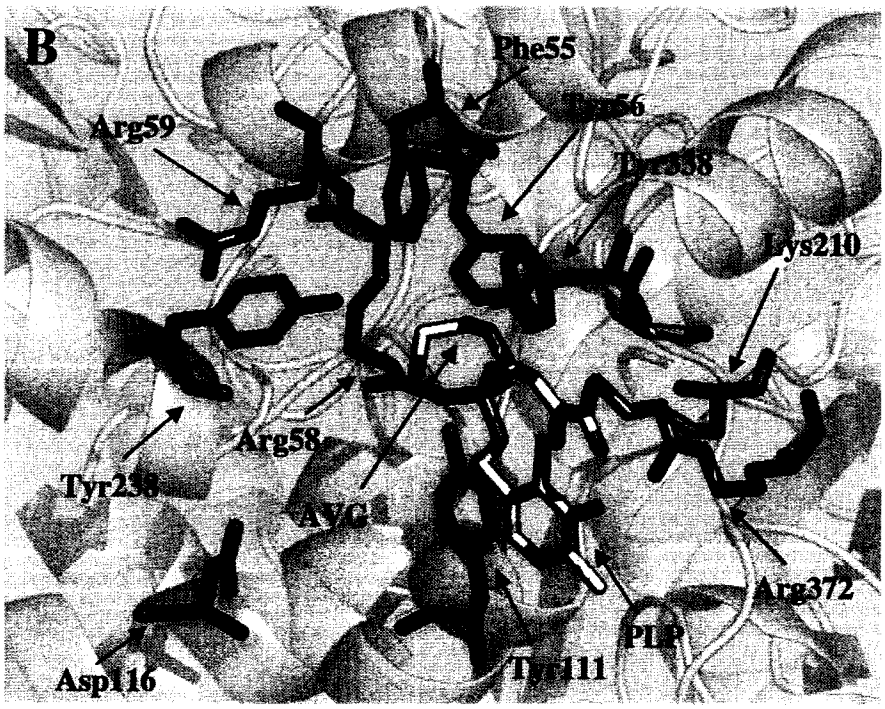

8.6. Hypothesis

The goal of my M.Sc. project was to investigate the role of a pair of active-site residues, in catalysis and substrate binding and as determinants of reaction specificity, in *E. coli* cystathionine β-lyase (eCBL) and yeast cystathionine γ-lyase (yCGL), PLP-dependent enzymes with distinct mechanisms but very similar active-site and overall structures. The pseudo-symmetric compound L-cystathionine is the substrate for the β-elimination and γ-elimination reactions catalyzed by eCBL and yCGL, respectively. Based on the crystal structures of eCBL, the eCBL-aminoethoxyvinylglycine complex and yCGL (Clausen *et al.*, 1996; Clausen *et al.*, 1997b; Messerschmidt *et al.*, 2003), I hypothesized that active-site residues Phe55 and Tyr338 of eCBL, and the corresponding residues Glu48 and Glu333 of yCGL, play an important role as determinants of productive substrate binding and reaction specificity in these enzymes.

9. Methods

9.1. Construction of *E. coli metB::aadA* gene replacement strain

Contamination with wild-type host enzymes is a concern when employing recombinant expression to produce enzymes for kinetic characterization, particularly when expressing site-directed mutants of enzymes found in the host species (*i.e.* recombinant expression of site-directed mutants of an *E. coli* enzyme in *E. coli*). This problem can be circumvented by the use of a mutant, knockout or gene replacement strain that lacks the ability to produce the wild-type enzyme. Although there are many commercially-available mutant strains of *E. coli*, most have not been thoroughly characterized. Additionally, the possibility of reversion to the wild-type genotype exists for insertions and point mutants. Another disadvantage of commercial strains is that the genetic background may not be well suited to the application. Therefore, a more rigorous approach is to engineer a knockout or gene replacement in a strain in an appropriate genetic background. Gene replacement was selected for this study as it offers the advantage of providing a selectable marker for the engineered strain, *via* replacement of the target gene with one encoding resistance to a specific antibiotic. A method involving homologous recombination between the *E. coli* chromosome and a plasmid (pKO3-*metB*/*aadA*) was employed to replace the *metB* gene, encoding CGS, with the aminoglycoside adenyltransferase (*aadA*) gene, affording spectinomycin and streptomycin resistance (Link *et al.*, 1997). The pKO3 plasmid contains a temperature-sensitive origin of replication (*RepA*), the chloramphenicol acetyltransferase (*Cat*) gene and the *Bacillus subtilis sacB* gene, encoding levansucrase. It was modified by inserting

the *aadA* gene, flanked by regions of the *E. coli* chromosomal bordering the *metB* gene, to produce the pKO3-*metB*/*aadA* plasmid (Figure 10).

The gene replacement procedure involves integration of the pKO3-*metB*/*aadA* plasmid, in its entirety, into the *E. coli* chromosome by homologous recombination. The temperature-sensitive origin of replication enables selection of cells, in which integration of the plasmid has occurred, by growth at 43°C, a non-permissive temperature for plasmid replication. The integrated plasmid is subsequently excised from the chromosome, substituting the targeted gene, *metB*, for another, in this case the *aadA* gene (Figure 10).

The first step in the construction of the pKO3-*metB*/*aadA* gene replacement plasmid was amplification of the 5' and 3' flanking regions of the *metB* gene from the *E. coli* chromosome. Genomic DNA of wild-type *E. coli,* strain JM103 (American Type Culture Collection) was prepared from 300 µL of an overnight culture, grown in Luria broth (LB) media. Cells were centrifuged for 2 minutes at 12000 rpm followed by resuspension in 300 µL of autoclaved dH_2O. This step was repeated twice prior to incubation at 95°C for 3 minutes to lyse cells. Lysates were placed on ice for immediate use or stored at -20°C.

Figure 10. Overview of the gene replacement method (Link *et al.*, 1997). The pKO3-*metB*/*aadA* plasmid is transformed into *E. coli* and then plated at 43°C, which is a non-permissive temperature for the pKO3 *RepA* origin of replication, thereby selecting for cells in which the plasmid has integrated into the chromosome. Subsequent growth in the presence of sucrose provides a selective advantage to those cells that have excised and lost the plasmid, which contains the *SacB* gene, encoding levansucrase. The plasmid may be excised from the chromosome by recombination within the same flanking region (crossover point 1) in which the insertional recombination event occurred, regenerating the original plasmid, or within the other flanking region (crossover point 2), resulting in replacement of the *metB* gene with the *aadA* gene in the *E. coli* chromosome.

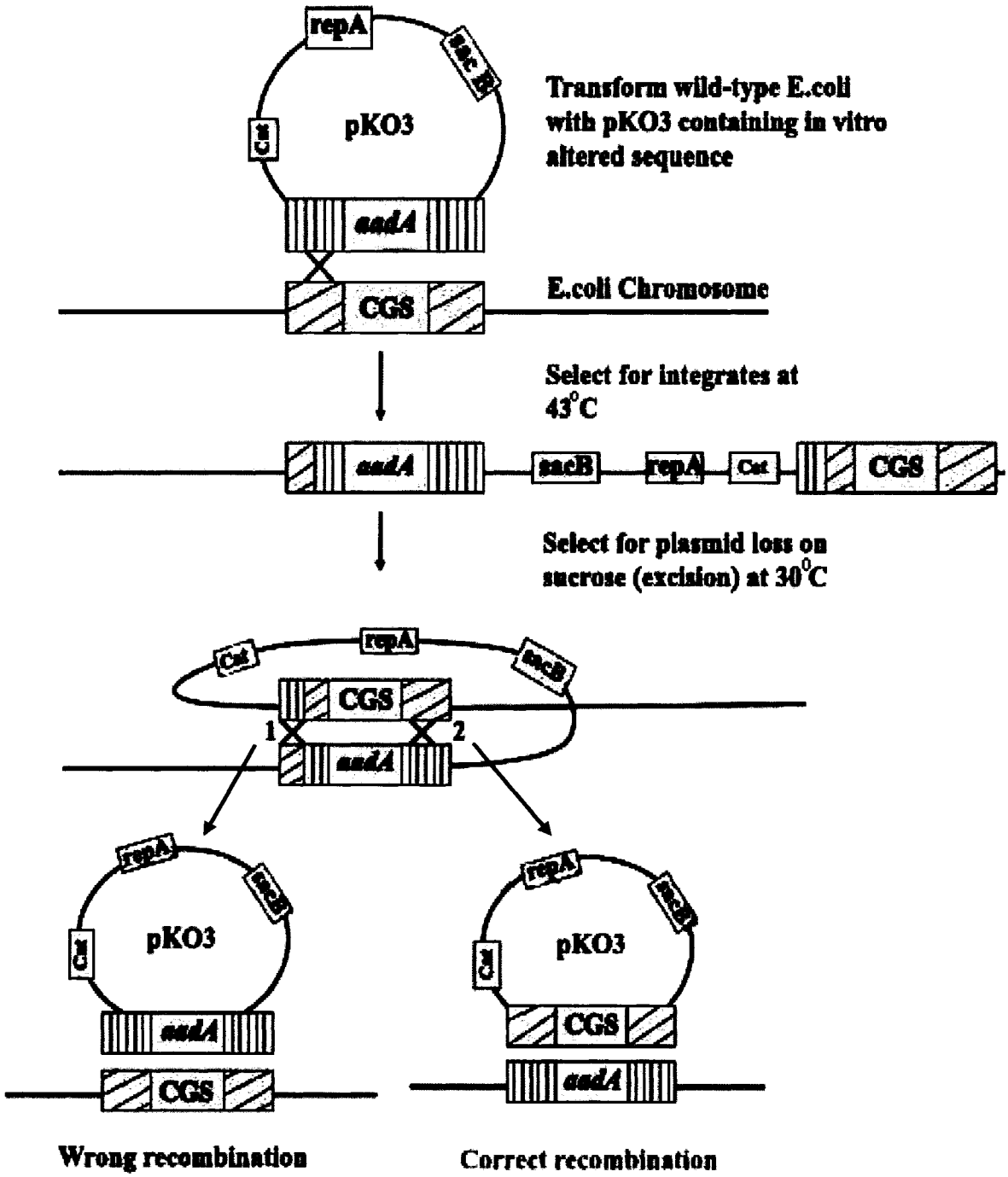

Oligonucleotide primers were designed to amplify ~700 bp segments of the 5' (primers N_o and N_i) and 3' (primers C_o and C_i) *E. coli* chromosomal regions bordering the *metB* gene (Table 2). The N_o and C_o primers have an internal *BamH*I site and the N_i and C_i primers have a complementary 21-base tail, designed to allow overlap extension to merge the amplified N_o-N_i and C_i-C_o regions, that incorporates a *Pst*I site. These two restriction endonuclease sites were selected because there is a unique *BamH*I site in pKO3, within the multiple cloning site, but no *Pst*I site, and there are no *BamH*I or *Pst*I sites in either the amplified *metB* flanking regions or the *aadA* gene. The ~700 bp chromosomal regions flanking the *E. coli metB* gene were amplified by polymerase chain reaction (PCR). Each PCR reaction (30 cycles of: 95°C for 1 min; 65°C for 2 min; 72°C for 2 min) consisted of 10 µL of the cell lysate, 0.2 mM dNTPs, 1 mM $MgCl_2$, 0.2 µM of each primer, taq polymerase, and 5% glycerol in a final volume of 100 µL. Amplified products were subjected to agarose (1.0%, w/v; Fisher Scientific) gel electrophoresis and were excised and purified using the GFX gel extraction kit (Amersham Biosciences). The N_o-N_i and C_i-C_o amplification products, corresponding to the 5' and 3' *metB* flanking regions, respectively, were subsequently annealed at the 21-bp overlapping region and amplified by PCR using the N_o and C_o primers (Figure 11). The resulting N_o-N_i/C_i-C_o fusion product and the pKO3 plasmid were digested with *BamH*I (New England BioLabs). The plasmid was subsequently treated with Antarctic phosphatase (New England BioLabs) to remove the 5'-phosphate group, thereby preventing self-ligation of the vector. The digested PCR and pKO3 fragments were gel purified, ligated with T4 DNA ligase (New England BioLabs) and transformed into *E. coli* strain DH10B *via* the heat shock method (Mandel, 1970).

Table 2. Primers employed in the construction and verification of the *E. coli metB::aadA* gene replacement strain.

Primer	**Sequence**	**Tm (°C)**
N_o	5'-cgcggatccgctcgttgtttatgccggatg	67.2
N_i	5'-ttgcccctgcagtaaacttaagacatctaaacttctttgc	63.4
C_o	5'-cgcggatccctccagatggttacgcgagaaacac	67.9
C_i	5'-ttaagtttactgcaggggcaagggctgcaaacaaggggta	68.8
CGS-F	5'-gggtactgaccgtaaacccgcatagttta	61.3
CGS-Fc	5'-ggaacttcatcccatggcgcgtaaacagg	64.5
CGS-seqBf	5'-tttttgaaacctggcgatctgctggttgcg	64.7
CGS-seqCf	5'-gtggccggcgtggtgattgctaaagacccg	68.9
CGS-R	5'-caccgatttgtgtcgcggaatagtcggaac	63.8
CGS-Rc	5'-ccttgttgattaggtaccgcagacatcagacgt	63.6
Spec-F(+P)	5'-cgaaaaactgcagcgctcgttcgccagcc	68.4
Spec-F	5'-cgaaaaactgcagatgagggaagcggtg	63.2
Spec-R	5'-cgaaaaactgcagttatttgccgactacctt	60.8

Figure 11. Procedure for construction of the pKO3-*metB*fl plasmid (Link *et al.*, 1997). The location of the N_o/N_i and C_o/C_i primers used to amplify the 5' and 3' *E. coli* chromosomal segments, respectively, flanking the *metB* gene are shown. The N_i and C_i primers contain a complementary 21-nucleotide segment, including a unique *Pst*I site, at their 5' ends, enabling fusion of the 5' and 3' flanking regions by overlap-extension PCR. The N_o and C_o primers incorporate a *BamH*I site at their 5' ends to allow insertion of the fusion product at the unique *BamH*I site of the pKO3 plasmid, to produce the pKO3-*metB*fl construct.

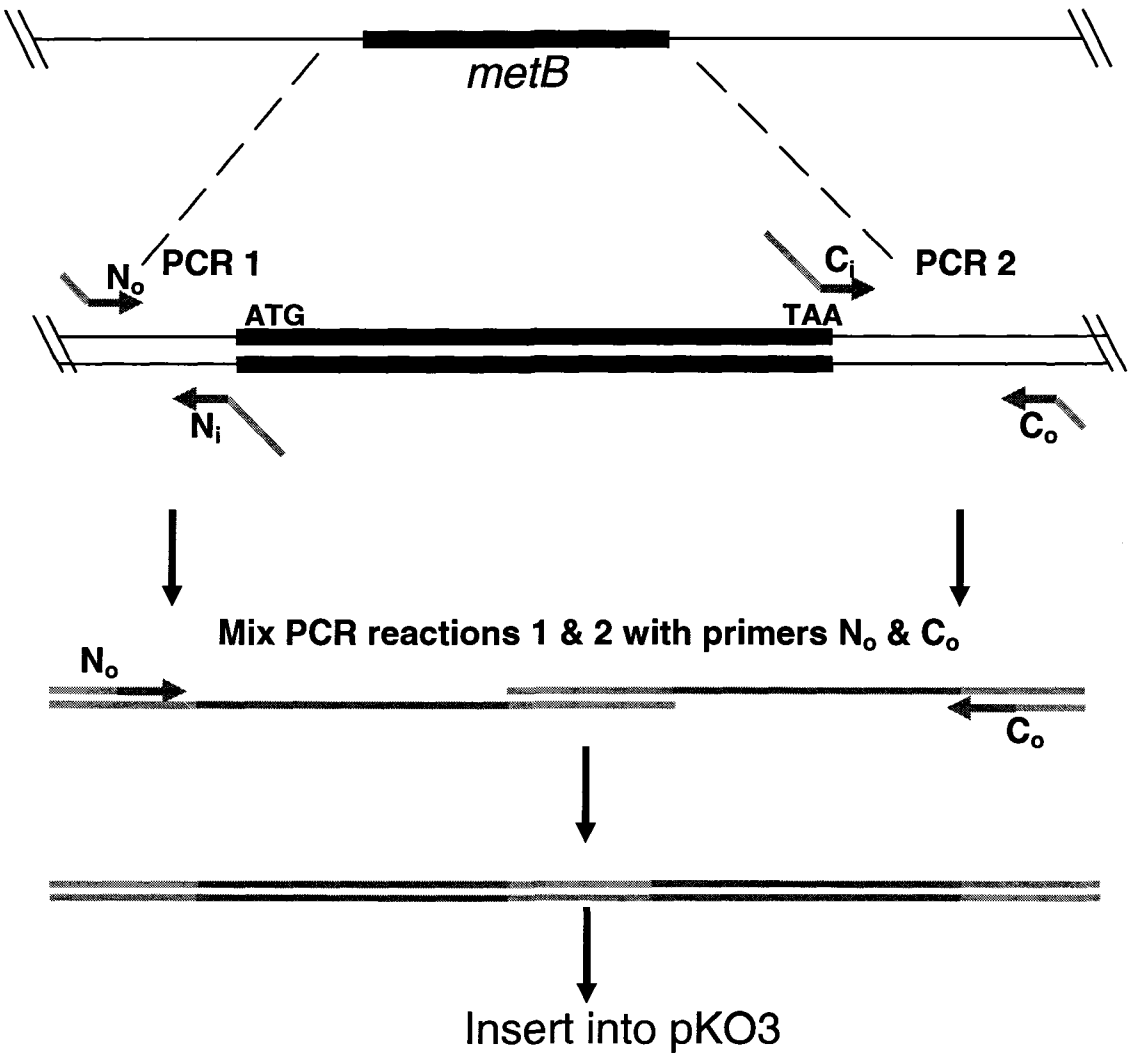

Transformants were plated on LB agar plates containing 100 μg/mL chloramphenicol (Chlor) and incubated overnight at 30°C. A colony containing the fused *metB* flanking regions in the pKO3 vector (pKO3-*metB*fl) was identified and plasmid DNA was isolated (Promega midiprep kit, Fisher Scientific).

The selectable marker chosen for gene replacement was the *aadA* gene, which confers spectinomycin (Spec) resistance. It is important not to use Chlor or ampicillin (Amp) for the gene replacement because the pKO3 plasmid, used for this procedure, carries the *Cat* gene, encoding Chlor resistance, and many expression plasmids use the β-lactamase gene, which confers Amp resistance, as a selectable marker. The PNN602S plasmid was used as the source for amplification of the *aadA* gene alone or with its promoter (Ma *et al.*, 1996) *via* PCR using the Spec-F and Spec-F(+P) primers, respectively, with the Spec-R primer (Table 2). The amplified fragments were digested with *Pst*I and inserted into the pKO3-*metB*fl construct at the unique *Pst*I site. Following transformation, colonies were screened for growth on 50 μg/mL spectinomycin (Spec). Growth was observed only for the construct with the *aadA* gene and promoter, therefore it was selected for use in the gene replacement procedure. Plasmid DNA was isolated from five colonies (Promega miniprep kit, Fisher Scientific) and screened, *via* digestion with *BstE*II, to verify the correct ligation. *BstE*II restriction endonuclease was chosen because the *aadA* gene and the pKO3-*metB*fl plasmid both contain a *BstE*II restriction site.

E. coli strain KS1000 (F', lac^q, lac^+, pro^+/ara $\Delta(lac\text{-}pro)$, $\Delta(tsp)= \Delta(prc)::$ Kan^R, $eda51::Tn10(Tet^R)$, $gyrA(Nal^R)$, *rpoB*, *thi-1*, *argI(am)*) (New England BioLabs) was

selected for the gene replacement because the lack of a periplasmic protease (*tsp*) in this strain will facilitate purification of overexpressed proteins. KS1000 cells were transformed with the pKO3-*metB*::*aadA* plasmid and plated on LB agar containing 50 μg/mL each of Chlor, Spec and kanamycin (Kan), which are the pKO3 selectable marker, the replacement gene for *metB* and the KS1000 selectable marker, respectively. Cells from a selection of colonies were selected, resuspended together in 100 μL of LB, serially diluted and plated in duplicate on LB agar plates containing 50 μg/mL each of Chlor, Spec and Kan (Figure 12). All plates were incubated overnight, with one set at 30°C and the duplicate set at 43°C. The pKO3 plasmid contains a temperature-sensitive origin of replication, such that the plasmid cannot replicate at 43°C. Therefore, colonies able to grow at this temperature have undergone a recombination event, incorporating the plasmid into the chromosome (Link *et al.*, 1997). Five-to-ten colonies were selected from the 43°C plates, resuspended in 100 μL of LB, serially diluted and plated in duplicate on LB agar plates. One set of plates, containing 5% sucrose, and 50 μg/mL each of Spec and Kan, was incubated at 30°C, while the other set, containing 50 μg/mL each of Spec, Kan and Chlor, was incubated at 43°C. The pKO3 plasmid contains the *sacB* gene, encoding the levansucrase gene, that produces a product toxic to *E. coli* cells grown in the presence of sucrose. Therefore, only cells which had excised the plasmid from their genomic DNA in the correct manner and eliminated the plasmid from the cell would have replaced the *metB* gene with the *aadA* gene (Figure 12) and, therefore, be able to grow in the presence of both sucrose and Spec. The excision frequency is the ratio of colonies observed on the 30°C plates containing sucrose, Spec and Kan *versus* those grown at 43°C on plates containing Spec, Kan and Chlor. Colonies from the 30°C, sucrose-containing plates were

replica-plated on LB agar, containing 50 μg/mL each Spec and Kan, of which only one set of plates also contained 50 μg/mL Chlor. The plates were incubated overnight at 30°C. The KS1000 *ΔmetB::aadA* cells are sensitive to Chlor, the selectable marker of the pKO3 plasmid, but resistant to Spec, the *metB* gene replacement selectable marker. In contrast, false positives, such as those colonies in which the *SacB* gene or its promoter have been mutated, maintain the pKO3 plasmid and are resistant to Chlor. The single colony that grew in the presence of 50 μg/mL each of Kan and Spec, but for which no growth was observed in the presence of 50 μg/mL Chlor was selected. The *metB::aadA* gene replacement was confirmed by PCR, using combinations of primers flanking the targeted *metB* open reading frame in the *E. coli* chromosome, within the *aadA* gene and within the *metB* gene (Table 2).

Figure 12. Schematic representation of the gene replacement procedure.

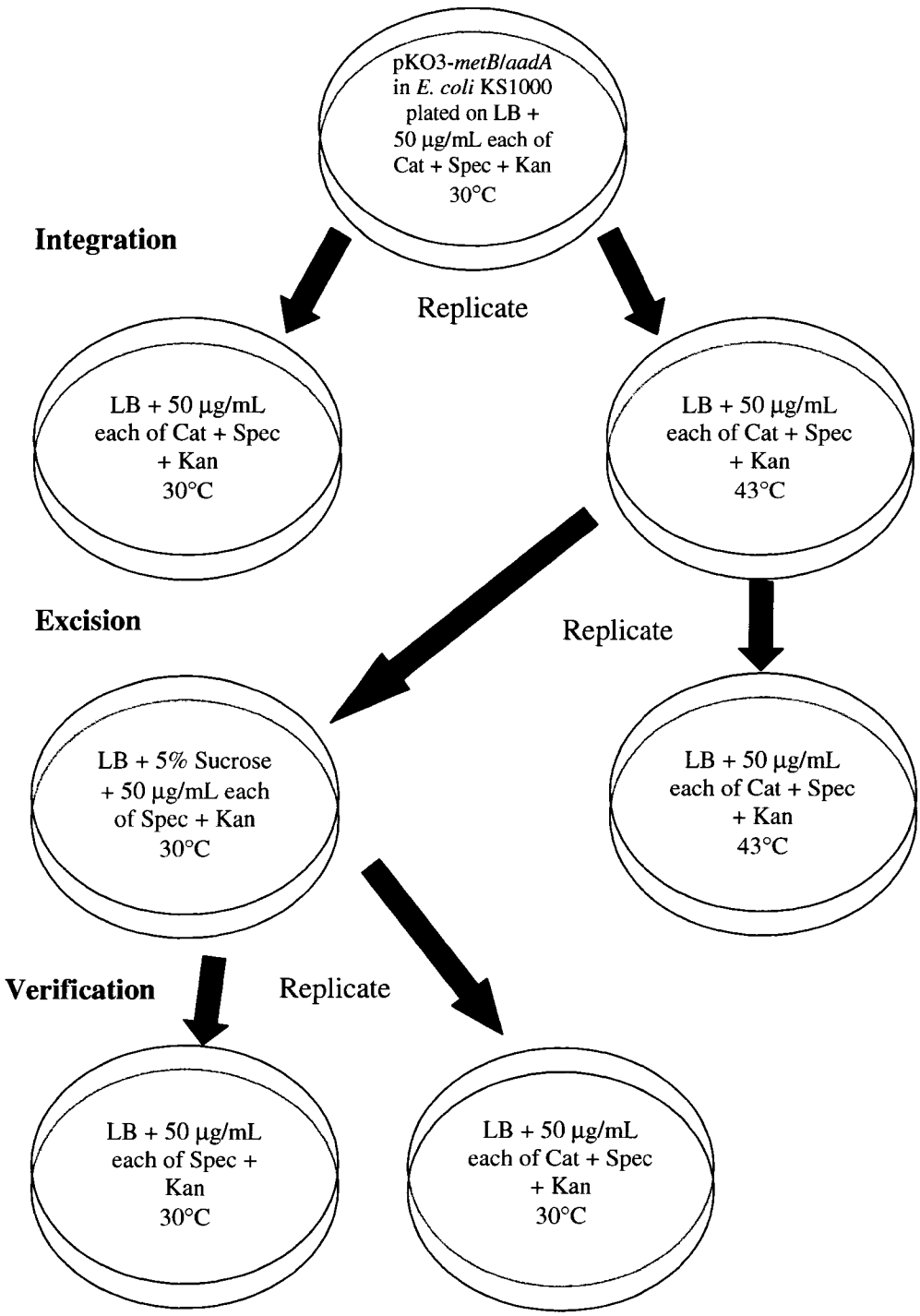

9.2. Verification and complementation of KS1000 Δ*metB::aadA* strain

The methionine auxotrophy of the KS1000 Δ*metB*::*aadA* strain was verified by analysis of the ability of cells to grow on minimal media. Both KS1000 and the KS1000 Δ*metB*::*aadA* strains were grown on M9 minimal media (20% dextrose, M9 salts, 1mM $MgSO_4$ and 1mg/mL thiamine) containing 150 μg/mL arginine (L-Arg) and 50 μg/mL Kan in the presence and absence of 75 μg/mL L-Met. The *E. coli* KS1000 strain is auxotrophic for L-Arg (*argI*) and is therefore, unable to grow in the absence of exogenously-supplied L-Arg. The ability of the genes encoding eCGS, yCGL and eCBL to complement the methionine auxotrophy of the KS1000 Δ*metB*::*aadA* strain was tested by transformation with the pTrc-99a plasmid, in which genes are under the control of the isopropyl-β-*D*-thiogalactopyranoside (IPTG)-inducible *trc* promoter. Cells were replica plated in triplicate on agar plates containing M9 minimal media, and 50 μg/mL each of Spec and Amp, the selectable markers of the KS1000 Δ*metB*::*aadA* strain and the pTrc-99a plasmid, respectively, either alone or in the presence of 1 mM IPTG or 75 μg/mL L-Met. Growth on the M9 and M9+IPTG plates was subsequently compared to the L-Met-containing control plates.

9.3. Introduction of C-terminal 6-His tag

Pairs of oligonucleotide primers were designed for amplification of the wild-type genes encoding eCBL and yCGL, from the pTrc-99a expression vector, with the

concomitant addition of a C-terminal 6-His tag. The 5' primers, CBL-Fc-NdeI and CGL–Fc-NdeI, incorporate a *Nde*I restriction endonuclease site, situated at the start codon. The 3' primers, CBL-Rc-His-XmaI and CGL-Rc-His-XmaI, include a 6-His tag, stop codon and a *Xma*I site (Table 3). A modified version of the pTrc-99a vector (pTrc-99a2 - engineered by Quazi and Aitken) was selected for expression, as the *Nco*I site (CCATGG) of the multiple cloning site of this plasmid has been replaced with a *Nde*I site (CATATG). The eCBL and yCGL amplification products were digested with *Nde*I and *Xma*I, ligated into the corresponding sites of the pTrc-99a2 vector and transformed into *E. coli* strain KS1000 *ΔmetC::Cat* (constructed by Lodha, Pearce and Aitken), in which the gene encoding eCBL has been replaced by that encoding chloramphenicol acetyltransferase.

9.4. Engineering of the pTrc-99a3 expression vector

The pTrc-99a2 expression vector was modified to incorporate a 6-His tag and linker with a Factor Xa proteolytic cleavage site at the 5' end of the multiple cloning site, such that proteins expressed will have a protease-cleavable, N-terminal 6-His tag to facilitate purification. The affinity-tag-containing linker was constructed by designing top and bottom strand oligonucleotide primers that would produce the requisite *Nde*I sticky ends, on both the 5' and 3' ends, when annealed. The sequence of the pET-16b vector (Novagen) was employed for guidance in the design of the proteolytic cleavage site and linker sequence.

Table 3. Primers employed in the construction and verification of expression constructs and site-directed mutants of eCBL and yCGL and in modification of the pTrc-99a expression vector.

Primer	Sequence	Tm (°C)
CBL-Fc-NdeI	5'-ggaaacagcatatggcggacaaaaagc	60.8
CGL-Fc-NdeI	5'-ggaaacagcatatggcggacaaaaagc	60.8
CBL-Rc-His-XmaI	5'-tccccccgggttaatggtggtgatggtggtgtacaatccgcgcaaaaccggcgtcc	74.8
CGL-Rc-His-XmaI	5'-tccccccgggttaatggtggtgatggtggtggttggtggcttgtttcaaggcttgc	73.9
pSECseq0	5'- ggcgtcaggcagccatcggaagctg	67.8
pSECseq7r	5'-gcccgccaccctccgggccgttgcttcgc	76.2
NdeI-linker-ver	5'-catagcagcggccatatcg	56.0
pTrc-MetF	5'-cacacaggaaacagataatgcatcatcatc	57.9
pTrc-MetR	5'-gatgatgatgcattatctgtttcctgtgtg	57.9
CBL-F55Df	5'-cgccaatggagagttggattatggacggcgcgg	68.9
CBL-Y338Ef	5'-cagtttattcagcatggccgaatcgtggggcggg	68.8
CGL-E48Af	5'-ccctatcggtacttacgcgtactccagatctc	62.9
CGL-E48Df	5'-ccctatcggtacttacgattactccagatctc	59.9
CGL-E48Ff	5'-ccctatcggtacttacttctactccagatctc	59.6
CGL-E333Af	5'-ctgttcacattggccgcgtcccttggtgg	68.0
CGL-E333Yf	5'-ctgttcacattggcctattcccttggtgg	62.7

Top primer sequence (his-Xa-NdeI-top - his-tag underlined):

5'-TAGCCATCATCATCATCATCATAGCAGCGGCCATATCGAAGGTCGTCA-3'

Bottom primer sequence (his-Xa-NdeI-bottom – his-tag underlined):

5'-TATGACGACCTTCGATATGGCCGCTGCTATGATGATGATGATGATGGC-3'

The linker was prepared by incubating a mixture of 1 nmol of each oligonucleotide primer at 70°C for 5 minutes, to ensure full denaturation, followed by the addition of annealing buffer (to a final concentration of 100 mM Tris HCl, pH 7.5, 70 mM $MgCl_2$) and incubation at 70°C for a further 5 minutes prior to gradual cooling, over a period of one hour. The annealed linker (10 pmol) was ligated, using T4 DNA ligase, overnight at 4°C with 0.3 pmol (100 ng) of plasmid, which had been digested with *Nde*I and treated with Antarctic phosphatase, prior to transformation into *E. coli* strain DH10B *via* the heat shock method (Mandel, 1970). Transformants were plated on LB agar plates containing 100 μg/mL ampicillin and incubated at 30°C overnight. Following the isolation of plasmid DNA, the presence of the linker was confirmed by PCR with the NdeI-linker-ver, pSECseq0 and pSECseq7r primers (Table 3).

The *Nde*I site was selected for insertion of the linker because it is the first site in the multiple cloning site of the pTrc-99a2 plasmid and in order to preserve the *Nde*I site of the vector, which is ideal as the 5' insertion site for genes because it: (i) minimize the number of amino acids remaining at the N-terminus of expressed proteins following proteolytic cleavage of the linker by Factor Xa, (ii) ensures that gene inserts will be in-frame with the linker sequence and (iii) ensures that the amino acid residue in the second coding position of expressed proteins is unaltered (Figure 13). The 5' *Nde*I site of the linker was designed to have the appropriate 5' overhang to enable ligation of the linker,

but to produce a site (CATAGC) which would not be cleaved by *Nde*I (CATATG) following ligation, as this would result in loss of the linker sequence from the vector upon cleavage with *Nde*I. Destruction of the 5' *Nde*I site of the linker without alteration of its 5' overhang was accomplished by changing the sequence at the 5' end of the linker from TATG to TAGC. This resulted in the loss of the ATG start codon of the vector, requiring subsequent engineering, *via* whole plasmid PCR mutagenesis, to replace the translation initiation site without reintroducing the 5' *Nde*I restriction site. The PCR reaction comprised 100 ng of template DNA (pTrc-99a2 containing the linker), 0.2 mM dNTPs, 0.2 μM each of the pTrc-MetF and pTrc-MetR primers (Table 3), *pfu* polymerase, and *pfu* polymerase buffer (Stratagene), in a final volume of 100 μL. The resulting amplification product was purified (Qiaquick gel extraction kit, Qiagen), treated with 40 units of *Dpn*I restriction endonuclease (New England), to digest the methylated, template DNA, and transformed into *E. coli* strain DH10B. Transformed cells were plated on LB agar plates containing 100 μg/mL Amp and incubated overnight at 30°C. A well-isolated colony was selected and grown in 100 mL of LB media, containing 100 μg/mL Amp for purification of plasmid DNA (Promega midiprep kit, Fisher Scientific).

Figure 13. Flowchart of the construction of the pTrc-99a3 plasmid and insertion of the eCBL and yCGL wild-type genes and site-directed mutants. A N-terminal, 6-His tag with a linker, containing the Factor Xa proteolytic cleavage site, was inserted at the *Nde*I site of the pTrc-99a2 plasmid to enable Ni-nitrilotriacetate-mediated affinity purification as well as cleavage of the 6-His tag.

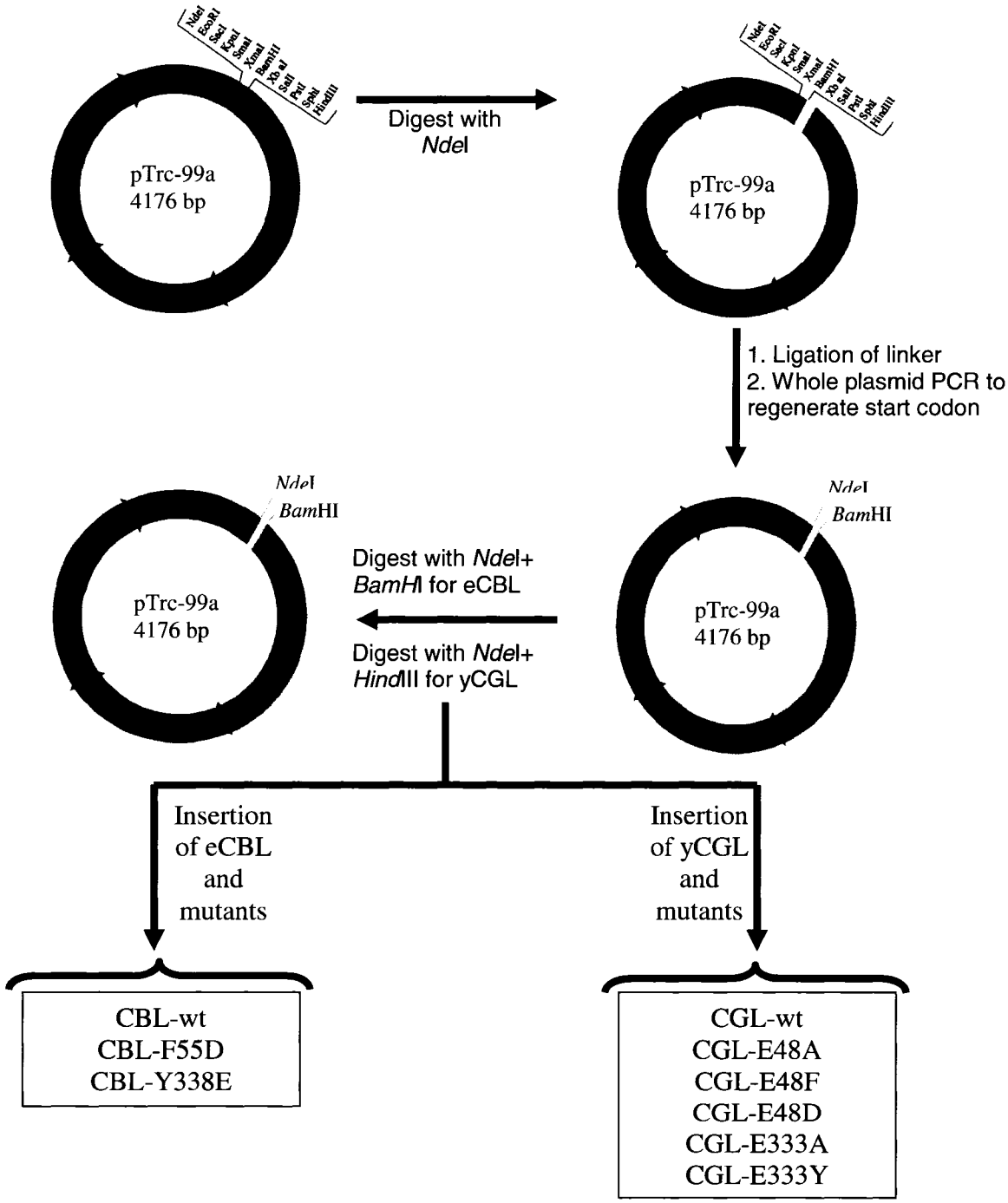

9.5. Site-directed mutagenesis and subcloning

Site-directed mutants were constructed by the overlap-extension method (Higuchi, 1990). The sequences of the mutagenic and flanking primers employed are presented in Table 3. The eCBL site-directed mutants and the yCGL Y333A and Y333E mutants were constructed previously by Susan Aitken. Dave Chitty assisted in the construction of the yCGL E48A, E48D and E48F mutants. The eCBL wild-type and site-directed mutant genes were amplified from the pTrc-99a expression vector with the CBL-Fc-NdeI and pSECseq7r primers. Similarly, the yCGL wild-type gene and site-directed mutants were amplified with the CGL-Fc-NdeI and pSECseq7r primers. The amplification products were gel purified (GFX kit, Amersham Biosciences) and digested with the appropriate restriction enzymes, *Nde*I and *BamH*I for eCBL and *Nde*I and *Hind*III for yCGL (Figure 13). The digested products were separated *via* agarose gel (1%, w/v) electrophoresis, gel extracted and purified (GFX kit, Amersham Biosciences). The plasmid was digested with the appropriate restriction endonucleases for insertion of the yCGL and eCBL genes and treated with Antarctic phosphatase (New England BioLabs) to remove the 5'-phosphate group, thereby preventing recircularization of the plasmid. The digested plasmids and inserts were then ligated with T4 DNA ligase (New England Biolabs) and transformed into *E. coli* strain DH10B (Amersham Biosciences). Transformants were plated and plasmid DNA was isolated, as described above, for each wild-type gene and mutant and transformed into *E. coli* strain KS1000 Δ*metC*::*Cat* for protein expression. Each insert was also sequenced (DNA Landmarks) using the

pSECseq0 and pSECseq7r primers, which are ~300 bp 5' and 3', respectively of the multiple cloning site of pTrc-99a3.

9.6. Purification of wild-type eCBL and yCGL

A 100-mL overnight culture of *E. coli* strain KS1000 Δ*metC*::*Cat* cells containing the yCGL or eCBL gene in the high copy expression plasmid pTrc-99a was grown in LB media (10 g/L tryptone, 5 g/L yeast extract and 10 g/L NaCl) containing 100 μg/mL ampicillin. The overnight culture was used to inoculate three litres of LB media (at a 1:50 ratio of inoculant to media), prewarmed to 32°C, in baffled, 2.8-L Fernbach flasks (1 L per flask). Cells were grown at 32°C in a shaking incubator (~300 rpm) until the OD_{600} reached 0.5. At this point IPTG was added to a final concentration of 0.1 mM and the cells were grown for additional 6-8 hours. The cells were harvested by centrifugation at 5000 rpm for 15 minutes at 4°C and the cell pellets were washed by resuspension in 100 mL of 0.85% NaCl followed by centrifugation at 5000 rpm for 15 minutes. Cell pellets were resuspended in 40 mL of buffer B (50 mM potassium phosphate, pH 7.8, 20 μM PLP) containing lysozyme (1 mg/mL; Sigma-Aldrich), DNase I (10 μg/mL; Roche) and one "EDTA-free" protease inhibitor tablet (Roche). The resuspended cells were incubated at room temperature for 30 minutes, to allow digestion of the cell wall and DNA by lysozyme and DNase I, respectively, before being further disrupted by sonication (8 cycles of 30 sec at 50% duty cycle). The cell lysate was centrifuged at 15000 rpm for 40 minutes at 4°C to remove cell debris. Following centrifugation of the cell lysate, ammonium sulfate was added to the supernatant to a final concentration of

30% saturation (at 4°C), the solution was stirred on ice for 20 min and centrifuged at 15000 rpm for 30 minutes at 4°C. The supernatant was loaded on a 50-mL butyl hydrophobic interaction column (Tosohaas), equilibrated with buffer B containing 30% ammonium sulfate. The column was subsequently washed with 10 column volumes of buffer B, containing 30% ammonium sulfate, and eluted with a 400-mL linear gradient of 30 – 0% ammonium sulfate in buffer B. Protein fractions (~8 mL) were tested for purity *via* sodium dodecyl sulfate polyacrylamide gel electrophoresis (SDS-PAGE) and then pooled, concentrated, and dialyzed against buffer B. The dialyzed protein was loaded on a 50-mL diethylaminoethyl (DEAE) anion exchange column (Pharmacia), equilibrated with buffer B, washed with 10 column volumes of buffer B, and eluted with a 400-mL linear gradient of 0 – 500 mM NaCl in buffer B. Protein fractions (~ 8 mL) were tested for purity *via* SDS-PAGE and then pooled, concentrated, and dialyzed against storage buffer (50 mM Tris, pH 7.8, 2 mM EDTA, 20 μM PLP). Glycerol was added to 20% (v/v) and samples were aliquoted and stored at -80°C. The protein concentration was determined by the Bradford method (BioRad), using bovine serum albumin (BSA) as a standard (Bradford, 1976).

9.7. Purification of 6-His-tagged eCBL and yCGL

Cells expressing the eCBL and yCGL genes, wild-type and site-directed mutants, bearing either a N-terminal or C-terminal 6-His tag were grown, harvested and lysed as described in the wild-type purification protocol, with the exception that buffer A (50 mM potassium phosphate, pH 7.8, 20 μM PLP, 10 mM imidazole) was employed in place of

buffer B. The supernatant was loaded on a ~10-mL Ni-nitrilo triacetic acid (Ni-NTA) column (Qiagen), equilibrated with buffer A. The column was subsequently washed with 10 column volumes of buffer A and the protein was eluted with a 200-mL linear gradient of 10-200 mM imidazole in buffer A. The protein fractions (~4 mL) were tested for purity *via* SDS-PAGE and those containing pure yCGL or eCBL enzyme were pooled, concentrated and dialyzed overnight in storage buffer. Glycerol was added to 20% (v/v) and samples were aliquoted and stored at -80°C. The protein concentration was determined by the Bradford method (BioRad), using bovine serum albumin (BSA) as a standard (Bradford, 1976).

9.8. Cleavage of the N-terminal linker

Factor-Xa cleaves after the arginine residue in its preferred cleavage site Ile-Glu-Gly-Arg, present in the linker sequence of proteins expressed from the engineered pTrc-99a3 expression vector, and 1 μg of Factor Xa is reported to cleave 50 μg of fusion protein to 95% completion within 6 hours at room temperature in 20 mM Tris-HCl, pH 8.0, containing 100 mM NaCl and 2 mM $CaCl_2$ (New England BioLabs). These conditions were employed to test the ability of Factor Xa protease to remove the affinity tag of the expressed eCBL and yCGL proteins.

9.9. Determination of steady-state kinetic parameters

The L-Cth lyase activity of the yCGL and eCBL enzymes was measured in a total volume of 1 mL with a MultiSpec-1501 (Shimadzu) spectrophotometer or in a total volume of 100 µL with a Spectramax 340 microtiter plate spectrophotometer (Molecular Devices). Enzyme activity was detected *via* the reaction of DTNB (5,5'-Dithiobis-(2-Nitrobenzoic Acid)) with the free thiol of the product, L-cysteine for the γ-elimination reaction and L-homocysteine for the β-elimination reaction, releasing the TNB thiolate ion that absorbs at 412 nm (Ellman, 1959; Yamagata *et al.*, 1993; Aitken *et al.*, 2003). Samples were equilibrated at 25°C and a background reading was recorded before initiation of the reaction by the addition of enzyme. All enzyme assays were carried out under the following conditions: 50 mM Tris (pH 8.0), 20 µM PLP, 2 mM DTNB, 0.15 – 20 mM L-Cth and 9.0×10^{-3} – 1.2 µM of enzyme. Data were fit to the Michaelis-Menten equation (equation 1) by nonlinear regression using the SAS software package (SAS Institute) to determine the kinetic parameters K_m and k_{cat} and to equation 2 to determine k_{cat}/K_m (Aitken and Kirsch, 2003).

$$\frac{v}{[E]} = \frac{k_{cat} \times [L-Cth]}{K_m + [L-Cth]} \qquad \text{(equation 1)}$$

$$\frac{v}{[E]} = \frac{k_{cat}/K_m \times [L-Cth]}{1 + [L-Cth]/K_m} \qquad \text{(equation 2)}$$

9.10. Product analysis *via* thin layer chromatography

The DTNB assay does not distinguish between cleavage of L-Cth *via* the CBL-catalyzed β-elimination reaction and the CGL-catalyzed γ-elimination reaction, which produce L-Hcys and L-Cys, respectively. Therefore, determination of the reaction specificity of these enzymes requires the development of a product analysis assay. Identification of the amino acid product of the CGL and CBL reactions *via* separation by thin layer chromatography (TLC) followed by derivatization to allow visualization was chosen as it is a quick procedure. Several spray reagents for the selective and non-selective detection of amino acids on TLC plates have been described, including ninhydrin, which is one of the most commonly employed (Mahler and Cordes, 1968; Laskar and Basak, 1988; Basak and Laskar, 1990). Amino acid standards (0.1 and 1 mg/mL) were prepared in 10 mM potassium phosphate buffer, pH 8.0. These solutions were spotted, 1 μL at a time, on chromatographic plates, comprised of a 0.1-mm thick layer of silica gel on an aluminum support (Sigma), and developed with a mobile phase of n-propanol/water (70:30, v/v), for a distance of 10 cm. TLC plates were subsequently dried, sprayed with a solution of 2.5 mg/mL ninhydrin in ethanol and dried, prior to heating for 15 min at 100°C (Basak and Laskar, 1990).

10. RESULTS

10.1. Construction of *metB*::*aadA* gene replacement plasmid

Approximately 700 bp of the 5' and 3' *E. coli* chromosomal segments bordering the *metB* gene were amplified with the N_o and N_i and the C_i and C_o primers (Table 2), respectively. The N_o-N_i and C_i-C_o fragments, which overlap by a 21-bp region containing a unique *Pst*I site, were fused by overlap-extension and amplified with N_o and C_o primers (Table 2), both of which contain a *BamH*I site. The resulting ~1400-bp N_o-N_i/C_i-C_o fusion product (Figure 14A) was subsequently inserted at the unique *BamH*I site of the pKO3 vector (Link *et al.*, 1997) to create the pKO3-*metB*fl construct.

The *aadA* gene, alone and in combination with a 441-bp region 5' of the gene, containing the promoter and ribosome binding site, was amplified from the pNN602 plasmid (Ma *et al.*, 1996) using the Spec-F and Spec-F(+P) primers, respectively, in combination with the Spec-R primer (Table 2), each of which contains a *Pst*I restriction site. Diagnostic agarose gel electrophoresis demonstrated that the resulting amplicons were of the predicted size: ~800 bp and ~1200 bp for the amplification of the *aadA* gene alone and in conjunction with the promoter region, respectively (Figure 14A). Both amplicons were inserted into the unique *Pst*I site of the pKO3-*metB*fl plasmid to create pKO3-*metB*::*aadA*(-p), which lacks the *aadA* promoter, and pKO3-*metB*::*aadA*, which comprises the *aadA* gene and its promoter region. The synthesis of both constructs was necessary as, although the pKO3-*metB*::*aadA* construct was expected to be optimal, the effect of combining the *metB* 5' flanking region and the *aadA* promoter, on the

expression of the *aadA* gene was unknown. Upon transformation of the pKO3-*metB*::*aadA*(-p) and pKO3-*metB*::*aadA* plasmids into *E. coli* strain DH10B, colonies were observed in the presence of 50 μg/mL Spec for cells containing the pKO3-*metB*::*aadA* plasmid, but not for cells containing the pKO3-*metB*::*aadA*(-p) plasmid, indicating that the *aadA* promoter and ribosome binding site are necessary for expression.

The restriction endonuclease *BstE*II was selected for restriction digestion analysis of the pKO3-*metB*::*aadA* plasmid because the *aadA* gene and the pKO3-*metB*fl plasmid (within the 3' *metB* flanking region) both contain a unique *BstE*II restriction site, thereby enabling both confirmation of insertion and determination of orientation. Digestion of the pKO3-*metB*::*aadA* plasmid with *BstE*II produced the expected ~1200-bp and ~6500-bp fragments and indicated that the *aadA* gene and promoter region were inserted in the same orientation in four of the five colonies (Lanes 1 and 3-5 of Figure 14B) and in the opposite orientation in only one (Lane 2 of Figure 14B). Although the effect of the orientation of the *aadA* gene in the final *E. coli ΔmetB::aadA* strain is unknown, it was predicted that maintenance of a common orientation, between the native *metB* and the *aadA* replacement gene would be an effective strategy. Therefore, the appropriate version (Lanes 1 and 3-5 of Figure 14B) of the pKO3-*metB*::*aadA* plasmid was selected, based on the diagnostic restriction digestions with *BstE*II, for use in the gene replacement procedure.

Figure 14. Verification of amplification products and correct ligation in the construction of the pKO3-*metB*::*aadA* gene replacement plasmid. (**A**) Agarose gel (1% w/v) of PCR amplification products from *E. coli* genomic DNA and the pNN602 plasmid. **Lane 1:** 1kb DNA ladder; **lane 2:** product of the overlap-extension reaction, combining the N_o-N_i and C_i-C_o fragments, corresponding to the 5' and 3' genomic regions flanking the *E. coli* *metB* gene, amplified with the N_o and C_o primers; **lane 3:** PCR amplicon of the *aadA* gene and a 441-bp 5' non-coding region, including the promoter region and ribosome binding site, amplified with the SpecR and SpecF+P primers; **lane 4:** PCR amplicon of the *aadA* gene alone amplified with the SpecR and SpecF primers. **B)** Screening, *via* diagnostic digestion with *BstE*II restriction endonuclease, of pKO3-*metB*::*aadA* plasmids isolated from five transformants (lanes 1 – 5). Lane 6: 1kb DNA ladder.

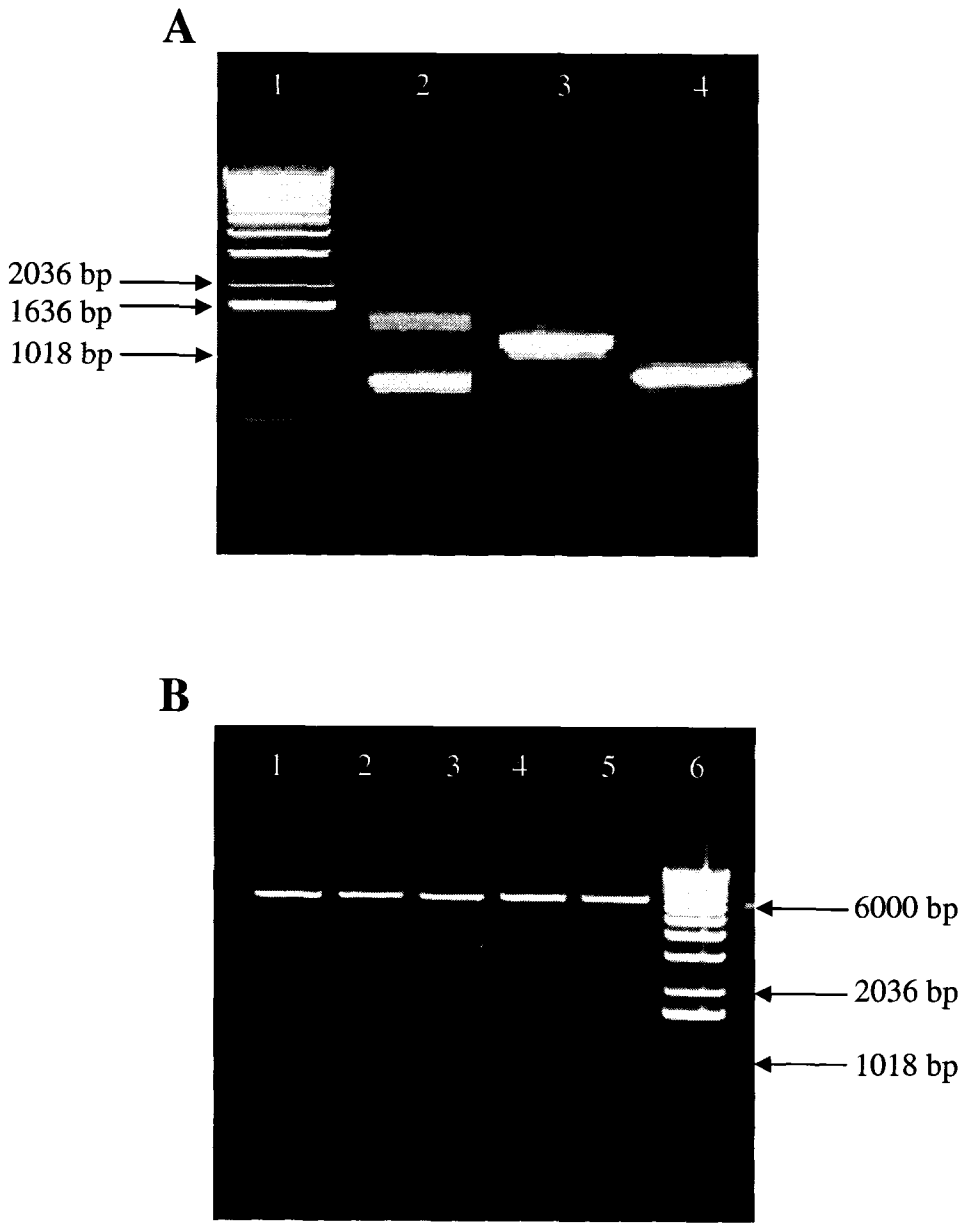

10.2. Construction of KS1000 Δ*metB*::*aadA* strain

The gene replacement strategy employed relies on the site-specific insertion into the *E. coli* genome and subsequent excision, of a plasmid containing the substitute gene, such as the selectable marker for Spec resistance, bordered by the flanking regions of the *E. coli* gene targeted for replacement (Link *et al.*, 1997). *E. coli* strain KS1000 was selected as the genetic background for creation of the Δ*metB*::*aadA* gene replacement strain because it lacks the periplasmic protease, thereby facilitating purification of homogeneous protein samples. The KS1000 strain was tested, prior to construction of the Δ*metB*::*aadA* gene replacement, to confirm that it does not have the ability to grow on Amp or Spec, the selectable markers of many expression vectors and of the Δ*metB*::*aadA* gene replacement, respectively, and that it is not a methionine auxotroph. The KS1000 strain is auxotrophic for arginine (Silber and Sauer, 1994); therefore requiring that M9 minimal media be supplemented with this amino acid.

KS1000 cells containing the pKO3-*metB*::*aadA* construct were replica plated at 30°C and 43°C on LB agar containing 50 μg/mL each of Chlor, Spec and Kan, the selectable markers of the pKO3 plasmid, the replacement gene and the KS1000 strain, respectively. Since the origin of replication of the pKO3 plasmid is temperature sensitive, only those cells in which recombination had occurred were able to grow at 43°C on the media containing Kan, Chlor and Spec. The ratio of colonies at 43°C compared to 30°C demonstrated that integration of the pKO3-*metB*::*aadA* plasmid into the *E. coli* genome occurred in less than 25% of cells. The subsequent selection of cells which have excised and lost the plasmid relies on the growth of cells on LB agar supplemented with 5%

sucrose, which is converted to levan, a toxic metabolite for *E. coli* cells, by levansucrase, encoded by the *SacB* gene (Lawes and Maloy, 1995). The recombination event, resulting in plasmid excision, may occur within either of the two *metB* flanking regions that border the *aadA* gene in the pKO3-*metB*::*aadA* construct (Figure 10). Gene replacement, whereby the *metB* gene in the *E. coli* genome is exchanged for the *aadA* gene, occurs only in cells that have excised the plasmid correctly. In order to distinguish between these two possibilities, colonies from the LB plates containing 5% sucrose were replica plated on LB agar plates containing 50 μg/mL each of Chlor, Spec and Kan and 50 μg/mL each of Spec and Kan only. Only one colony, of approximately 500 selected, did not display growth on the plate containing Chlor, suggesting that mutation of the *sacB* gene or its promoter is much more prevalent than excision of the plasmid from the *E. coli* genome.

10.3. Verification and complementation of the KS1000 Δ*metB::aadA* strain

The *metB*::*aadA* gene replacement was confirmed using PCR. The primers chosen for the diagnostic reactions were located in the regions flanking the locus corresponding to the *metB* gene, within *metB* gene, and within the *aadA* gene (Figure 15A and B). With the exception of one reaction, which was not predicted to yield an amplification product, fragments of the predicted size were observed (Figure 15C, Table 4). The reaction with primers 4 (CGSseq-Cf), and 10 (CGS-R), designed to anneal within the *metB* gene its 3' flanking region, respectively, produced an amplification product that was not expected (reaction 4, Table 4). This reaction product was not observed when the amplification was repeated with a higher annealing temperature (65°C *versus* 50°C), indicating it was likely an artifact resulting from mis-priming.

Figure 15. PCR-based verification of the *E. coli* KS1000 *metB*::*aadA* gene replacement strain. The targeted annealing location of the oligonucleotide primers employed to verify the *metB*::*aadA* gene replacement within the (**A**) wild-type *E. coli* KS1000 chromosome and (**B**) the KS1000 *metB*::*aadA* gene replacement strain are shown. (**C**) Agarose gel (1%, w/v) of PCR reactions (described in Table 4) designed to confirm gene replacement in the KS1000 Δ*metB*::*aadA* strain. **Lanes 1-5** and **7-10** correspond to PCR reactions 1-5 and 7-10 (Table 4), respectively; **lane 6:** 1kb DNA ladder.

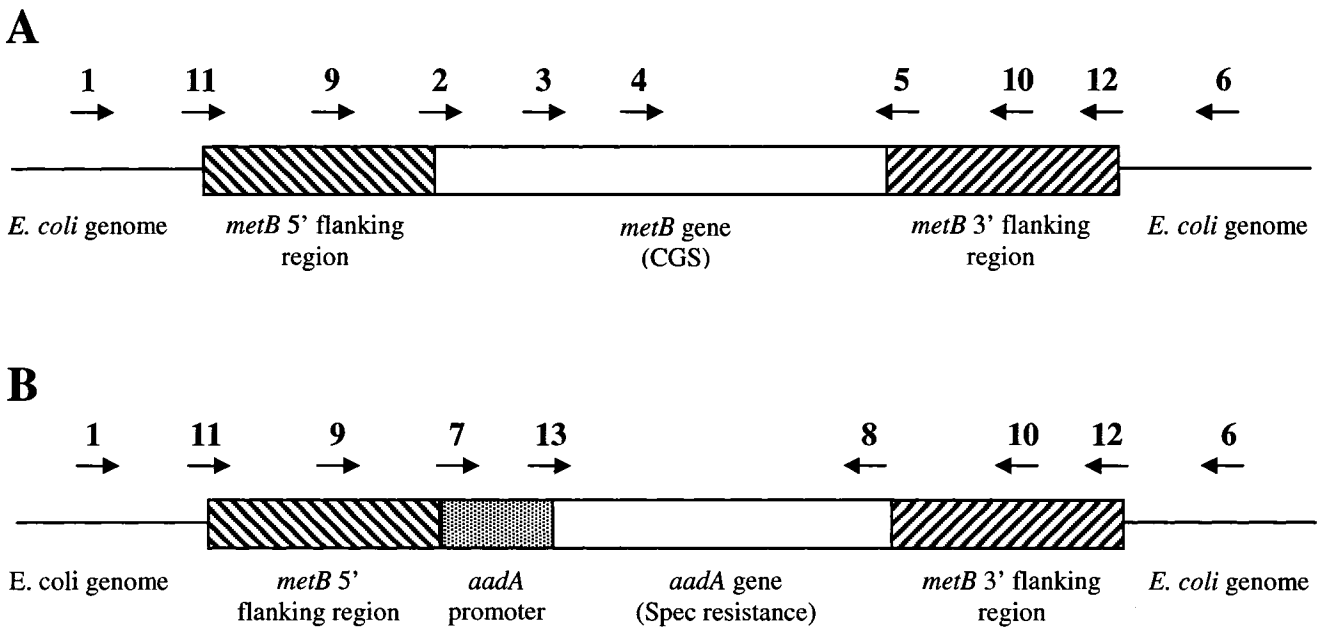

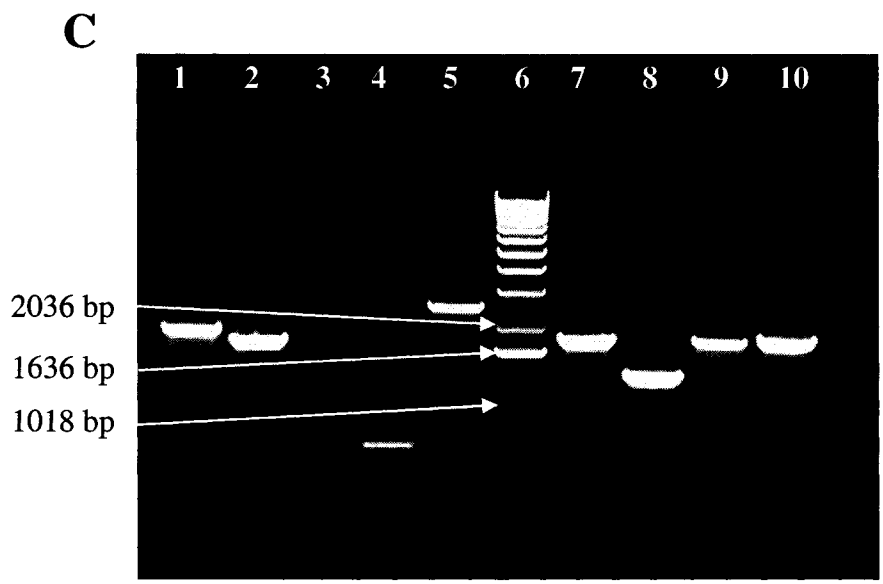

Table 4. List of PCR reactions used to verify the KS1000 Δ*metB*::*aadA* strain.[a]

[b]Reaction number	5' primer	3' primer	Expected amplicon (bp)	Observed amplicon (bp)
1	9 – CGS-F	10 - CGS-R	~2000	~2000
2	9 – CGS-F	5 – CGS-Rc	~1800	~1800
3	3-CGS-seqBf	10 - CGS-R	No band	No band
4	4-CGS-seqCf	10- CGS-R	No band	~700
5	11-CGS-No	12-CGS-Co	~2500	~2500
6	Corresponds to lane with 1 kb DNA ladder in Figure 15			
7	11-CGS-No	8-Spec-R	~1800	~1800
8	9 – CGS-F	8-Spec-R	~1300	~1300
9	7-Spec-F(+P)	10- CGS-R	~1900	~1900
10	7-Spec-F(+P	12-CGS-Co	~2000	~2000

[a]Annealing temperature of 50°C.
[b]Reaction numbers correspond to lane numbers in Figure 15C.

Mutation of the *metB* gene has been demonstrated to result in methionine auxotrophy in *E. coli* (Hacham *et al.*, 2002). Therefore, the Δ*metB*::*aadA* gene replacement strain was predicted to be unable to grow in the absence of exogenous methionine. To verify this, KS1000 Δ*metB*::*aadA* cells were plated on M9 minimal media in the presence and absence of methionine. Growth was observed in the presence of Spec, resistance to which is provided by the *aadA* gene, but only when the media was supplemented with both arginine, as the KS1000 parent strain is auxotrophic for arginine, and methionine (Figure 16A).

The KS1000 Δ*metB*::*aadA* strain was transformed with the pTrc-99a expression vector containing the genes encoding eCGS, eCBL and yCGL, under control of the IPTG-inducible *trc* promoter, as well as empty vector control, to determine the ability of these genes to complement the *metB* knockout. As expected, the pTrc-99a plasmid alone did not complement the methionine auxotrophy of KS1000 Δ*metB*::*aadA* (Figure 16B, plates 1 and 2). Similarly, the *E. coli metC* gene, encoding eCBL, did not enable growth of KS1000 Δ*metB*::*aadA* in the absence of exogenous methionine (Figure 16B, plates 5 and 6). The *metB* and *Cys3* genes, encoding eCGS and yCGL, respectively, did complement the methionine auxotrophy of KS1000 Δ*metB*::*aadA*. However, growth was observed only in the absence of IPTG in the case of *metB* (Figure 16B, plates 3 and 4) and, in contrast, only in the presence of IPTG for *Cys3* (Figure 16B, plates 7 and 8).

The F55D and Y338E mutants of eCBL and the E48A, E48D, E48F, E333A and E333Y mutants of yCGL, as well as the wild-type genes encoding eCGS, eCBL and yCGL, were tested for their ability to complement the methionine auxotrophy of the

KS1000 Δ*metB*::*aadA* and KS1000 Δ*metC*::*Cat* strains. Their growth on M9 minimal media and the effect of induction with 1mM IPTG is compared to growth on M9 minimal media supplemented with 75 μg/mL methionine in Tables 5 and 6. Only the wild-type yCGL gene and the yCGL-E48D site-directed mutant enabled KS1000 Δ*metB*::*aadA* cells to grow, in the presence of IPTG, which induces expression via the *trc* promoter of the vector (Table 5). The KS1000 Δ*metC*::*Cat* strain, which lacks the gene encoding eCBL, is complemented by only the wild-type and mutants of the *metC* gene, encoding eCBL, in the absence of IPTG. In the presence of IPTG, this strain is complemented by all but the wild-type *metB* gene, encoding eCGS, and the yCGL-E333Y site-directed mutant (Table 6).

Figure 16. Verification and complementation of the methionine auxotrophy of *E. coli* strain KS1000 Δ*metB*::*aadA*. (**A**) Growth of KS1000 Δ*metB*::*aadA* on (**plate 1**) M9 minimal media containing 100 μg/mL Spec and supplemented with (**plate 2**) 75 μg/mL methionine, (**plate 3**) 150 μg/mL arginine and (**plate 4**) both 75 μg/mL of methionine and 150 μg/mL arginine. (**B**) Complementation of KS1000 Δ*metB*::*aadA* with the pTrc-99a plasmid without gene insert, as empty vector control (**plates 1** and **2**), or containing the genes encoding eCGS (**plates 3** and **4**), eCBL (**plates 5** and **6**) and yCGL (**plates 7** and **8**), under the control of the IPTG-inducible *trc* promoter. Cells were grown on M9 minimal media containing 100 μg/mL Spec, 100 μg/mL Amp and 150 μg/mL arginine in the absence (**plates 1, 3, 5** and **7**) or presence (**plates 2, 4, 6** and **8**) of 1 mM IPTG.

A

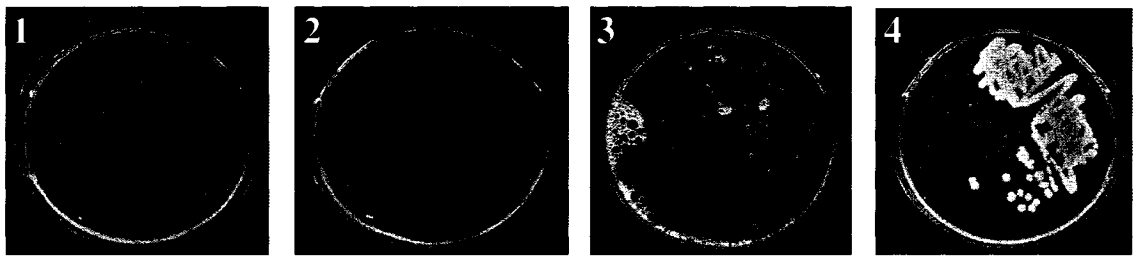

B

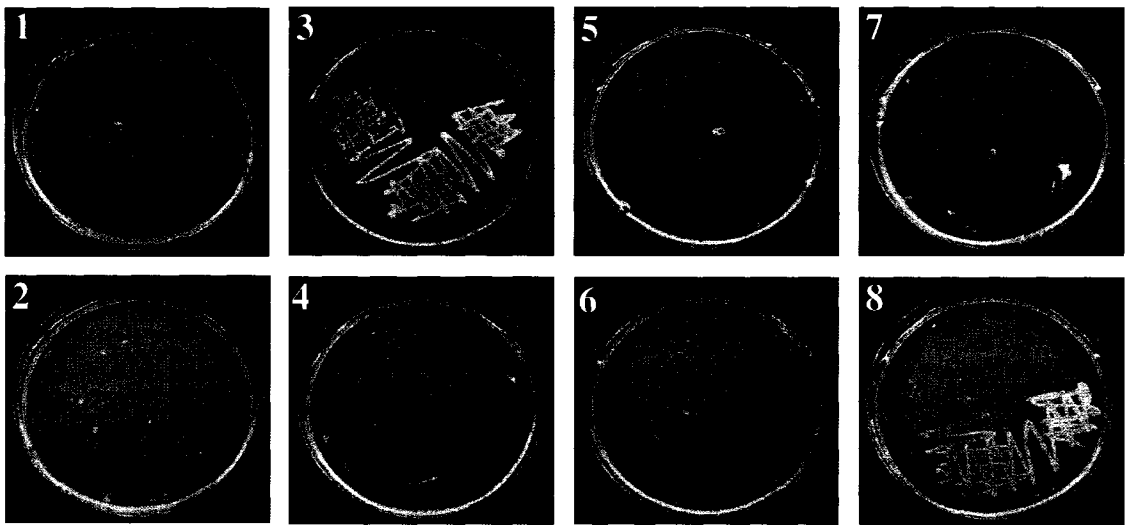

Table 5. Relative ability of wild-type and site-directed mutants of eCBL, eCGS, and yCGL genes to complement the methionine auxotrophy of the *E. coli* KS1000 Δ*metB*::*aadA* strain (lacking eCGS enzyme). Cells were grown for 86 hours on M9 minimal media containing 100 μg/mL Amp, 100 μg/mL Spec, 150 μg/mL arginine, and supplemented with 1mM IPTG or 75 μg/mL methionine.[a]

Enzyme	M9 media	M9 media + 1 mM IPTG	M9 media + 75 μg/mL L-Met.
eCBL	○	○	●
eCBL-F55D	○	○	●
eCBL-Y338E	○	○	●
eCGS	●	○	●
yCGL	○	●	●
yCGL-E48A	○	○	●
yCGL-E48D	○	●	●
yCGL-E48F	○	○	●
yCGL-E333A	○	○	●
yCGL-E333Y	○	○	●

[a]Filled (●) and open circles (○) indicate growth observed and lack of growth, respectively.

Table 6. Relative ability of wild-type and site-directed mutants of eCBL, eCGS, and yCGL genes to complement the methionine auxotrophy of the *E. coli* KS1000 Δ*metC*::*Cat* strain (lacking eCBL enzyme). Cells were grown for 86 hours on M9 minimal media containing 100 μg/mL Amp, 100 μg/mL Chlor, 150 μg/mL arginine, and supplemented with 1mM IPTG or 75 μg/mL methionine.[a]

Enzyme	M9 media	M9 media + 1 mM IPTG	M9 media + 75 μg/mL L-Met.
eCBL	●	●	●
eCBL-F55D	●	●	●
eCBL-Y338E	●	●	●
eCGS	○	○	●
yCGL	○	●	●
yCGL-E48A	○	●	●
yCGL-E48D	○	●	●
yCGL-E48F	○	●	●
yCGL-E333A	○	●	●
yCGL-E333Y	○	○	●

[a]Filled (●) and open circles (○) indicate growth observed and lack of growth, respectively.

10.4. Addition of N- and C-terminal 6-His affinity tags to eCBL and yCGL and analysis of their effect on the purification and properties of the enzymes

Although purification of yCGL *via* a single anion exchange chromatography step has been reported (Yamagata *et al.*, 1993), this method was found to produce enzyme of less than 50% purity (Figure 17A). Refinement of the purification protocol by addition of a hydrophobic interaction chromatography step also did not yield sufficiently pure protein (Figure 17B) for the reliable determination of kinetic parameters. A 6-His affinity tag was subsequently added to the wild-type eCBL and yCGL enzymes to facilitate purification and improve the yield and purity of the expressed proteins.

Two methods were employed to incorporate the 6-His affinity tag. The first involved the use of an oligonucleotide primer, comprising the nucleotide sequence encoding the 6-His sequence, to incorporate a C-terminal 6-His tag *via* PCR, followed by insertion of the amplified gene into the pTrc-99a2 expression vector. The presence of the resulting C-terminal 6-His tag on the eCBL and yCGL genes was verified by DNA sequencing (DNA Landmarks). The second method involved engineering the pTrc-99a2 expression vector to insert a 48-bp linker, encoding a N-terminal 6-His tag and Factor Xa protease cleavage site (Figure 18A), at the *Nde*I site of the plasmid. Insertion of the linker was confirmed using PCR and the expected ~400 and ~600 bp amplicons were observed for the NdeI-linker-ver and pSECseq7r and the pSECseq0 and pSECseq7r primer pairs (Figure 18A and B). The subsequent whole-plasmid PCR mutagenesis step, repairing the ATG start codon of the plasmid-linker construct, was completed successfully and verified by DNA sequencing (DNA Landmarks).

The N- and C-terminal 6-His tags were observed to be equally effective in the enabling purification to >95% homogeneity, as demonstrated by SDS-PAGE (Figure 19A). The yields of wild-type eCBL, eCBL-his (C-terminal) and eCBL-his (N-terminal) were 46, 55 and 137 mg, respectively and of wild-type yCGL, yCGL-his (C-terminal) and yCGL-his (N-terminal) were 15, 9 and 11 mg, respectively. Cleavage of the N-terminal 6-His tag and linker from the purified eCBL-his protein with 1 μg of Factor Xa protease was tested at protein concentrations of 50 μg/mL and 250 μg/mL and observed to be effective (Figure 19B).

The effect of adding an affinity tag on the kinetic parameters of eCBL and yCGL was investigated. The steady state kinetic parameters of the wild-type and 6-His tagged versions of eCBL and yCGL were determined (Figure 20 and Table 7). The difference in k_{cat}/K_m values of wild-type eCBL and yCGL enzymes and the corresponding N- and C-terminal 6-His tags are within ~2.5-fold, demonstrating that the effect of the 6-His tag is negligible. Although this result suggests that cleavage of the affinity tag is not required for the steady state characterization of these enzymes, future investigations, such as X-ray crystallography, may require its removal. Therefore, the N-terminal, removable 6-His method, employing the pTrc-99a3 vector, was selected for expression of the site-directed mutants. Each of the nine yCGL and eCBL wild-type and site-directed mutants were sequenced after subcloning into the pTrc-99a3 vector and found to contain no frame shifts or unanticipated mutations. The purity and approximate molecular weight (predicted from amino acid sequence: eCBL – 43,212 Da and yCGL – 42,542 Da) of expressed wild-type and mutant enzymes was verified by SDS-PAGE (Figure 19C).

Figure 17. SDS-PAGE of fractions from purification of wild-type eCBL using (**A**) anion exchange and (**B**) hydrophobic interaction chromatography. (**A**) Anion exchange chromatography. **Lanes 1** and **20:** protein ladder; **lane 2:** cell lysate pellet (following centrifugation); **lane 3:** cell lysate supernatant; **lane 4:** column flow-through following loading; **lanes 5-19** and **21-23:** even numbered protein fractions from 1-38.(**B**) Hydrophobic interaction chromatography. **Lanes 1** and **18:** protein ladder and **lanes 2-17** and **19-24:** even numbered protein fractions 2-44.

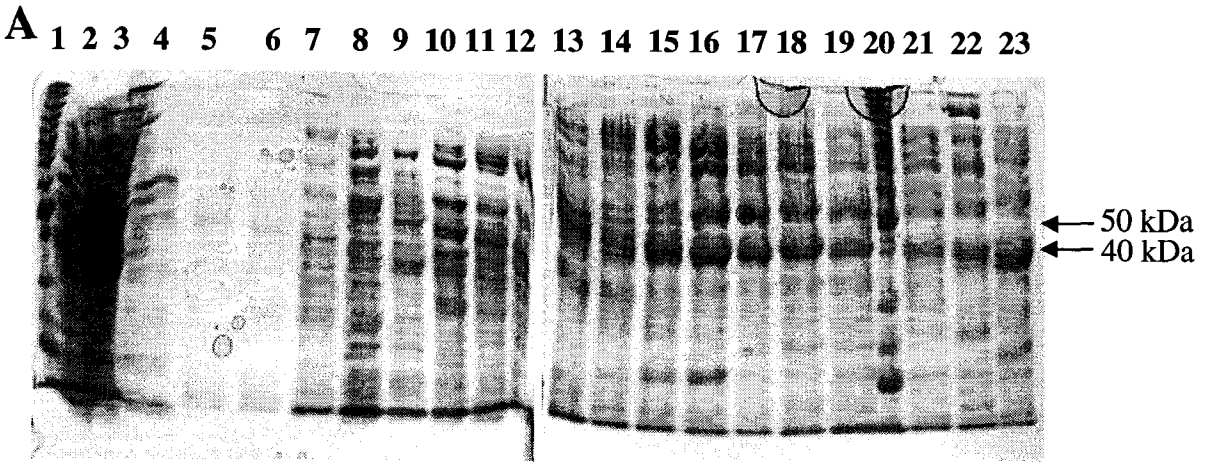

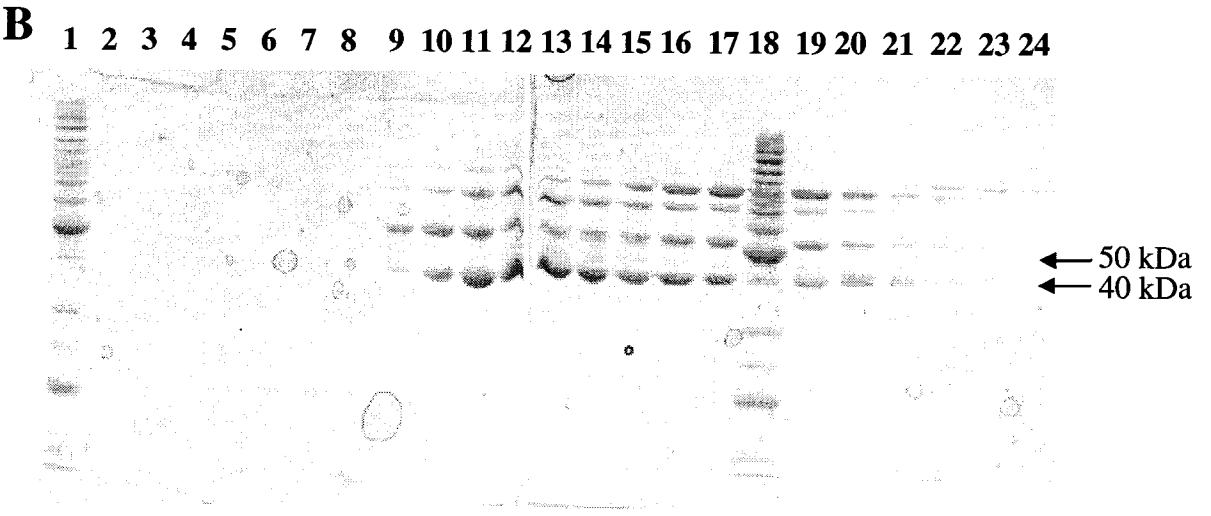

Figure 18. Linker sequence and PCR-based verification of the pTrc-99a3 vector. (**A**) Features of the linker and relative locations of the oligonucleotide primers employed to verify the correct insertion of the linker in the pTrc-99a2 plasmid. (**B**) Agarose gel (1%, w/v) of PCR products from reactions designed to confirm the correct insertion of the linker in the pTrc-99a plasmid. **Lane 1:** reaction with primers NdeI-linker-ver and pSECseq7r; **lane 2:** reaction with primers pSECseq0 and pSECseq7r; **lane 3:** reaction with primers pSECseq0 and NdeI-linker-ver; **lane 4: 1kb** DNA ladder.

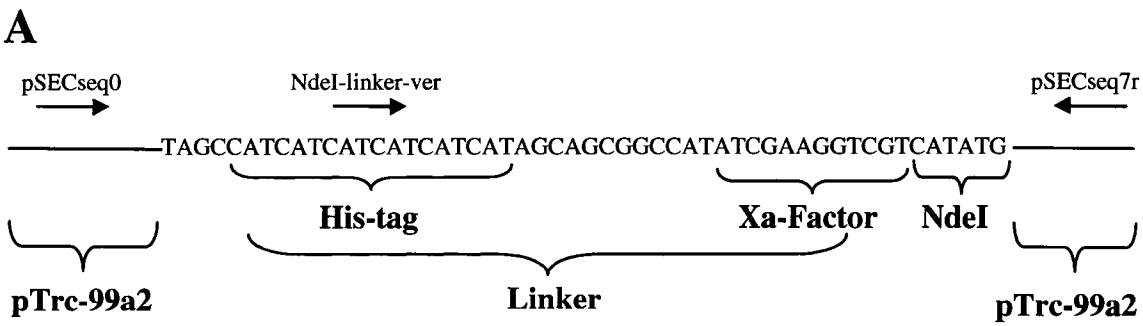

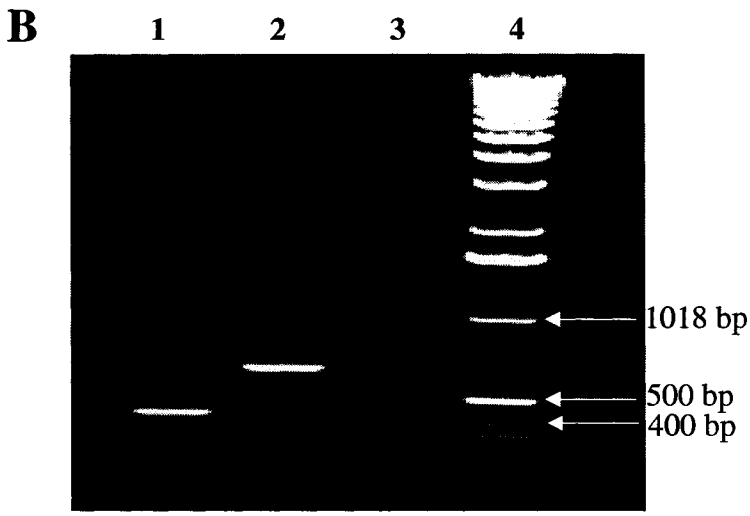

Figure 19. Demonstration of the protease cleavage and effectiveness in producing homogeneous enzyme preparations of the N-terminal 6-His tag and linker. (**A**) SDS-PAGE of Ni-NTA chromatography fractions of 6-His tagged eCBL. **Lanes 1** and **19:** protein ladder; **lane 2:** cell lysate supernatant (following centrifugation); **lane 3:** column-flow through following loading; **lanes 4–24:** column fractions 1-20. (**B**) SDS-PAGE of samples of the 50 μg/mL and 250 μg/mL solutions of N-terminally 6-His tagged eCBL following cleavage with 1 μg of Factor Xa protease for 12 hours at room temperature. **Lane 1:** protein ladder; **lane 2:** undigested 50 μg/mL 6-His-eCBL control; **lane 3:** 50 μg/mL 6-His-eCBL digestion; **lane 4:** 250 μg/ml 6-His-eCBL digestion. (**C**) SDS-PAGE gel demonstrating the purity of proteins (3 μg each) expressed with N-terminal 6-His tags in the engineered pTrc-99a3 construct. **Lane 1:** protein ladder; **lane 2:** eCBL; **lane 3:** eCBL-F55D; **lane 4:** eCBL-Y338E; **lane 5:** empty; **lane 6:** yCGL; **lane 7:** yCGL-E48A; **lane 8:** yCGL-E48F; **lane 9:** yCGL-E48D; **lane 10:** yCGL-E333A; **lane 11:** yCGL-E333Y.

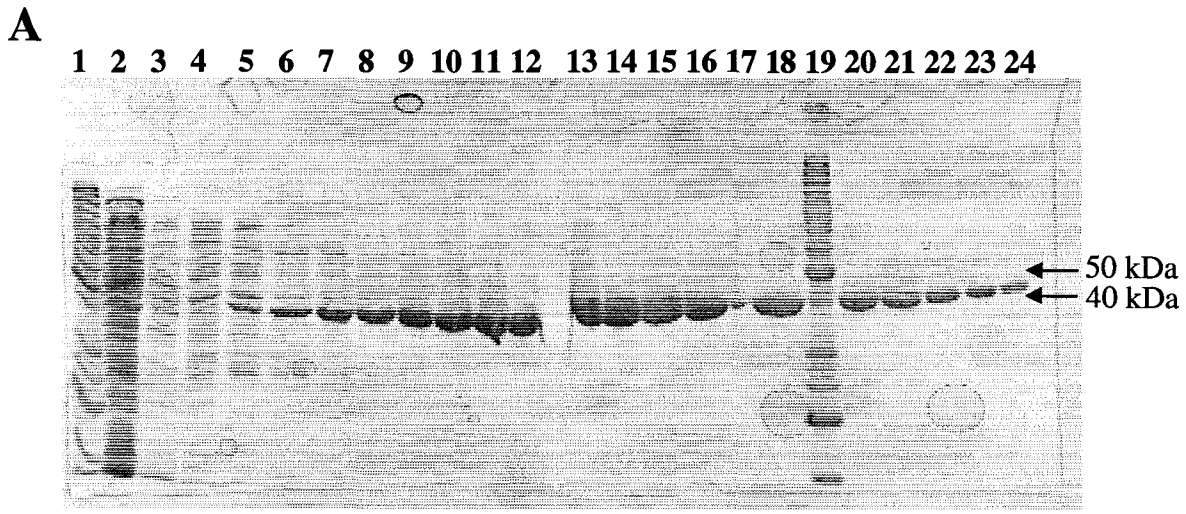

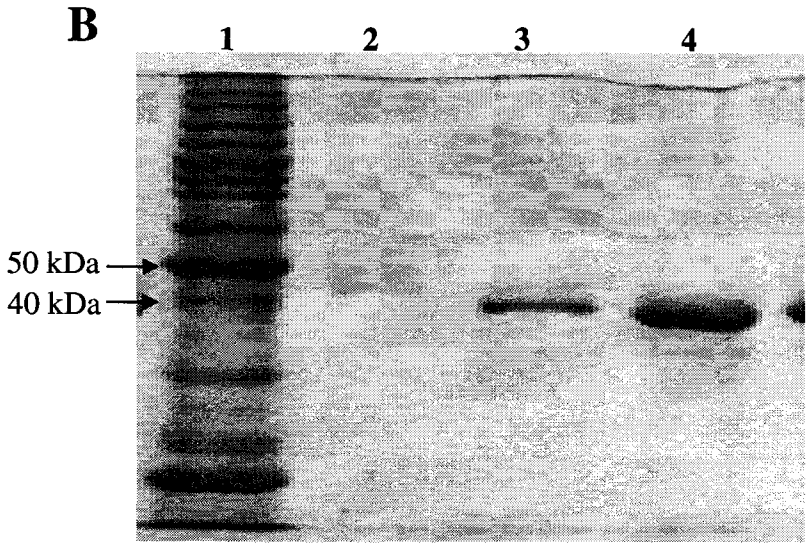

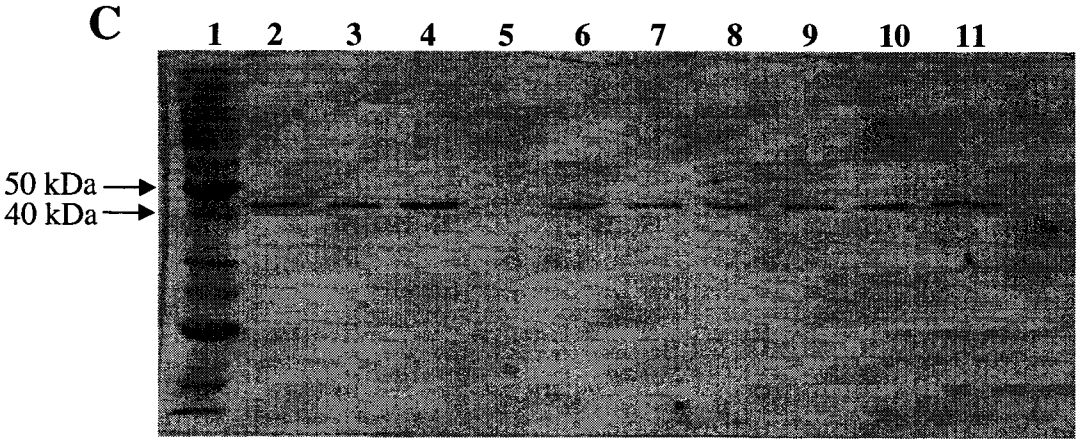

Figure 20. Michaelis-Menten plots of wild-type and 6-His tagged eCBL and yCGL: (**A**) wild-type eCBL, (**B**) C-terminally 6-His tagged eCBL, (**C**) N-terminally 6-His tagged yCGL, (**D**) wild-type yCGL, (**E**) C-terminally 6-His tagged yCGL and (**F**) N-terminally 6-His tagged yCGL Conditions: 100 mM potassium phosphate (pH 8.0), 20 μM PLP, 2 mM DTNB, 0.03-3.75 mM L-cystathionine and (**A**) 0.5-2.2 μM wild-type eCBL, (**B**) 0.6-1.3 μM C-terminally 6-His tagged eCBL, (**C**) 0.1 μM N-terminally 6-His tagged eCBL (**D**) 0.7μM wild-type yCGL, (**E**) 0.4 μM C-terminally 6-His tagged yCGL-his and (**F**) 0.22μM N-terminally 6-His tagged yCGL.

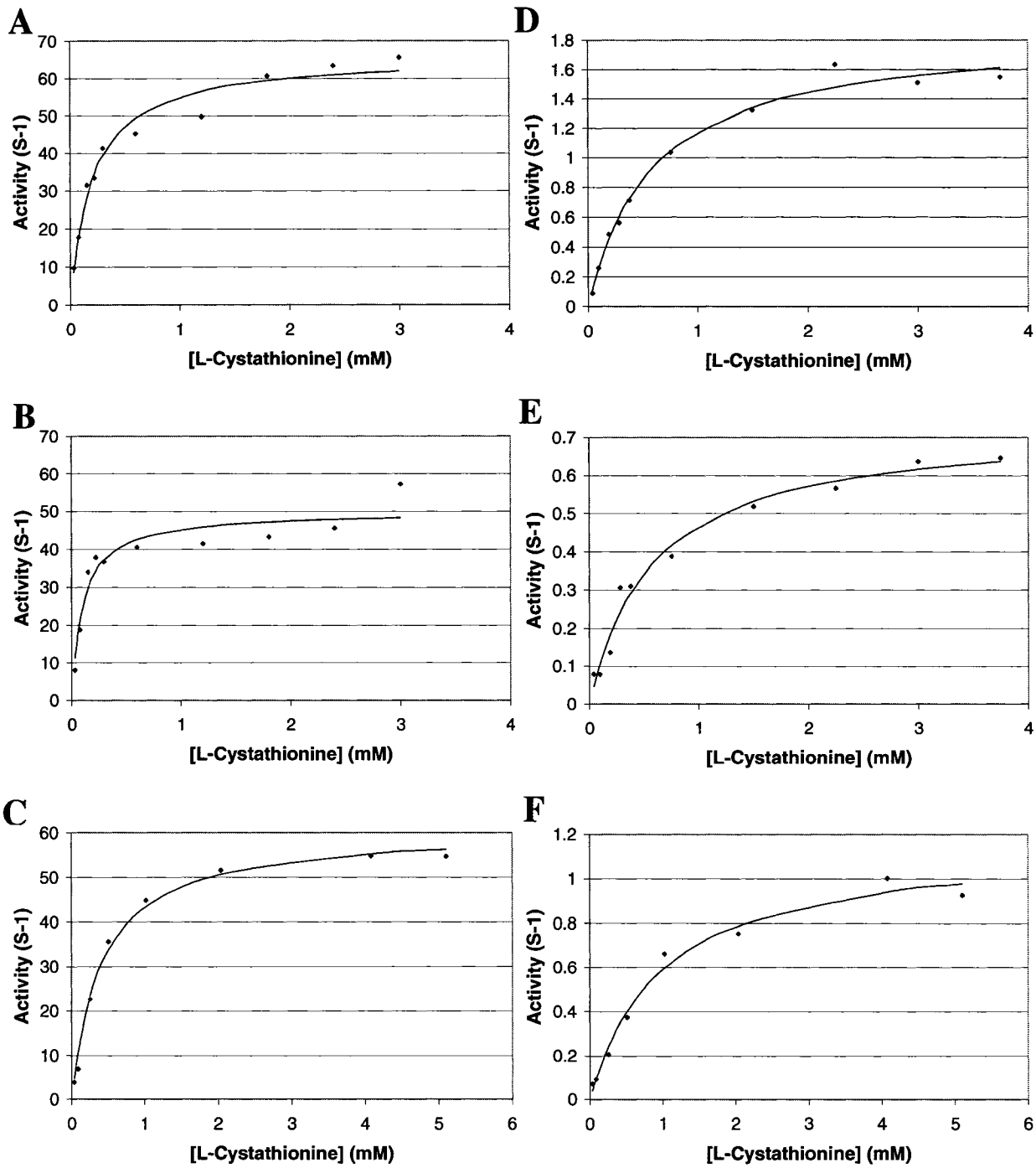

Table 7. Kinetic parameters of wild-type and 6-His tagged eCBL and yCGL.[a]

	K_m (mM)	k_{cat} (s^{-1})	k_{cat}/K_m ($M^{-1}s^{-1}$)
eCBL	0.203 ± 0.03	66.1 ± 2.5	$(3.3 \pm 0.4) \times 10^5$
eCBL-his (C)	0.10 ± 0.03	49.9 ± 2.7	$(5 \pm 1) \times 10^5$
eCBL-his (N)	0.41 ± 0.1	61 ± 2.1	$(1.5 \pm 0.1) \times 10^5$
yCGL	0.588 ± 0.1	1.87 ± 0.1	$(3.2 \pm 0.3) \times 10^3$
yCGL-his (C)	0.570 ± 0.1	0.734 ± 0.04	$(1.3 \pm 0.2) \times 10^3$
yCGL-his (N)	0.97 ± 0.2	1.2 ± 0.07	$(1.2 \pm 0.2) \times 10^3$

[a]C-terminal and N-terminal 6-His tags denoted by (C) and (N), respectively.

10.5. Steady state kinetics of site-directed mutants

The eCBL and yCGL wild-type and site-directed mutant enzymes were purified (Figure 19C, Table 8) and their kinetic parameters for the L-Cth hydrolysis reaction were determined (Table 9). The catalytic efficiency (k_{cat}/K_m) of the F55D and Y338E mutants of eCBL are reduced by 82-fold and 3400-fold, respectively, compared to the wild-type enzyme (Table 9, Figure 21), demonstrating that Tyr338 plays a more significant role in substrate binding and catalysis than Phe55. The k_{cat}/K_m values of the E48F and E48A mutants of yCGL are similar to the wild-type enzyme, whereas those of the E48D, E333A and E333Y mutants are reduced by 4.8-fold, 5-fold and 7.3-fold, respectively (Table 9, Figure 22), suggesting that Glu333 plays a more significant role in substrate binding and catalysis than Glu48. Although no role has been proposed for Tyr338 in eCBL, Messerschmidt *et al.* (2003) suggested that the corresponding residue in yCGL (Glu333) interacts with the substrate and is a key determinant of reaction specificity.

Table 8. Yield and concentration of purified eCBL and yCGL wild-type and mutants.[a]

Protein	Concentration (mg/mL)	Final yield (mg)
eCBL-wild type	19.1	137
eCBL-F55D	0.7	8.2
eCBL-Y338E	2.6	39
yCGL-wild type	1.0	10.5
yCGL-E48D	4.5	47.5
yCGL-E48A	4.2	50.5
yCGL-E48F	4.3	34.5
yCGL-E333A	5.1	61.2
yCGL-E333Y	6.0	71.5

[a]All enzymes expressed using pTrc-99a3 vector and bearing the N-terminal 6-His tag and linker.

Figure 21. Michaelis-Menten plots of wild-type and site-directed mutants of N-terminally 6-His tagged eCBL. Conditions: 50 mM Tris (pH 8.0), 20 μM PLP, 2 mM DTNB, 0.038-5 mM L-Cth and (**A**) 0.1 μM eCBL, (**B**) 0.16μM eCBL-F55D and (**C**) 1.2μM eCBL-Y338E.

A

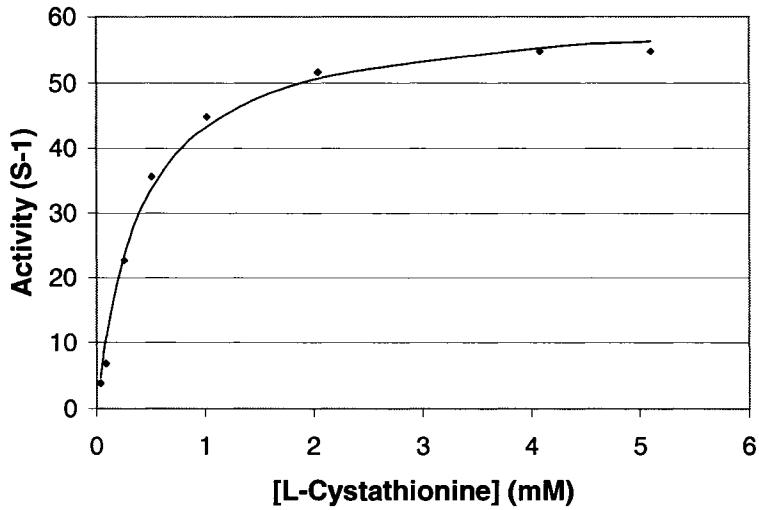

B

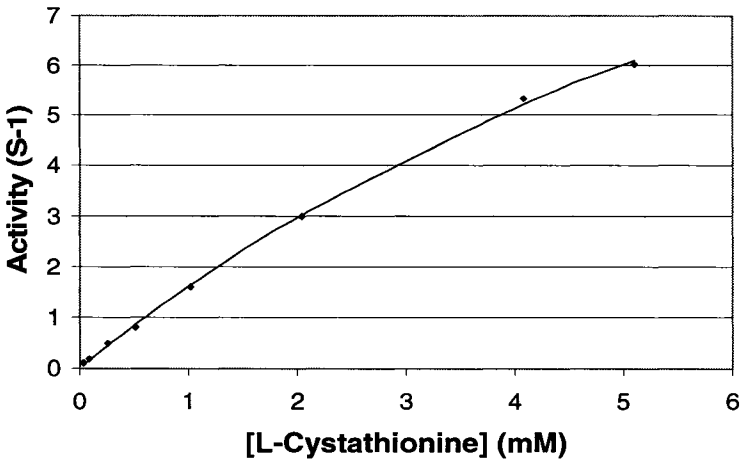

C

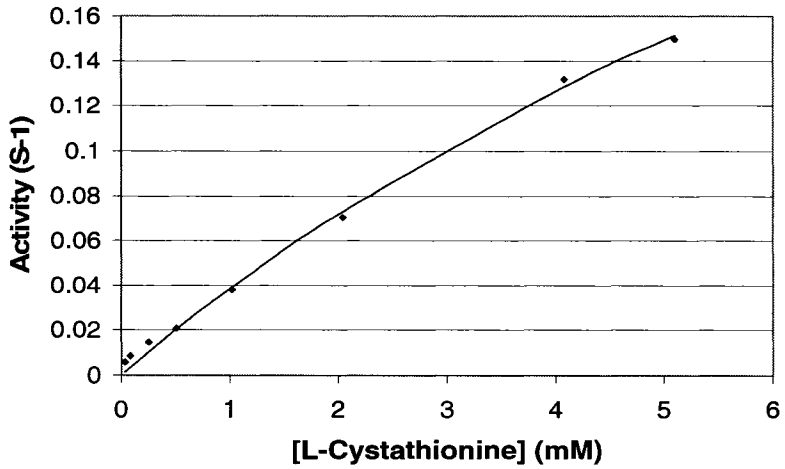

Figure 22. Michaelis-Menten plots of wild-type and site-directed mutants of N-terminally 6-His tagged yCGL. Conditions: 50 mM Tris (pH 8.0), 20 μM PLP, 2 mM DTNB, 0.038-5 mM L-Cth and (**A**) 0.22μM yCGL, (**B**) 0.4 μM yCGL-E48A, (**C**) 0.42μM yCGL-E48D, (**D**) 0.41μM yCGL-E48F, (**E**) 0.48μM yCGL-E333A and (**F**) 0.56μM yCGL-E333Y.

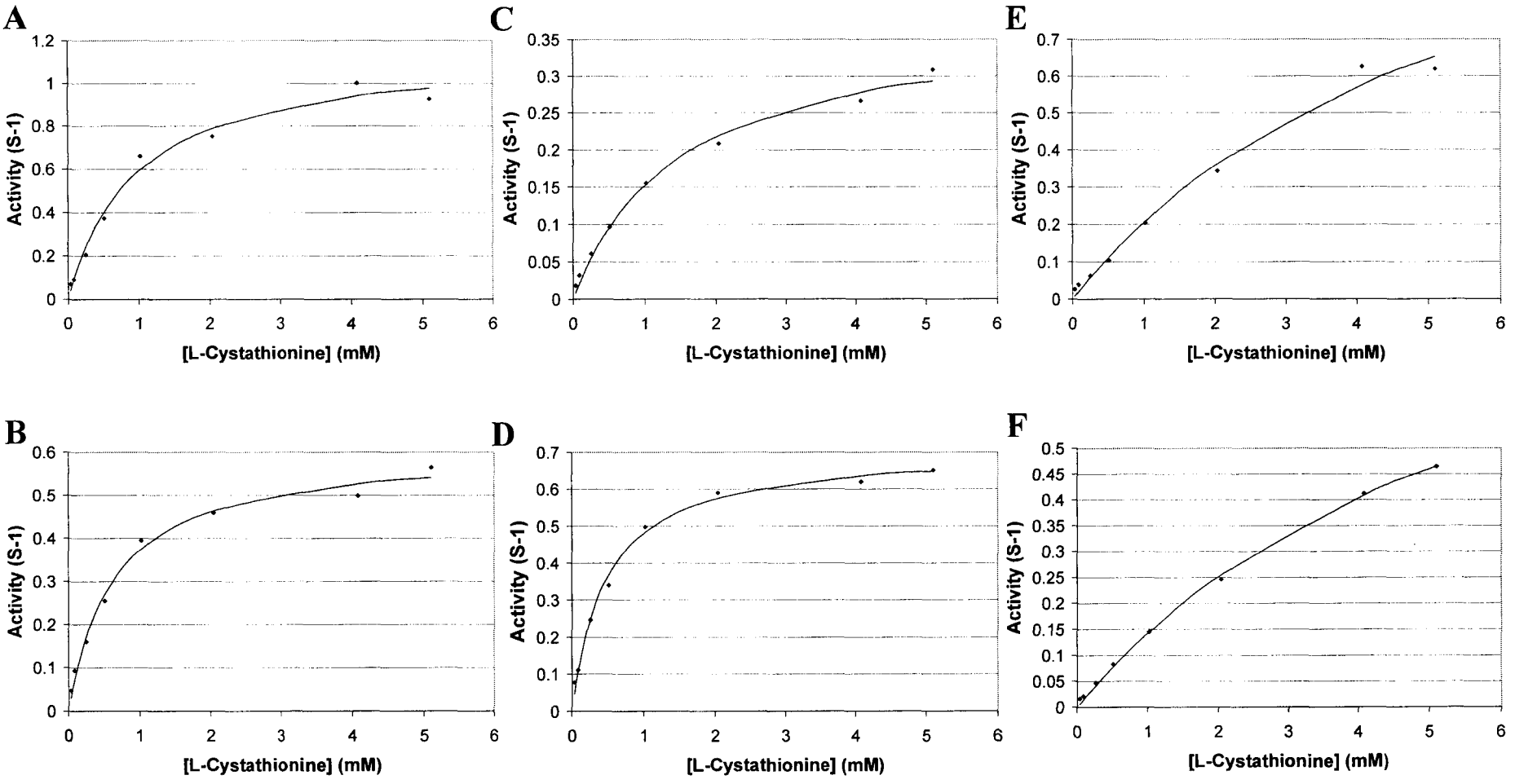

Table 9. Kinetic parameters of wild-type eCBL and yCGL and site-directed mutants.[a]

	K_m (mM)	k_{cat} (s^{-1})	k_{cat}/K_m ($M^{-1}S^{-1}$)
eCBL	0.4 ± 0.1	61 ± 2	(1.5 ± 0.1)× 10^5
eCBL-F55D	11 ± 3	19 ± 3	(1.8 ± 0.1) × 10^3
eCBL-Y338E	13 ± 4	0.5 ± 0.1	40 ± 3
yCGL	1.0 ± 0.2	1.20 ± 0.07	(1.2 ± 0.2) × 10^3
yCGL-E48D	1.50 ± 0.05	0.38 ± 0.02	(2.5 ± 0.3) × 10^2
yCGL-E48A	0.64 ± 0.08	0.61 ± 0.02	(1.0 ± 0.1) × 10^3
yCGL-E48F	0.48 ± 0.05	0.71 ± 0.02	(1.5 ± 0.1) × 10^3
yCGL-E333A	6 ± 2	1.4 ± 0.3	(2.4 ± 0.3) × 10^2
yCGL-E333Y	6 ± 1	1.10 ± 0.07	(1.6 ± 0.1) × 10^2

[a]All enzymes expressed using pTrc-99a3 vector and bearing the N-terminal 6-His tag and linker.

10.6. Product analysis *via* thin-layer chromatography

The reaction specificity of eCBL and yCGL were tested, *via* product analysis, by separation of reaction products by TLC, followed by derivatization with ninhydrin, for detection of amino acids. In the transsulfuration pathway, eCBL reacts with L-Cth to produce L-Hcys, pyruvate, and ammonia (Figure 3). Comparison of the reaction products, following incubation of eCBL with L-Cth (Lanes 6-8 of Figure 23A), with the L-Cth and L-Hcys standards (Lanes 1-5 and 10 of Figure 23A) confirm the production of L-Hcys by eCBL. The eCBL protein standard (Lane 9 of Figure 23A) demonstrates the lack of background resulting from the presence of enzyme and buffer in the reactions. In the reverse-transsulfuration pathway, yCGL reacts with L-Cth to produce L-Cys, α-ketobutyrate, and ammonia (Figure 3). L-Cys is not observed as product of the reaction of yCGL with L-Cth (Lanes 6-8 of Figure 23B), in comparison with the L-Cys, L-Cth and L-Hcys standards (Lanes 1-5 and 9-10 of Figure 23B). This is likely due to the rapid conversion of the produced L-Cys, to pyruvate, hydrogen sulfide and ammonia, by yCGL, *via* a β-elimination reaction. The β-lyase activity yCGL is confirmed by observation of the production of L-Hcys upon incubation of the enzyme with L-Cth (Lanes 6-8 of Figure 23B).

Figure 23. Product analysis of the amino acid products of L-Cth hydrolysis by eCBL and yCGL. Reaction products and amino acid standards were separated by TLC and derivatized with ninhydrin. **A)** L-Hcys and L-Cth standards and *eC*BL reaction products: **lane 1:** 1 mg/mL L-Hcys; **lane 2:** 0.1 mg/mL L-Hcys; **lane 3:** 1 mg/mL L-Cth; **lane 4:** 0.1 mg/mL L-Cth; **lane 5:** L-Hcys + L-Cth (1 mg/mL of each); **lane 6:** 1 mg/mL L-Cth + 1.74 mM eCBL; **lane 7:** 1 mg/mL L-Cth + 174 μM eCBL; **lane 8:** 1 mg/mL L-Cth + 17.4 μM eCBL; **lane 9:** 1.74 mM eCBL; **lane 10:** 1 mg/mL L-Hcys. **(B)** L-Cys, L-Hcys and L-Cth standards and yCGL reaction products: **lane 1:** 1 mg/mL L-Cys; **lane 2:** 0.1 mg/mL L-Cys; **lane 3:** 1 mg/mL L-Cth; **lane 4:** 0.1 mg/mL L-Cth; **lane 5:** L-Hcys + L-Cys + L-Cth (1 mg/mL of each); **lane 6:** 1 mg/mL L-Cth + 86 μM yCGL; **lane 7:** 1 mg/mL L-Cth + 8.6 μM yCGL; **lane 8:** 1 mg/mL L-Cth + 0.86 μM yCGL; **lane 9:** L-Cth + L-Cys (1 mg/mL of each); **lane 10:** 1 mg/mL L-Cys.

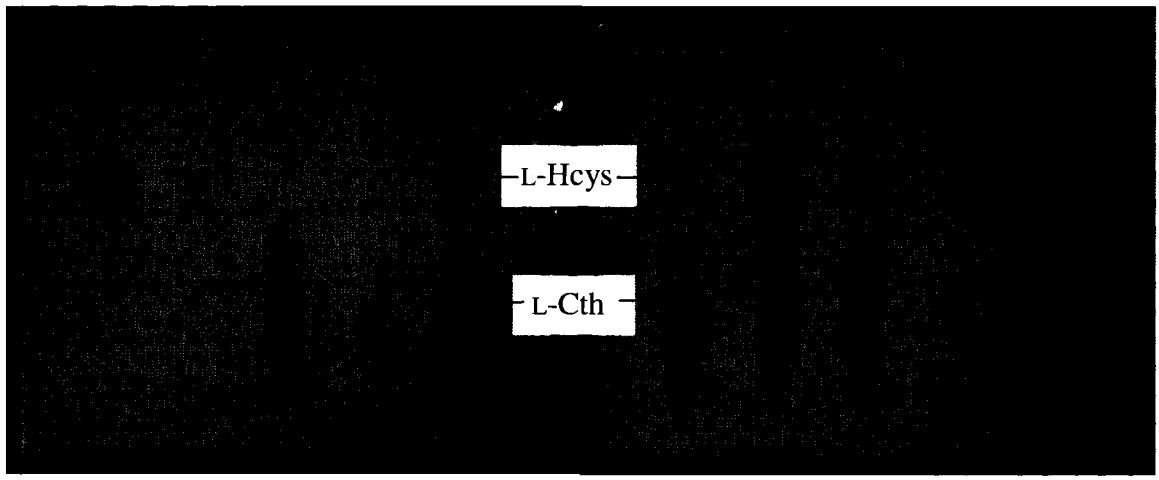

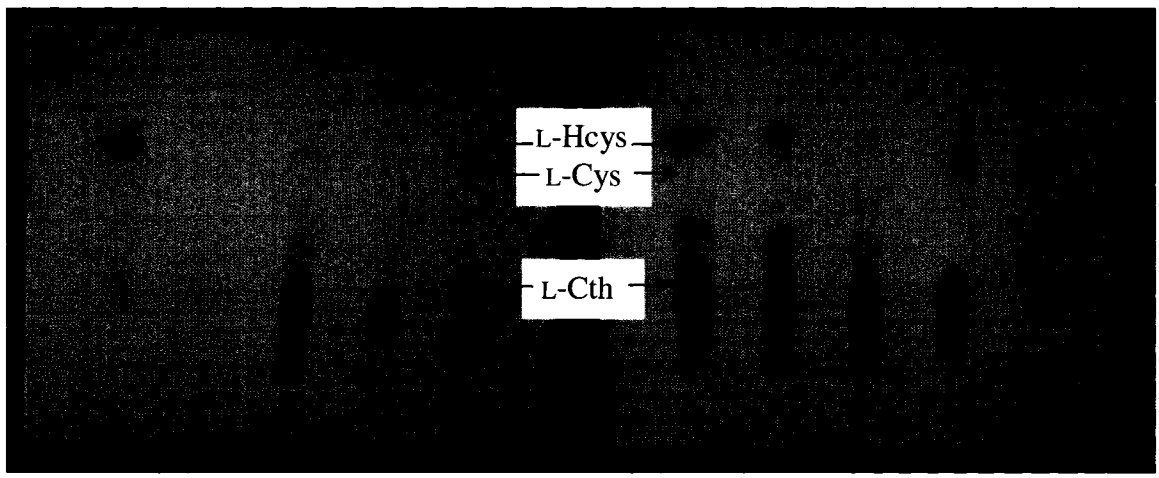

11. DISCUSSION

The goal of this research was the investigation of the role of a pair of active-site residues in substrate binding and catalysis, and as determinants of reaction specificity, in *E. coli* cystathionine β-lyase (eCBL) and yeast cystathionine γ-lyase (yCGL), the second enzymes of the transsulfuration and reverse-transsulfuration pathways, respectively. Although eCBL and yCGL are very similar in structure and both catalyze the hydrolysis of the pseudo-symmetric compound L-cystathionine (L-Cth), their mechanisms and reaction products are distinct. This study demonstrates that although the active-site residues, Phe55 and Tyr338, of eCBL, and the corresponding residues of yCGL, Glu48 and Glu333, are not the sole determinants of reaction specificity in these enzymes, they are involved in the formation of a productive enzyme-substrate complex, which is essential for efficient catalysis.

11.1. Construction of the *E. coli* KS1000 *metB*::*aadA* gene replacement strain

The development of gene replacement strains, lacking the genes encoding eCGS and eCBL, was necessary for both the *in vivo*, complementation, and *in vitro*, protein expression, aspects of this project. Mutant strains deficient in eCGS and eCBL activity, encoded by the *metB* and *metC* genes, respectively, are available. However, many such strains have been made by chemical or UV mutagenesis. Therefore, they are not knockout or gene replacement strains and, as such, may be able to revert to the wild-type genotype and produce a functional enzyme product. This would result in a bacterial strain

that would no longer be auxotrophic and which would yield false positives in complementation experiments. Contamination of site-directed mutants with wild-type enzyme is also a concern for *in vitro* studies, particularly when expressing mutants of host enzymes (*i.e.* expressing site-directed mutants of *E. coli* enzymes in *E. coli*). Therefore, in order to avoid these problems, the *E. coli* KS1000 *metB*::*aadA* gene replacement strain was constructed, in which the *metB* gene, encoding eCGS, was replaced with the *aadA* gene, which provides spectinomycin resistance. The *E. coli* KS1000 *metC*::*Cat* gene replacement strain (constructed by P. Lodha, J. Pearce and S. Aitken), in which the *metC* gene, encoding eCBL, is replaced by the *Cat* gene, which provides chloramphenicol resistance, was also employed in this study. The KS1000 strain (New England BioLabs) was selected as the genetic background for both gene replacement strains because it lacks the periplasmic protease, thereby facilitating protein expression.

The gene replacement strategy employed in construction of the *E. coli* KS1000 *metB*::*aadA* and KS1000 *metC*::*Cat* strains is similar to the pop-in/pop-out method used in *Saccharomyces cerevisiae* and the hit-and-run procedure used in mouse embryonic stem cells (Link, 1997; Hasty, 1991; Rothstein, 1991; Scherer, 1979). This method involves homologous recombination between the *E. coli* chromosome and the pKO3 plasmid containing the replacement gene, bordered by the flanking regions of the target gene, *aadA* and *metB*, respectively, in the case of the *metB*::*aadA* strain (Figure 10). Restriction analysis with *BstE*II, which cleaves the *aadA* gene and 3' *metB* flanking region, confirmed the successful construction of pKO3-*metB*::*aadA* plasmid (Figure

14B). Subsequently, *E. coli* KS1000 *metB*::*aadA* strain was produced, using the recombination method of Link *et al.*, 1997, and verified *via* PCR.

The transsulfuration pathway is the sole biosynthetic source of L-Met in *E. coli* and disruption of this pathway by elimination of the *metB* or *metC* genes gives rise to methionine auxotrophy in *E. coli*. Therefore, observation of methionine auxotrophy was employed as a final verification of the successful construction of both the KS1000 *metB*::*aadA* (Figure 16A) and KS1000 *metC*::*Cat* (P. Lodha, unpublished results) strains. It also enabled the use of complementation as an *in vivo* test for reaction specificity, as only wild-type enzymes and site-directed mutants with CGS and CBL activity can rescue the *ΔmetB* and *ΔmetC* strains, respectively.

11.2. Complementation of *E. coli* KS1000 *metB*::*aadA*

E. coli KS1000 Δ*metB*::*aadA* cells were transformed with the wild-type *metB*, *metC* and *Cys3* genes, encoding eCGS, eCBL and yCGL, respectively, as well as site-directed mutants of *metC* and *Cys3*, in order to determine the ability of these genes to complement the methionine auxotrophy of this strain. The empty pTrc-99a plasmid, employed as a negative control, did not enable growth of the KS1000 Δ*metB*::*aadA* strain in the absence of exogenous L-Met (Figure 16B). Similarly, the *E. coli metC* gene, encoding eCBL, was unable to complement the methionine auxotrophy of this strain (Figure 16B, Table 5), demonstrating that the eCBL enzyme does not catalyze the γ-replacement reaction of eCGS *in vivo*. The F55D and Y338E site-directed mutants of

eCBL were also unable to support the growth of this strain (Table 5), indicating that the conversion of Phe55 and Tyr338 to the corresponding residues of eCGS is not sufficient to switch the reaction specificity of eCBL from β-lyase to γ-synthase. This result demonstrates the importance of the larger structural context of enzymes as a determinant of function and illustrates the challenges facing rational redesign studies (Luong and Kirsch, 2001).

The observed complementation of the *ΔmetB* strain by *Cys3* demonstrates that, like eCGS, yCGL is able to catalyze the synthesis of L-Cth, although at low levels compared to eCGS as complementation by *Cys3* was not observed in the absence of IPTG (Figure 16B, Table 5). Of the five yCGL site-directed mutants, only the E48D mutant complemented the KS1000 Δ*metB*::*aadA* strain (Table 5). Replacement of the glutamate side chain of Glu48 in the wild-type enzyme by aspartate is a conservative change, as both are acidic amino acids, in which only the placement of the side chain carboxylate is altered, a change that does not eliminate the γ-synthase activity of yCGL. The inability of the other Glu48 and Glu333 mutants to complement the methionine auxotrophy of the *ΔmetB* strain suggests that these residues have a role in substrate binding or maintenance of appropriate active-site architecture in yCGL.

As expected, the *ΔmetB* strain was complemented by the *metB* gene, although only in the absence of induction by IPTG (Figure 16B, Table 5). The presence of growth upon complementation with the *metB* gene in the absence of induction is due to the leaky *trc* promoter of the pTrc-99a plasmid (Terpe, 2006; Anthony *et al.*, 2004), which allows a low, constitutive level of expression that is sufficient to allow KS1000 Δ*metB*::*aadA* cells

containing the pTrc-99a-*metB* plasmid to produce adequate L-Met for growth. In contrast, complementation by *metB* was blocked in the presence of IPTG. Methionine synthesis diverges from the threonine branch of the family of amino acids derived from aspartate (Galili, 2002). In *E. coli* L-homoserine is the branch-point intermediate of L-threonine and L-Met biosynthesis and is the common substrate for homoserine kinase and homoserine *O*-succinyltransferase, which produce *O*-phosphohomoserine and *O*-succinyl-L-homoserine, respectively (Voet *et al.*, 2002). The shift in the flux of activated L-homoserine towards L-Met, resulting from *metB* overexpression, may result in insufficient production of L-threonine to sustain cell growth. Therefore, the observed lack of growth of the *ΔmetB* strain upon IPTG-induced expression of *metB* is likely due to the disruption of primary metabolism in the L-Met and L-threonine biosynthetic pathways. As mentioned above, the gene encoding yCGL rescues the methionine auxotrophy of KS1000 Δ*metB*::*aadA* (CGS knockout) only when overexpressed by induction with IPTG, suggesting that yCGL is able to synthesize L-cystathionine *in vivo*, but at a relatively low level in comparison with eCGS. This contrasts with the suggestion of Ono *et al.* (1999) that yCGL and eCGS have similar reaction specificity and that the *in vivo* activity of these enzymes is determined by substrate availability.

11.3. Complementation of *E. coli* KS1000 *metC*::*Cat*

The ability of the *metC* gene, encoding eCBL, to complement the methionine auxotrophy of the KS1000 Δ*metC*::*Cat* strain was unimpeded by IPTG (Figure 16B, Table 6). This contrasts with the effect of IPTG-induced expression of the *metB* gene,

encoding eCGS, discussed above. The eCGS and eCBL enzymes occupy the first and second positions, respectively, in the transsulfuration pathway (Aitken and Kirsch, 2005). Therefore, overexpression of eCBL does not have the same impact on the cellular metabolism of the *E. coli* cells because the substrate of this enzyme is not a branch-point metabolite.

Complementation of the KS1000 Δ*metC*::*Cat* strain upon induction by IPTG was observed for all genes tested, with the exception of wild-type eCGS and the yCGL-E333Y mutant (Table 6). The catalytic efficiency for the eCGS-catalyzed L-Cth hydrolysis reaction is one and three orders of magnitude lower than that of yCGL and eCBL, respectively (S. Aitken, unpublished results), and may not be sufficient to complement the *metB* gene. However, the inability of the *metB* gene to support growth may also be due to the effect of overexpression of this gene on cellular metabolite levels, as discussed above. Therefore, a plasmid in which expression is tightly regulated, in contrast with the leaky promoter of pTrc-99a, is required to distinguish between these mechanisms.

The observed complementation, upon induction with IPTG, of the *ΔmetC* strain by the wild-type yCGL and the E48A, E48D, E48F and E333A site-directed mutants (Table 6) confirms the report that yCGL has both β- and γ-lyase activities (Yamagata *et al.*, 1993). Only the genes encoding the wild-type and F55D and Y338E mutants of eCBL were able to complement the *ΔmetC* strain in the absence of IPTG (Table 6), demonstrating that the yCGL wild-type and mutant enzymes are less efficient in catalysis of the β-lyase activity than eCBL.

11.4. Protein purification

Yamagata *et al.* (1993) reported that yCGL, expressed recombinantly in *E. coli*, can be purified to approximately 90% homogeneity *via* a single anion exchange chromatography step. This method was found to be irreproducible as it yielded protein of less than 50% purity (Figure 17A). The addition of a second chromatography step, employing hydrophobic interaction resin, also did not yield sufficiently pure enzyme for the accurate determination of kinetic parameters (Figure 17B). Ni-NTA affinity chromatography is an effective method for the purification of recombinant proteins and has the advantage of requiring only a single chromatography step, thereby increasing yields, by minimizing losses during chromatrographic steps, and enabling the purification procedure to be completed in a single day (Arnau *et al.*, 2006). A disadvantage of Ni-NTA affinity chromatography is that it requires the incorporation of a 6-His tag, generally at the N- or C-terminal of the target protein (Arnau *et al.*, 2006). Therefore, the resulting protein is not truly wild-type and it is important to ensure that the introduction of the affinity tag does not alter the kinetic parameters of the enzyme (Aitken and Kirsch, 2004). Proteolytic cleavage of the tag is a common method to circumvent this problem if the presence of the affinity tag is observed to alter the properties of an enzyme (Arnau *et al.*, 2006).

A straightforward method for the incorporation of a 6-His tag is *via* PCR, in which one of the oligonucleotide primers includes a 3'-extension, comprising the 18-nucleotide sequence encoding the tag. An alternative is the use of an expression vector

that incorporates the 6-His tag and a linker, containing a protease recognition site to enable cleavage of the affinity tag. Both methods were employed in the optimization of the eCBL and yCGL expression protocol in order to determine which, if either, end of the protein was optimal for introduction of the affinity tag. A C-terminal 6-His tag was incorporated *via* PCR. The pTrc-99a2 expression vector was also engineered to incorporate a N-terminal 6-His-tag with a linker containing the Factor Xa proteolytic cleavage site, with the goal of enabling affinity purification followed by the optional removal of the 6-His tag (Figure 18A). This plasmid construct was determined to be effective for the expression and purification of homogeneous protein (Figure 19A) and protease cleavage of the affinity tag and linker region was demonstrated (Figure 19B).

The steady state kinetic parameters of the wild-type and 6-His tagged versions of eCBL and yCGL were measured in order to determine the effects of the N- and C-terminal affinity tags on enzyme activity. Comparison of the k_{cat}/K_m values for the wild-type and affinity-tagged versions of eCBL and yCGL demonstrated that the effect of the 6-His tags were negligible and therefore, proteolytic removal is not required. The pTrc-99a3 expression vector, which incorporates the removable, N-terminal 6-His tag was selected for expression of the site-directed mutants of eCBL and yCGL to provide consistency in future experiments, as removal of the affinity tag could be optimal for certain biophysical applications, such as X-ray crystallography (Arnau *et al.*, 2006).

11.5. Steady state characterization of the eCBL and yCGL site-directed mutants

The KS1000 *metC::Cat* strain was chosen for expression of the wild type and site-directed mutants of eCBL and yCGL to avoid contamination by wild-type eCBL. The 82-fold reduction in the k_{cat}/K_m of eCBL-F55D is dominated by a 28-fold increase in K_m as the k_{cat} of this mutant is reduced by only 3-fold (Table 9, Figure 21). Therefore, the introduction of a negatively-charged residue at this position, within the context of the eCBL structure (Figure 7), likely reduces the ability of the enzyme to bind its substrate rather than producing a non-productive binding conformation. In contrast, the k_{cat} and k_{cat}/K_m values of the eCBL-Y338E mutant are reduced by 120- and 3400-fold (Table 9, Figure 21), respectively, suggesting that the introduction of a negatively-charged glutamate residue at this position (Figure 7) not only reduces the ability of eCBL to bind L-Cth, but also forces the substrate into a less optimal conformation, thereby reducing the catalytic efficiency of the enzyme.

The positively-charged guanidinium group of Arg59 is proposed to interact, *via* a salt bridge, with the distal carboxylate group of L-Cth (Figure 7) (Clausen *et al.*, 1996). This interaction could be weakened in the F55D and Y338E mutants because the introduction of negatively-charged surface area at the entrance of the active site, within the context of the eCBL structure, may impede substrate binding *via* a repulsive electrostatic interaction with the distal carboxylate group of the substrate. The distal amino group of L-Cth may be hydrogen bonded to the side chains of Tyr111, Asp116 or Tyr238 when bound to eCBL (Figure 7) (Clausen *et al.*, 1996). The investigation of the D116R site-directed mutant of eCBL has demonstrated that Asp116 is not involved in

substrate binding or catalysis (S. Aitken, unpublished results) and examination of the structure of the eCBL-AVG complex reveals that a hydrogen bond and a water-mediated hydrogen bond are likely formed between the distal amino group of the substrate and the side chains of Tyr111 and Tyr238, respectively (Figure 9) (Clausen *et al.*, 1997b). As Tyr338 is predicted interact with L-Cth *via* van der Waals contacts, the replacement of its aromatic side chain with the acidic, carboxylate group of glutamate, in the Y338E mutant, may result in the formation of a hydrogen bond with the distal amino group of L-Cth, thereby pulling this group away from Tyr111. This would be expected to force the substrate into an alternate binding conformation, thereby resulting in the observed reduction in k_{cat} for the Y338E mutant. These results suggest that the structure-based prediction of the interaction of Tyr338 with the L-Cth substrate is likely correct (Clausen *et al.*, 1996; Clausen *et al.*, 1997b).

The k_{cat}/K_m values of the E48F and E48A mutants of yCGL are similar to the wild-type enzyme, whereas those of the E48D, E333A and E333Y mutants were reduced by 5-fold, 5-fold and 7-fold, respectively (Table 9, Figure 22). Although the slight increase in the K_m and decrease in the k_{cat} of the E48D mutant are significant, in comparison with the experimental error of the kinetic parameters (Table 9), they are negligible and indicate that while this residue does not play a role in binding or catalysis, its mutation may result in a subtle change in active-site architecture. The K_m values of the E333A and E333Y mutants increased by 6-fold, whereas the k_{cat} values remains essentially unchanged. This result suggests that the predicted hydrogen bond between Glu333 and the distal amino group of L-Cth (Messerschmidt *et al.*, 2003) either is not formed or does not play a major role in binding in the enzyme-substrate complex. An

alternative binding mode is that observed in the eCBL-AVG complex, in which the distal amino group of the inhibitor is hydrogen bonded to the hydroxyl group of the phenolic side chain of Tyr111 (Figure 9), as discussed above, which is conserved as Tyr103 in yCGL. This binding mode may be common to both eCBL and yCGL, such that the role of Glu333 may be simply to steer the substrate within the active site, as proposed by Messerschmidt *et al.* (2003).

Electrostatic repulsion between the carboxylate group of the Glu333 side chain, which, along with Glu48, forms a negatively-charged surface area at the entrance of the yCGL active site (Figure 8), and the sulfur atom of the L-Cth substrate was proposed to be an important determinant of the orientation of substrate binding and, therefore, reaction specificity in this enzyme (Messerschmidt *et al.*, 2003). However, both the *in vivo* and *in vitro* results of this study (Table 6 and Figure 23) are in agreement with an earlier report (Yamagata *et al.*, 1993) that the reaction specificity of yCGL is actually low, as it catalyzes both γ-elimination and the β-elimination reactions when presented with L-Cth as a substrate. In eCBL residues Phe55 and Tyr338, corresponding to Glu48 and Glu333 of yCGL, form a hydrophobic patch of surface area at the entrance of the active site (Figure 7). Additionally, Tyr338 is proposed to interact *via* van der Waals contacts with the L-Cth substrate, as discussed above. Although no model has been suggested to explain reaction specificity in eCBL, Clausen *et al.* (1996) proposed that L-Cth enters the active site of eCBL, to form the enzyme substrate complex, *via* a channel between residues Arg58 and Arg59, which were also proposed to form salt bridge interactions with the phosphate moiety of PLP and the distal carboxylate group of L-Cth, respectively (Figure 7) (Clausen *et al.*, 1996; Clausen *et al.*, 1997b). Therefore, it seems

likely that these residues play an important role in enforcing the appropriate binding conformation of L-Cth within the active site (Messerschmidt *et al.*, 2003).

Comparison of the active sites of eCBL and yCGL demonstrates that the latter is larger, due to the absence of bulky aromatic groups, including Phe55 and Tyr338 of eCBL. This demonstrates that, despite the overall similarity in the structures of these enzymes and the high degree of conservation of active-site residues, the architecture of the active sites is subtly different. The complementation results, discussed above, show that mutation of Phe55 and Tyr338 of eCBL and the corresponding Glu48 and Glu333 of yCGL is not sufficient to alter the reaction specificity of these enzymes *in vivo*. These findings illustrate the importance of the larger structural context of the enzyme in defining the architecture of the active site (Luong and Kirsch, 2001). Therefore, modification of the reaction specificity of eCBL and yCGL would likely require mutation of several residues, some of which may not be located within the primary shell of residues in the active site that directly contact the substrate.

11.6. Product analysis

The continuous, DTNB-based assay employed to determine the kinetic parameters for L-Cth hydrolysis does not distinguish between the β- and γ-elimination reactions catalyzed by eCBL and yCGL, respectively. Therefore, separation of reaction products by TLC followed by derivatization with ninhydrin was used to detect the amino acid products of L-Cth hydrolysis, which are L-Hcys and L-Cys for the β-lyase and γ-lyase

reactions, respectively. Qualitative comparison of the eCBL and yCGL reaction products with L-Cth, L-Hcys and L-Cys standards, demonstrated the production of L-Hcys by both enzymes (Figure 23). This substantiates the *in vivo* observation that yCGL complements the *ΔmetC* strain, which lacks eCBL activity (Table 6).

The lack of observed L-Cys, as product of the reaction of yCGL with L-Cth, is likely due to the quick turn over of the L-Cys produced to pyruvate by yCGL. Therefore, as both eCBL and yCGL catalyze the β-elimination of L-Cys (S. Aitken, unpublished results; Yamagata *et al.*, 2002), a novel product analysis assay is required as other methods reported for this purpose also rely on the detection of the amino acid products of the reaction (Yamagata et al., 1993; Gaitonde, 1967). One alternative to detection of the amino acid products of the β- and γ-hydrolysis of L-Cth is detection of the α-ketoacid products. Another option is the use of alternative substrates, such as L-homocystine, which can only undergo γ-elimination. However, the solubility of L-homocystine in aqueous solution is in the low micromolar range, thereby making it technically challenging to detect the formation of product.

11.7. Conclusion

E. coli cystathionine β-lyase and yeast cystathionine γ-lyase comprise an ideal model system to investigate the mechanism of regulation of reaction specificity in PLP-dependent enzymes. These two enzymes bind the same pseudo-symmetric substrate, L-Cth, but in opposite orientations. This distinction allows eCBL and yCGL to produce L-

Hcys and L-Cys, respectively, from the same substrate. Although the active-sites of the two enzymes are very similar, a prominent difference is the pair of aromatic residues Phe55 and Tyr338 in eCBL, which correspond to the acidic residues Glu48 and Glu333 in yCGL. A series of site-directed mutants of these residues were constructed to probe their role in substrate binding, catalysis and as determinants of reaction specificity. The ability of these mutants to complement methionine auxotrophy in *E. coli* strains lacking the enzymes of the transsulfuration pathway was observed to be no greater than the corresponding wild-type enzymes. The k_{cat}/K_m of the CBL F55D and Y338E mutants is reduced by two and three orders of magnitude, respectively, and a similar, although less pronounced, trend was observed for mutants of the corresponding residues in yCGL. The *in vivo* and *in vitro* results indicate that, although these residues are involved in maintaining appropriate active-site architecture, mutation of Phe55 and Tyr338 of eCBL and the corresponding Glu48 and Glu333 of yCGL is insufficient to modify the reaction specificity of these enzymes. This finding reveals the essential role of the larger context of the enzyme and demonstrates that the inter-conversion of the β- and γ-elimination activities of eCBL and yCGL, respectively, would require modification of the active-site topology, thereby likely necessitating the concomitant alteration of several residues.

12. REFERENCES

Ahuja, S.K., Ferreira, G.M., and Moreira, A.R. 2004. Utilization of enzymes for environmental applications. Crit. Rev. Biotech. 24: 125-154.

Aitken, S.M. and Kirsch, J.F. 2005. The enzymology of cystathionine biosynthesis: strategies for the control of substrate and reaction specificity. Arch. Biochem. Biophys. 433: 166-175

Aitken, S.M. and Kirsch, J.F. 2004. Role of active-site residues Thr81, Ser82, Thr85, Gln157, and Tyr158 in yeast cystathionine β-synthase catalysis and reaction specificity. Biochem. 43: 1963-71.

Aitken, S.M. and Kirsch, J.F. 2003. Kinetics of the yeast cystathionine beta-synthase forward and reverse reactions: continuous assays and the equilibrium constant for the reaction. Biochem. 42: 571-578.

Aitken, S.M., Kim, D.H., and Kirsch, J.F. 2003. *Escherichia coli* cystathionine γ-synthase does not obey ping-pong kinetics. Novel continuous assays for the elimination and substitution reactions. Biochem. 42: 11297-11306.

Alting, A.C., Engels, W.J.M., Van Schalkwijk, S., Exterkate, F.A. 1995. Purification and characterization of cystathionine β-lyase from *Lactococcus lactis* subsp. *cremoris* B78 and its possible role in flavor development in cheese. Appl. Environ. Microbiol. 61: 4037-4042.

Anthony, L.C., Suzuki, H., and Filutowicz, M. 2004. Tightly regulated vectors for the cloning and expression of toxic genes. J. Microbiol. Methods. 58: 243-250.

Ardö, Y.2006. Flavour formation by amino acid catabolism. Biotechnology Advances. 24: 238-242.

Arnau, J., Lauritzen, C., Petersen, G.E., and Pedersen, J. 2006. Current strategies for the use of affinity tags and tag removal for the purification of recombinant proteins. Protein Expr. Purif. 48: 1-13.

Bairoch, A. 2000. The enzyme database in 2000. Nuc. Acid Res. 28, 304-305.

Belfaiza, J., Parsot, C., Martel, A., Bouthier De La Tour, C., Margarita, D., Cohen, G.N., and Saint-Girons, I. 1986. Evolution in biosynthetic pathways: two enzymes catalyzing consecutive steps in methionine biosynthesis originate from a common ancestor and possess a similar regulatory region. Proc. Natl. Acad. Sci. U.S.A. 83: 867-871.

Bradford, M.M. 1976. A rapid and sensitive method for the quantitation of microgram quantities of protein utilizing the principle of protein-dye binding. Anal. Biochem. 72: 248-254.

Centerwall, S.A. and Centerwall, W.R. 2000. The discovery of phenylketonuria: The story of a young couple, two retarded children, and a scientist. Pediatrics. 105: 89-103.

Chica, R.A., Doucet, N., and Pelletier, J.N. 2005. Semi-rational approaches to engineering enzyme activity: combining the benefits of directed evolution and rational design. Curr. Opin. Biotech. 16: 378-384.

Christen, P. and Mehta, P.K. 2001. From cofactor to enzymes. The molecular evolution of pyridoxal-5'-phosphate-dependent enzymes. Chem. Rec. 1: 436-447.

Clausen, T. and Huber, R. Prade, L., Wahl, M.C. and Messerschmidt, A. 1998. Crystal structure of *Escherichia coli* cystathionine γ-synthase at 1.5Å resolution. EMBO J. 17: 6827-6838.

Clausen, T., Laber, B., and Messerschmidt, A. 1997a. Mode of action of cystathionine beta-lyase. Biol Chem. 378: 321-326.

Clausen, T., Huber, R., Messerschmidt, A., Pohlenz, H.-D., and Laber, B. 1997b. Slow-binding inhibition of *Escherichia coli* cystathionine β-lyase by L-aminoethoxyvinylglycine: a kinetic and X-ray study. Biochemistry. 36: 12633-12643.

Clausen, T. and Huber, R. Laber, B., Pohlenz, H.D., and Messerschmidt, A. 1996. Crystal structure of the pyridoxal 5'-phosphate dependent cystathionine β-lyase from *Escherichia coli* at 1.83 Å. J. Mol. Biol. 262: 202-224.

Cutin, A.C., McSweeney, P.L.H. 2004. Catabolism of amino acids in cheese during ripening. *In* Fox, P.F. (ed.), Cheese: chemistry, physics and microbiology. Vol. 1, pp. 435-454. Elsevier Ltd. London, England.

DeLano, W.L. 2002. The PyMOL Molecular Graphics System. DeLano Scientific. Palo Alto, CA, USA.

Dias, B., Weimer, B. 1998. Conversion of methionine to thiols by *Lactococci*, *Lactobacilli*, and *Brevibacteria*. Appl. Environ. Microbiol. 64: 3320-3326.

Dubourdieu, D., Tominaga, T., Masneuf, I., Peyrot des Gachons, C., Murat, M.L. 2006. The role of yeasts in grape flavor development during fermentation: the example of Sauvignon Blanc. Am. J. Enol. Vitic. 57:81-88.

Dunathan, H.C. 1966. Conformation and reaction specificity in pyridoxal phosphate enzymes. Proc. Natl. Acad. Sci. U.S.A. 55: 712-716

Eliot, A.C. and Kirsch, J.F. 2003. Avoiding the road less traveled: how the topology of enzyme-substrate complexes can dictate product selection. Acc. Chem. Res. 36: 757-765.

Eliot, A.C. and Kirsch, J.F. 2004. Pyridoxal phosphate enzymes: mechanistic, structural, and evolutionary considerations. Ann. Rev. Biochem. 73: 383-415.

Ellman, G. L. 1959. Tissue sulfhydryl groups. Arch. Biochem. Biophys. 82: 70-77.

Fernandez, M., Van Doesburg, W., Rutten, G.A.M., Marugg, J.D., Alting, A.C., Van Kranenburg, R., Kuipers, O.P. 2000. Molecular and functional analyses of the *metC* gene of *Lactococcus lactis*, encoding cystathionine β-lyase. Appl. Environ. Microbiol. 66: 42-48.

Flavin, M., Segal, A. 1964. Purification and properties of the cystathionine γ-cleavage enzymes of *Neurospora*. J. Biol. Chem. 239:2220-2227.

Gaitonde, M.K. 1967. A spectrophotometric method for the direct determination of cysteine in the presence of other naturally occurring amino acids. Biochem. J. 104: 627-633.

Galili, G. and Hofgen, R. 2002. Metabolic engineering of amino acids and storage proteins in plants. Metabolic Engineering. 4: 3-11.

György, P. 1971. Developments leading to the metabolic role of vitamin B6. Am. J. Clin. Nutr. 24: 1250-1256.

Hacham, Y., Avraham, T., and Amir, R. 2002. The N-terminal region of Arabidopsis cystathionine gamma-synthase plays an important regulatory role in methionine metabolism. Plant Phys. 128: 454-462.

Hasty, P., Ramirez-Solis, R., Krumlauf, R., and Bradley, A. 1991. Introduction of a subtle mutation into the Hox-2,6 locus in embryonic stem cells. Nature 350: 243-246.

Hermann, T. 2003. Industrial production of amino acids by Coryneform bacteria. J. Biotech. 204: 155-172.

Higuchi, R. 1990. Recombinant PCR. *In* Innis, M.A., Gelfand, D.H., Sninsky, J.J., White, T.J., eds. PCR protocols: a guide to methods and applications. pp. 177-183. Academic Press. San Diego.

Howell, K.S., Swiegers, J.H., Elsey, G.M., Siebert, T.E., Bartowsky, E.J., Fleet, G.H., Pretourius, I.S., de Barros Lopes, M.A. 2004. Variation in 4-mercapto-4-methyl-pentan-2-one release by *Saccharomyces cerevisiae* commercial wine strains. FEMS Microbiol. Lett. 240:125-129.

Hult, K., Berglund, P. 2003. Engineered enzymes for improved organic synthesis. Curr Opin. Biotechnol. Aug; 14: 395-400.

Hyde, C.C., Ahmed, S.A., and Padlan, E.A., Miles, E.W., Davies, D.R. 1988. Three-dimensional structure of the tryptophan synthase $\alpha_2\beta_2$ multienzyme complex from *Salmonella typhimurium*. J. Biol. Chem. 263: 17857-17871.

Jansonius, J.N. 1998. Structure, evolution and action of vitamin B6-dependent enzymes. Curr. Opin. Struct. Biol. 8: 759-769.

Koch, K.A., Capitani, G., Gruetter, M.G., and Kirsch, J.F. 2001. The human cDNA for a homologue of the plant enzyme 1-aminocyclopropane-1-carboxylate synthase encodes a protein lacking that activity. Gene. 272: 75-84.

Kuchner, O. and Arnold, F.H. 1997. Directed evolution of enzyme catalysts. Trends Biotechnol. 15: 523-530.

Kyte. J. 1995. Mechanism in Protein Chemistry. Garland Publishing, Inc., New York.

Laskar, S., Basak, B. 1988. Detection of amino acids on thin layer plates. J. Chromatogr. 436: 341–343.

Lawes, M. and Maloy, S. 1995. MudSacI, a transposon with strong selectable and counterselectable markers: use for rapid mapping of chromosomal mutations in *Salmonella typhimurium*.J. Bacteriol. 177: 1383-1387.

Lee, W.J., Banavara, D.S., Hughes, J.E., Christiansen, J.K., Steele, J.L., Broadbent, J.R., Rankin, S.A. 2007. Role of cystathionine β-lyase in amino acid catabolism to sulfur volatiles by genetic variants of *Lactobacillus helveticus* CNRZ32. Appl. Environ. Microbiol. [epub ahead of print].

Leuchtenberger, W., Huthmacher, K., and Drauz, K. 2005. Biotechnological production of amino acids and derivatives: current status and prospects. Appl. Microbiol. Biotechnol., 69: 1-8.

Link, A.J., Phillips, D., Church, G.M. 1997. Method for generating precise deletions and insertions in the genome of wild-type *Escherichia coli*: Application to open reading frame characterization. J. Bacteriol. 179: 6228-6237.

Luong, T.N. and Kirsch, J.F. 2001. A general method for the quantitative analysis of functional chimeras: applications from site-directed mutagenesis and macromolecular association. Protein Sci. 10: 581-591.

Ma, D., Alberti, M., Lynch, C., Nikaido, H., and Hearst, J. E. 1996. The local repressor AcrR plays a modulating role in the regulation of acrAB genes of *Escherichia coli* by global stress signals. Mol. Microbiol. 19: 101–112.

Mandel, M. and Higa, A. 1970. Calcium-dependent bacteriophage DNA infection. J. Molec. Biol. 53, 159-162.

Mahler, H.R., Cordes, E.H. 1968. Basic biological chemistry, 3rd Edn. pp. 40. Harper & Row, New York.

Messerschmidt, A. Worbs, M., and Steegborn, C. Wahl, M.C., Huber, R., Laber, B., and Clausen, T. 2003. Determinants of enzymatic specificity in the Cys-Met-metabolism PLP-dependent enzymes family: crystal structure of cystathionine gamma-lyase from yeast and intrafamiliar structure comparison. Biol. Chem., 384: 373-386.

Mudd, S. H., Levy, H. L., and Skovby, F.1989. Disorder in transsulfuration In: The Metabolic Basis of Inherited Disease (Scriver, C. R., Beaudet, A. L., Sly, W. S., and Valle, D., Eds.) pp. 693-734, McGraw-Hill, New York.

Nagasawa, T. Kanzaki, H., and Yamada, H. 1984. Cystathionine gamma-lyase of Streptomyces phaeochromogenes. The occurrence of cystathionine gamma-lyase in filamentous bacteria and its purification and characterization. J. Biol. Chem. 259: 10393-10403.

Ono, B.I., Hazu, T., Yoshida, S., Kowato, T., Shinoda, S., Brzywczy, J., and Paszewski, A. 1999. Cysteine biosynthesis in *Saccharomyces cerevisiae*: a new outlook on pathway and regulation. Yeast. 15: 1365-1375.

Percudani, R. and Peracchi, A. 2003. A genomic overview of pyridoxal-phosphate-dependent enzymes. EMBO Rep. 4: 850-854.

Ravanel, S., Gakiere, B., Job, D., and Douce, R. 1998. The specific features of methionine biosynthesis and metabolism in plants. Proc. Natl. Acad. Sci. USA. 95: 7805-7812.

Rothstein, R. 1991. Targeting, disruption, replacement, and allele rescue: integrative DNA transformation in yeast. Methods Enzymol. 194: 281-301.

Sarrazin, E., Shinkaruk, S., Tominga, T., Bennetau, B., Frerot, E., and Dubourdieu, D. 2007. Odorous impact of volatile thiols on the aroma of young botrytized sweet

wines: identification and quantification of new sulfanyl alcohols. J. Agric. Food Chem. 55: 1437-1444.

Scherer, S., and R. W. Davis. 1979. Replacement of chromosome segments with altered DNA sequences constructed in vitro. Proc. Natl. Acad. Sci. U.S.A. 76: 4951-4955.

Shike, M. (Ed.) 2006. Modern nutrition in health and disease. Lippincott, Williams and Wilkins. Philadelphia.

Silber, K.R. and Sauer, R.T. 1994. Deletion of the prc (tsp) gene provides evidence for additional tail-specific proteolytic activity in Escherichia coli K-12. Mol. Gen. Genet. 242: 237-240.

Steegborn, C., Clausen, T., Sondermann, P., Jacob, U., Worbs, M., Martinkovic, S., Huber, R., and Wahl, M.C. 1999. Kinetics and inhibition of recombinant human cystathionine γ-lyase. J. Biol. Chem. 274: 12675-12684.

Sugio, S., Petsko, G.A., and Manning, J.M. 1995. Crystal structure of a D-amino acid aminotransferase: how the protein controls stereoselectivity. Biochem. 34: 9661-9669.

Swiegers, J.H., Pretorius, I.S. 2007. Modulation of volatile sulfur compounds by wine yeast. Appl Microbiol Biotechnol. 74: 954-960.

Terpe, K. 2006. Overview of bacterial expression systems for heterologous protein production: from molecular and biochemical fundamentals to commercial systems. Appl. Microbiol. Biotechnol. 72: 211-22.

Tominaga, T., Masneuf, I., Dubourdie, D. 1995. A *S*-cysteine conjugate, precursor of aroma of white sauvignon. J. Int. Sci. 29: 227-232.

Tominaga, T., Peyrot des Gachons, C., Dubourdieu, D. 1998a. A new type of flavour precursors in *Vitis vinifera* L. cv. Sauvignon Blanc: S-cysteine conjugates. J. Argic. Food Chem. 46: 5215-5219.

Tominaga, T., Furrer, A., Henry, R., Dubourdieu, D. 1998b. Identification of new volatile thiols in the aroma of *Vitis vinifera* L. var. Sauvigonon Blanc wines. Flavour Fragr. J. 13: 159-162.

Tominaga, T., Blanchard, L., Darriet, P., Dubourdieu, D. 2000. A powerful aromatic volatile thiol, 2-furanmethanethiol, exhibiting roast coffee aroma in wines made from several *Vitis vinifera* grape varieties. J. Agric. Food Chem. 48:1799-1802.

Uren, J.R., Ragin, R., Chaykovsky, M. 1978. Modulation of cysteine metabolism in mice - effects of propargylglycine and l-cyste(e)ine-degrading enzymes. Biochem Pharmacol. 27: 2807-2814.

Voet, D., Voet, J.G., and Pratt, C.W. 2002. Fundamentals of Biochemistry. John Wiley & Sons Inc., New York.

Wada, M. and Takagi, H. 2006. Metabolic pathways and biotechnological production of L-cysteine. Appl. Microbiol. Biotechnol., 73: 48-54.

Wang, J. and Hegele, R.A. 2003. Genomic basis of cystathioninuria (MIM 219500) revealed by multiple mutations in cystathionine gamma-lyase (CTH). Hum. Genet. 112: 404-408.

Weimer, B., Seefeldt, K., and Dias, B. 1999. Sulfur metabolism in bacteria associated with cheese. Antonie Van Leeuwenhoek. 76: 247-261.

Yamagata, S., Isaji, M., Yamane, T., and Iwama, T. 2002. Substrate inhibition of L-cysteine α,β-elimination reaction catalyzed by L-cystathionine γ-lyase of *Saccharomyces cerevisiae*. Biosci. Biotechnol. Biochem. 66: 2706-2709.

Yamagata, S., D'Andrea, R.J., and Fujisaki, S., Isaji, M., Nakamura, K.1993. Cloning and bacterial expression of the *Cys3* gene encoding cystathionine γ-lyase of *Saccharomyces cerevisiae* and the physicochemical and enzymatic properties of the protein. J. Bacteriol 75: 4800-4808.